

การสังเคราะห์ซิลิกาไลต์ และซิลิกาไลต์เมมเบรนจากแกลบข้าวโดยวิธี  
ไฮโดรเทอร์มัล สำหรับการแยกเอทานอลออกจากสารละลายในน้ำ



นายชัยวัฒน์ คงมันกลาง

วิทยานิพนธ์นี้เป็นส่วนหนึ่งของการศึกษาตามหลักสูตรปริญญาวิทยาศาสตรดุษฎีบัณฑิต

สาขาวิชาเคมี

มหาวิทยาลัยเทคโนโลยีสุรนารี

ปีการศึกษา 2557

**HYDROTHERMAL SYNTHESIS OF SILICALITE AND  
SILICALITE MEMBRANE FROM RICE HUSK  
FOR ETHANOL SEPARATION FROM  
AQUEOUS SOLUTION**

**Chaiwat Kongmanklang**



**A Thesis Submitted in Partial Fulfillment of the Requirements for the  
Degree of Doctor of Philosophy in Chemistry  
Suranaree University of Technology  
Academic Year 2014**

**HYDROTHERMAL SYNTHESIS OF SILICALITE AND  
SILICALITE MEMBRANE FROM RICE HUSK FOR  
ETHANOL SEPARATION FROM AQUEOUS SOLUTION**

Suranaree University of Technology has approved this thesis submitted in partial fulfillment of the requirements for the Degree of Doctor of Philosophy.

Thesis Examining Committee

---

(Assoc. Prof. Dr. Jatuporn Wittayakun)

Chairperson

---

(Asst. Prof. Dr. Kunwadee Rangriwatananon)

Member (Thesis Advisor)

---

(Asst. Prof. Dr. Aahiruk Chaisena)

Member

---

(Asst. Prof. Dr. Sanchai Prayoonpokarach)

Member

---

(Asst. Prof. Dr. Thanaporn Manyum)

Member

---

(Prof. Dr. Sukit Limpijumngong)

Vice Rector for Academic Affairs  
and Innovation

---

(Prof. Dr. Santi Maensiri)

Dean of Institute of Science

ชัยวัฒน์ คงมันกลาง : การสังเคราะห์ซิลิกาไลต์ และซิลิกาไลต์เมมเบรนจากแกลบข้าว  
โดยวิธีไฮโดรเทอร์มัล สำหรับการแยกเอทานอลออกจากสารละลายในน้ำ

(HYDROTHERMAL SYNTHESIS OF SILICALITE AND SILICALITE MEMBRANE  
FROM RICE HUSK FOR ETHANOL SEPARATION FROM AQUEOUS SOLUTION)

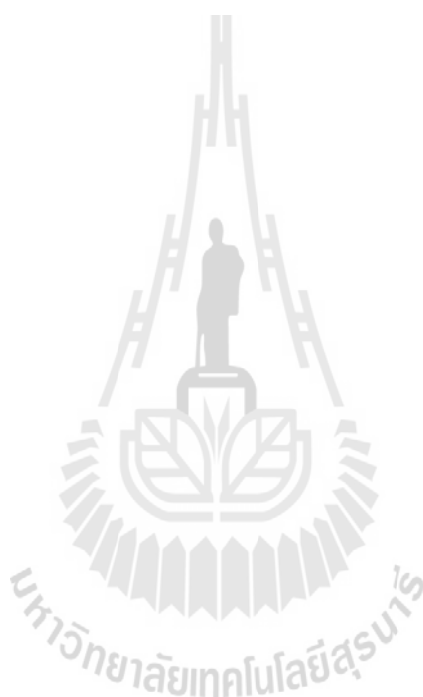
อาจารย์ที่ปรึกษา : ผู้ช่วยศาสตราจารย์ ดร.กมลวิดี รัมย์พัฒนานนท์, 97 หน้า.

ในการศึกษานี้ สามารถสังเคราะห์ซิลิกาไลต์ชนิดซิลิกาไลต์ด้วยวิธีไฮโดรเทอร์มัล ที่อุณหภูมิ 187 องศาเซลเซียส ภายใต้ความดันออกโทจีเนียสจากเจลที่ประกอบด้วย ซิลิกา ค่าง น้ำ และ แคลตไอออนเอมีนอินทรีย์ที่ใช้เป็นเทมเพลต เถ้าแกลบความบริสุทธิ์สูงที่ใช้เป็นแหล่งของซิลิกาเตรียมได้จากการชะละลายแกลบข้าวด้วยกรดที่เหมาะสม และเผาที่อุณหภูมิ 700 องศาเซลเซียส เป็นเวลา 4 ชั่วโมง ซิลิกาเจลที่ได้จากเถ้าแกลบเตรียมขึ้นเพื่อเพิ่มความบริสุทธิ์ และเพิ่มพื้นที่ผิวของซิลิกา ซิลิกาไลต์ที่มีความเป็นผลึกสูงสุดเตรียมได้เมื่ออัตราส่วนโดยโมลของ  $\text{NaOH}/\text{SiO}_2$   $\text{H}_2\text{O}/\text{NaOH}$  และ  $\text{SiO}_2/\text{TPABr}$  มีค่าเท่ากับ 0.24 1.55 และ 30 ตามลำดับ โดยใช้เวลาในการสังเคราะห์เพียง 6 ชั่วโมง ซิลิกาไลต์ที่ได้จากซิลิกาเจลมีขนาดเล็กกว่าที่ได้จากเถ้าแกลบ และซิลิกาไลต์ที่เตรียมได้ทั้งหมดมีรูปร่างผลึกเป็นคอปฟินและรูปลูกบาศก์

ได้ศึกษาการสังเคราะห์ซิลิกาไลต์ให้มีขนาดผลึกต่าง ๆ กันจากเถ้าแกลบ การสังเคราะห์ใช้วิธีไฮโดรเทอร์มัลอย่างง่าย โดยใช้แหล่งซิลิกาจากเถ้าแกลบ โซเดียมซิลิเกตและโพแทสเซียมซิลิเกต ซึ่งโซเดียมซิลิเกตและโพแทสเซียมซิลิเกต เตรียมได้จากการละลายเถ้าแกลบด้วยโซเดียมไฮดรอกไซด์และโพแทสเซียมไฮดรอกไซด์ ขนาดผลึกของซิลิกาไลต์สามารถเตรียมได้ในช่วง 3 ถึง 23 ไมครอน โดยการปรับอัตราส่วนโมล  $\text{NaOH}:\text{SiO}_2$  หรือ  $\text{KOH}:\text{SiO}_2$  ในระบบของ  $\text{SiO}_2$ -TPABr-NaOH/KOH- $\text{H}_2\text{O}$  ผ่านกระบวนการสังเคราะห์ที่อุณหภูมิ 187 องศาเซลเซียส เป็นเวลา 6 ชั่วโมง

ด้วยคุณสมบัติของซิลิกาไลต์ที่ดูดซับสารอินทรีย์ได้ดีจึงสามารถนำมาใช้ในการดูดซับและการแยกสารอินทรีย์ได้ จึงได้ศึกษาการแยกเอทานอลจากสารละลายผสมระหว่างเอทานอลน้ำด้วยซิลิกาไลต์เมมเบรนด้วยวิธีเพอเวอเรนซ์ ได้สังเคราะห์ซิลิกาไลต์เมมเบรนบนแผ่นรองรับมีลไลต์รูพรุนจากสารละลายที่มีองค์ประกอบเจล  $0.80\text{KOH}:\text{SiO}_2:0.03\text{TPABr}:123\text{H}_2\text{O}$  การเกิดผลึกของซิลิกาไลต์ใช้อุณหภูมิในการสังเคราะห์ 2 ชั้น ที่ 90 องศาเซลเซียส เป็นเวลา 17 ชั่วโมง และ 170 องศาเซลเซียส เป็นเวลา 24 ชั่วโมง เพื่อเป็นการเพิ่มคุณสมบัติในการดูดซับสารอินทรีย์ซิลิกาไลต์เมมเบรนได้ถูกคัดแปรด้วย phenyltriethoxysilane (PhTES) โดยการรีฟลักซ์ซิลิกาไลต์เมมเบรนด้วย PhTES ในโทลูอีน ที่อุณหภูมิ 80 องศาเซลเซียส เป็นเวลา 6 ชั่วโมง ผลิตภัณฑ์ที่ได้นำมาวิเคราะห์ลักษณะด้วยเทคนิค XRD XRF SEM  $\text{N}_2$  adsorption-desorption analysis FT-IR laser particle size analysis และ  $^{29}\text{Si}$   $^{27}\text{Al}$  NMR การแยกเอทานอลจากสารผสมเอทานอล/น้ำ ด้วยซิลิ-

กาไลท์เมมเบรนด้วยกระบวนการเพอเวพอเรชันของสารละลายเอทานอลที่มีความเข้มข้น ร้อยละ 5  
โดยน้ำหนัก พบว่าแฟลคเตอร์การแยกและฟลักซ์ มีค่า 8.43 และ  $0.42 \text{ kg/m}^2 \cdot \text{h}$  ตามลำดับ



สาขาวิชาเคมี  
ปีการศึกษา 2557

ลายมือชื่อนักศึกษา \_\_\_\_\_  
ลายมือชื่ออาจารย์ที่ปรึกษา \_\_\_\_\_

CHAIWAT KONGMANKLANG : HYDROTHERMAL SYNTHESIS OF  
SILICALITE AND SILICALITE MEMBRANE FROM RICE HUSK FOR  
ETHANOL SEPARATION FROM AQUEOUS SOLUTION.

THESIS ADVISOR : ASST. PROF. KUNWADEE

RANGSRIWATANANON, Ph.D. 97 PP.

RICE HUSK ASH/ SILICALITE/ ZSM-5/ SIZE CONTROLLED/ SILICALITE  
MEMBRANE

In this study, silicalite was hydrothermally synthesized at 187°C under autogeneous pressure from a gel composed of silica, alkaline, water and organic amine cation, which was used as a template. High purity rice husk ash (RHA), used as a silica source, was obtained from appropriate acid leaching and burning of the husk at 700°C for 4 h. Silica gel (SG) produced from rice husk ash was prepared to increase the purity and surface area. Silicalite with the highest crystallinity was obtained at a reaction time of only 6 h with the mole ratios of NaOH/SiO<sub>2</sub>, H<sub>2</sub>O/NaOH, and SiO<sub>2</sub>/TPABr of 0.24, 155, and 30, respectively. The particle size of the silicalite obtained from SG was smaller than that from RHA. The morphologies of all silicalite samples were coffin and cubic-like shape.

The facial hydrothermal synthesis of size-controlled silicalite crystals from rice husk ash was further studied. The silicalite was successfully obtained through the simplest hydrothermal method with the following materials as silica RHA, sodium silicate and potassium silicate (prepared by dissolving RHA with NaOH and KOH, respectively). Its crystal size could be easily tuned from 3 μm to 23 μm by adjusting

the molar ratio of NaOH:SiO<sub>2</sub> or KOH:SiO<sub>2</sub> in the system of SiO<sub>2</sub>-TPABr-NaOH/KOH-H<sub>2</sub>O through the synthesis process with the temperature at 187°C for 6 h.

Due to the high hydrophobicity and organophilicity of silicalite, it is a promising material as a high capacity adsorbent in adsorption and separation processes. A pure silicalite membrane was hydrothermally synthesized on a porous support of mullite discs from clear solutions with a gel compositions of 0.80KOH:SiO<sub>2</sub>:0.03TPABr:123H<sub>2</sub>O. Crystallization was carried out with 2 temperature stage of 90°C for 12 h and 170°C for 24 h. To improve the hydrophobicity, a modified silicalite membrane was prepared by refluxing silicalite membrane with PhTES in toluene at 80°C for 6 h. All of the products were characterized by XRD, XRF, SEM, N<sub>2</sub> adsorption-desorption analysis, FT-IR, laser particle size analysis, and <sup>29</sup>Si, <sup>27</sup>Al NMR. Separation of ethanol/water mixtures through the silicalite membrane was carried out by pervaporation. High ethanol permselectivity with a separation factor of 8.43 and flux of 0.42 kg/m<sup>2</sup>h was achieved for a 5 wt% aqueous ethanol solution at 60°C.

School of Chemistry

Academic Year 2014

Student's Signature \_\_\_\_\_

Advisor's Signature \_\_\_\_\_

## **ACKNOWLEDGEMENTS**

I would like to express my deepest and sincerest gratitude to my advisor, Asst. Prof. Dr. Kunwadee Rangriwatananon for her kindness to give me a good opportunity to study in this field, her supervision and her valuable suggestions.

I am also grateful to the lecturers in the School of Chemistry. I am extremely thankful and indebted for sharing expertise, and sincere and valuable guidance and encouragement extended to me.

I would like to highly acknowledge the Suranaree University of Technology Research and Development Support Fund for financial support and the Center for Scientific and Technological Equipment for facility support in carrying out this research.

Finally, I take this opportunity to express gratitude to all of the Department faculty members for their help and support. I also thank my parents for the unceasing encouragement, support and attention.

Chaiwat Kongmanklang

# CONTENTS

	<b>Page</b>
ABSTRACT IN THAI.....	I
ABSTRACT IN ENGLISH .....	III
ACKNOWLEDGEMENTS.....	V
CONTENTS.....	VI
LIST OF TABLES .....	X
LIST OF FIGURES .....	XI
LIST OF ABBREVIATIONS.....	XIV
<b>CHAPTER</b>	
<b>I INTRODUCTION.....</b>	<b>1</b>
1.1 Zeolite molecular sieves.....	2
1.1.1 Synthesis.....	4
1.1.2 Synthesis mechanism .....	6
1.2 Zeolite membrane.....	9
1.2.1 Membrane synthesis .....	9
1.2.2 Membranes characterization .....	11
1.3 Pervaporation .....	12
1.3.1 Introduction .....	12
1.3.2 Factors affecting pervaporation performance of MFI membranes .....	15

## CONTENTS (Continued)

	<b>Page</b>
1.3.3 Non-zeolite pores .....	16
1.4 References .....	19
<b>II LITERATURE REVIEWS.....</b>	<b>26</b>
2.1 Silicalite synthesis .....	26
2.2 Size-controlled synthesis of silicalite.....	28
2.3 Silicalite membrane and pervaporation.....	33
2.4 References .....	39
<b>III HYDROTHERMAL SYNTHESIS OF SILICALITE FROM</b>	
<b>RICE HUSK ASH.....</b>	<b>45</b>
3.1 Abstract.....	45
3.2 Introduction.....	45
3.3 Materials and methods .....	47
3.3.1 Materials.....	47
3.3.2 Methods .....	47
3.3.3 Synthesis procedure.....	48
3.3.4 Ethanol adsorption.....	48
3.3.5 Characterization .....	48
3.4 Results and discussion .....	49
3.4.1 Fourier transform infrared spectroscopy .....	51
3.4.2 X-ray fluorescence .....	52
3.4.3 X-ray diffraction.....	52

## CONTENTS (Continued)

	<b>Page</b>
3.4.4 Scanning electron microscope.....	54
3.4.5 Ethanol adsorption properties.....	56
3.5 Conclusions.....	57
3.6 References.....	57
<b>IV FACIAL HYDROTHERMAL SYNTHESIS OF SIZE-CONTROLLED SILICALITE CRYSTALS FROM RICE HUSK ASH .....</b>	<b>60</b>
4.1 Abstract.....	60
4.2 Introduction.....	61
4.3 Materials and methods .....	63
4.3.1 Materials.....	63
4.3.2 Methods.....	63
4.3.3 Synthesis procedure.....	64
4.3.4 Characterization .....	65
4.4 Results and discussion .....	65
4.4.1 Silica source properties .....	65
4.4.2 Fourier transform infrared spectroscopy .....	66
4.4.3 X-ray power diffraction.....	67
4.4.4 <sup>29</sup> Si and <sup>27</sup> Al NMR .....	68
4.4.5 Scanning electron microscope.....	70
4.5 Conclusions.....	73
4.6 References.....	73

## CONTENTS (Continued)

	<b>Page</b>
<b>V SEPARATION OF ETHANOL FROM ETHANOL/WATER</b>	
<b>MIXTURES USING PERVAPORATION MEMBRANE .....</b>	<b>78</b>
5.1 Abstract .....	78
5.2 Introduction .....	79
5.3 Materials and methods .....	81
5.3.1 Materials .....	81
5.3.2 Methods .....	81
5.3.3 Characterization .....	82
5.4 Results and discussion .....	83
5.4.1 Mullite disc porous support .....	83
5.4.2 Time dependent layer morphology .....	84
5.4.3 Silicalite crystallinity .....	86
5.4.4 Modified silicalite membrane .....	87
5.4.5 Pervaporation .....	89
5.5 Conclusions .....	92
5.6 References .....	93
SUMMARY .....	95
CURRICULUM VITAE .....	97

## LIST OF TABLES

<b>Table</b>		<b>Page</b>
2.1	Separation factors and fluxes for the MFI membranes .....	35
3.1	The chemical compositions and BET surface areas of silica sources.....	49
3.2	Mole ratios of gel compositions for silicalite synthesis.....	50
3.3	The chemical compositions of silicalite SL13 and SL18.....	52
3.4	Ethanol adsorption of silicalite (2.5 wt% to 10 wt% ethanol solutions, 100 mg/mL) .....	57
4.1	The chemical composition of the local RHA determined by XRF .....	65
4.2	Molar ratios of gel composition and crystal size of silicalite synthesized at 187°C for 6 h .....	66
5.1	Mole ratios of chemical compositions of preparation condition of silicalite membranes synthesis at 2 stage temperature for 24 h .....	84
5.2	Pervaporation performance of silicalite membrane and silicalite membrane modified for ethanol/water mixture separation.....	92

## LIST OF FIGURES

<b>Figure</b>	<b>Page</b>
1.1 Zeolite framework and pore system: MFI topologies.....	3
1.2 Mechanism of structure direction and crystal growth in the synthesis of TPA-Si-ZSM-5 as investigated by Burkett and Davis (1994).....	8
1.3 Schematic representation of a typical experimental set up for pervaporation .....	13
1.4 Representation of non-zeolite pores in the intercrystalline boundaries of a zeolite membrane layer .....	17
1.5 Representation of transport of an organic/water mixture through: (a) hydrophobic zeolite membrane, (b) hydrophobic zeolite membrane containing non-zeolite pores .....	18
3.1 FT-IR spectra of silica source: RHA(a), SG(b) and silicalite samples: SL1(c), SL12(d), SL13(e), and SL18(f) with different gel compositions (see Table 3.2) .....	51
3.2 X-ray diffraction patterns of silica source: RHA(a), SG(b) and silicalite sample: SL1(c), SL12(d), SL13(e), and SL18(f) with different gel compositions (see Table 3.2).....	53
3.3 Scanning electron micrographs of SL1(a), SL2(b), SL10(c), SL11(d), SL12(e), SL13(f) and SL18(g) referred in Table 3.2.....	55
3.4 Particle size distribution of silicalite synthesized from RHA (SL13) in solid line and SG (SL18) in dash line .....	56

## LIST OF FIGURES (Continued)

<b>Figure</b>	<b>Page</b>
4.1	FT-IR spectra of as-synthesized silicalite prepared from RHA1(a), RHA2(b), SS2(c), and KS2(d).....67
4.2	X-ray diffraction patterns of RHA1(a), RHA2(b), SS2(c), and KS2(d).....68
4.3	<sup>29</sup> Si MAS NMR signal of SS3 sample .....69
4.4	<sup>27</sup> Al NMR spectra of SS3 sample .....70
4.5	Scanning electron micrographs of as-synthesized silicalite samples RHA1(a), RHA2(b), SS1(c), SS2(d), SS3(e), KS1(f), KS2(g), and KS3(h) .....71
5.1	SEM of the mullite (a) mullite disc with diameter 5 cm, (b) surface and (c) cross-section of mullite disc .....83
5.2	SEM imaging of silicalite membrane formation against time, tc. Top views of single layered membranes after tc = 0 h (a), 2 h (b), 4 h (c), 12 h (d) and 24 h (e) .....85
5.3	Cross-sections through the layered of zeolites membrane corresponding to synthesis times of 24 h .....86
5.4	X-ray diffraction patterns of the (a) mullite disc support and (b) silicalite membrane synthesized with reaction time of 24 h .....87
5.5	Surface of silicalite membrane (a) and silicalite membrane modified with PhTES (b) .....88
5.6	FT-IR spectra of PhTES (a), silicalite membrane after modified with PhTES (b), and silicalite membrane (c) .....89

**LIST OF FIGURES (Continued)**

<b>Figure</b>	<b>Page</b>
5.7 Influence of feed temperature on pervaporation performances through silicalite membrane modified with PhTES. Feed ethanol concentration: 5 wt% .....	90
5.8 Influence of feed ethanol concentration on pervaporation performance. Feed temperature: 60°C.....	91



## LIST OF ABBREVIATIONS

AAS	=	Atomic Absorption Spectrometer
BET	=	Brunauer Emmett Teller
FT-IR	=	Fourier Transform Infrared Spectrometer
GC	=	Gas Chromatography
kV	=	kilovolts
MAS NMR	=	Magic Angle Spin Nuclear Magnetic Resonance
ND	=	Not Detected
OTCIS	=	Octadecyltrichlorosilane
PDMS	=	Polydimethylsiloxane
PhCIOS	=	Phenylchloroethoxysilane
PhTES	=	Phenyltriethoxysilane
PTFE	=	Polytetrafluoroethylene
PVDF	=	Polyvinylidene fluoride
RHA	=	Rice Husk Ash
S.F.	=	Separation Factor
SEM	=	Scanning Electron Microscope
TPABr	=	Tetrapropylammonium bromide
XRD	=	X-ray diffraction or X-ray diffractometer
XRF	=	X-ray Fluorometer

# CHAPTER I

## INTRODUCTION

The conversion of biomass into an energy source by fermentation processes to produce chemicals and fuels such as bioethanol, replacing the use of fossil energy resources is receiving substantial interests. This is due to the increasing petroleum prices and concerns over climate change. Ethanol fermentation can transform the biomass into a useful energy source as pure ethanol or gasohol. The ethanol must be concentrated because the ethanol concentration requested for gasohol is over 99.5° Gay-Lussac (G.L). The ethanol fermenter used for energy should be operated efficiently. The current method used for ethanol recovery and purification in the fermentation process is distillation followed by molecular sieve adsorption. The recovery and purification of ethanol from fermentation broth generally involves distillation which is energy intensive and complex. It has been estimated to consume more than half of the total energy in the production of alcohol by fermentation. To make bioethanol processes competitive with fossil energy resources, production costs must be reduced.

Pervaporation is a membrane based system permeation that removes ethanol from the fermenter. It can be a solution to overcome the disadvantages of conventional ethanol fermentation systems. A membrane separation system has been employed for continuous operation at room temperature. Thus, an ethanol permselective membrane system has been used for the extraction of ethanol from fermentation broth.

Silicalite membranes exhibited preferential organic compound permeation from water such as ethanol/water mixtures because silicalite not only has a strong hydrophobicity but also preferentially adsorbs organic compounds. Thus, it is necessary to develop efficient procedure for the fabrication of silicalite membranes with high fluxes and high separation factors.

### 1.1 Zeolite molecular sieves

Zeolites are microporous crystalline silicates or aluminosilicate with a 3-dimensional, open anion framework consisting of oxygen-sharing  $TO_4$  tetrahedra, where T is Si or Al. Their framework structures contain interconnected voids that are filled with adsorbed molecules or cations. The uniform molecular-sized pores give zeolite the capacity to separate material mixtures on the molecular level, allowing them to be designated as molecular sieves. The general empirical formula is:



where m is the valence of cations M, n is the water content and  $0 \leq x \leq 1$ . The flexibility of the zeolite Si-O-Si bond explains the fact that more than 200 structures have been determined. Indeed, there is little energetic difference (10-12 kJ/mol) between these remarkable porous silicates and higher density phases such as quartz. Several properties account for their commercial use: they are strong adsorbents, they show a very high selectivity and they are excellent solid acid catalysts.

ZSM-5 zeolite is a high silica zeolite, which was first synthesized by Argauer and Landolt of Mobil Oil Corporation, in 1972 (Argauer and Landolf, 1972). Zeolite ZSM-5 of MFI structure (Mobil Five), contains two intersecting channel systems

composed of straight and sinusoidal channels with 10-membered ring opening of  $5.3 \times 5.6 \text{ \AA}$  and  $5.5 \times 5.1 \text{ \AA}$  in dimension, respectively (Kokotailo, Lawton, Olson, and Meier, 1972). The structure of ZSM-5 zeolite can exist over a wide span of Si/Al ratios, with its silica content approaching to 100%.

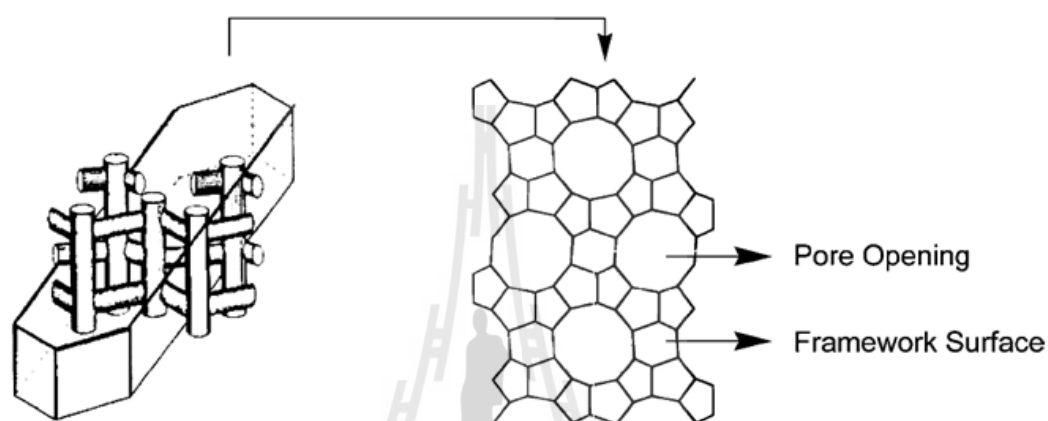


**Figure 1.1** Zeolite framework and pore system: MFI topologies.

Silicalite, which is crystalline silica having channel structure similar to that of ZSM-5 zeolite, is essentially the aluminium-free end member of the isostructural ZSM-5 series. The silicalite is highly hydrophobic and organophilic, and therefore selectively adsorbs organic molecules over water. This remarkable property makes the silicalite an ideal sorbent for removing selectively from aqueous solutions the organic molecules smaller than its limiting pore size. Also, because of its peculiar shape-selectivity behavior and little or no catalytic activity at higher temperatures, the silicalite has shown high promise as a potential adsorbent in adsorption separation processes (Oumi, Miyajima, Miyamoto, and Sano, 2002; Delgado et al., 2012).

### 1.1.1 Synthesis

The synthesis of zeolites is carried out under hydrothermal conditions. An aluminate solution and a silicate solution are mixed together in an alkaline medium to form a milky gel or in some instances, clear solutions. Various cations or anions can be added to the synthesis mixture. Synthesis proceeds at elevated temperatures (60-200°C) where crystals form through a nucleation step. The following sections give a general overview on the parameters effective during zeolite synthesis.

#### a) Molar composition

Although this is not an independent parameter, every zeolite has a specific molar composition range often represented graphically in a ternary compositional phase diagram ( $\text{Na}_2\text{O}$ ,  $\text{Al}_2\text{O}_3$  and  $\text{SiO}_2$ ). On the other hand, each structure also depends on the amount of Al that can incorporate the structure. High-silica molecular sieves such as ZSM-5 can be synthesized over a wide range of Si/Al ratios (Si/Al from 10 to infinity (Shirazi, Jamshidi, and Ghasemi, 2008)).

#### b) Mineralizer

A mineralizer is a species which enables the formation of a more stable solid phase from a less stable solid phase via dissolution and crystallization. Supersaturation can be reached by dissolution and these soluble species are then available for nucleation and crystal growth. In most cases, hydroxyl ions act as mineralizing agents. Indeed,  $\text{OH}^-$  increases the solubility of silica by depolymerizing amorphous silica particles. Oligomeric species are then present in solution. Condensation of specific aluminosilicate species, facilitated by the presence of  $\text{OH}^-$ , occurs and leads to the appearance of the first crystals. In general high pH values increase crystal growth rates and shorten the nucleation period. Hydroxyl ion

concentration can also influence crystal morphology, crystal yield and final zeolite structure.

c) Inorganic cations

Inorganic cations have been regarded as an important parameter influencing the structure formed. They are involved in structure direction, solid yield, crystal morphology and purity. Most of the synthetic analogues of natural zeolites are obtained using alkali and alkaline earth metal cations. Nucleation and crystal growth can be optimized by the right choice of inorganic cations.

d) Temperature

Temperature can alter the zeolite structure as well as the induction period and crystal growth kinetics. As the temperature of the system increases the reaction rate increases, thus accelerating nucleation and crystal growth. Theoretical modeling of zeolite syntheses have shown that the rate of nucleation can be very sensitive to the changes in the temperature of system (Jia and Murad, 2006). The heat-up rate of the system can also be critical; a slow heating rate will result in a spreading-out of the nucleation period (Coker and Jansen, 1998).

e) Silica and alumina sources

Nucleation and growth kinetics can depend on the dissolution of the solid reagents and formation of aluminosilicate precursors. Mintova and Valtchev investigated the colloidal distribution of silicalite-1 synthesis mixtures containing different silica sources (Mintova and Valchev, 2002). It was found that a nutrient present in a monomeric form might more readily interact with other nutrients to form nuclei than one which is present in a polymeric form.

#### f) Structure direction in zeolite synthesis

Structure direction occurs when inorganic or organic molecules are used to direct the crystallization towards a specific zeolite structure. Structure-directing agents, commonly called templates, are generally:

(1) charged molecules which are mostly cations. Inorganic cations such as  $\text{Na}^+$ ,  $\text{K}^+$ ,  $\text{Li}^+$  and  $\text{Ca}^{2+}$  are frequently used (Choudhary and Akolekar, 1988). Organic molecules that are used are usually tetraalkylammonium, dialkyl and trialkyl amines or phosphonium compounds (Ban et al., 2005).

(2) neutral molecules. Water actually plays an important role in the structure direction encountered in zeolite synthesis. Water molecules act as void fillers in order to stabilize the porous oxide framework. Interactions of water molecules with cations are part of the template effect and therefore are of crucial importance. Other molecules include amines, ethers or alcohols.

(3) ionic pairs: salts ( $\text{NaCl}$ ,  $\text{KCl}$ ,  $\text{KBr}$ ) are occluded into the zeolite framework as guest.

The porous silicon dioxide framework is mainly uncharged. Defect sites are required to balance the charge of the cationic structure-directing agent. Interactions between organic molecules and silica are mostly the Van der Waals forces (Burkett and Davis, 1995).

### 1.1.2 Synthesis mechanism

Much effort has been made to study the crystallization of Silicalite-1 without the intermediary of a heterogeneous gel phase by performing the crystallization from a clear solution. In the TPAOH-TEOS- $\text{H}_2\text{O}$  system, the soluble aggregates with dimensions of 4 nm are the end product of the polycondensation and exist in the

solution prior to and throughout the process of crystallization. These aggregates apparently have the MFI topology and occluded TPA cations in channel intersections and thus have been considered to be correlated to the onset of crystallinity (Kirschhock et al., 1999).

Chang and Bell (1991) studied the formation of ZSM-5 from Al-free precursor gels at 90-95°C using XRD,  $^{29}\text{Si}$  MAS NMR spectroscopy, and ion exchanges in gel structure occur during the early stages of reaction. This was confirmed by the demonstration of ion sieve effects suggesting that, in the tetrapropylammonium (TPA) system, embryonic structures with  $\text{Si}/\text{TPA} = 20\text{-}24$  are formed rapidly upon heating. These first-formed units, approximating to channel intersections and each containing essentially one  $\text{TPA}^+$  cation, are initially randomly connected but in the time become ordered through repeated cleavage and recombination of siloxane bonds, mediated by hydroxide ion. The hydrophobic effect and the isomorphism between water and silicate structure are invoked to provide a possible mechanism for ZSM-5 nucleation with the following steps.

- (a) formation of clathrate-like water structure around the template
- (b) isomorphous substitution of silicate for water in these cages
- (c) progressive ordering of these entities into the final crystal structure

Burkett and Davis (1994) examined the role of TPA as structure directing agent in silicalite synthesis, primarily by MAS NMR spectroscopy.  $^1\text{H}$ - $^{29}\text{Si}$  CP MAS NMR results provide direct evidence for the existence of preorganized inorganic-organic composite structures during the synthesis, in which the TPA molecules adopt a conformation similar to that which they have in the zeolite product. The initial formation of the inorganic-organic composite is initiated by overlap of the hydrophobic

hydration spheres of the inorganic and organic components, with subsequent release of ordered water to establish favorable van der Waals interactions. Thereafter, aggregation of these composite species is responsible for nucleation. Crystal growth occurs through diffusion of the same species to the surface of the growing crystallites to give a layer-by-layer growth mechanism. These ideas are illustrated in Figure 1.2.

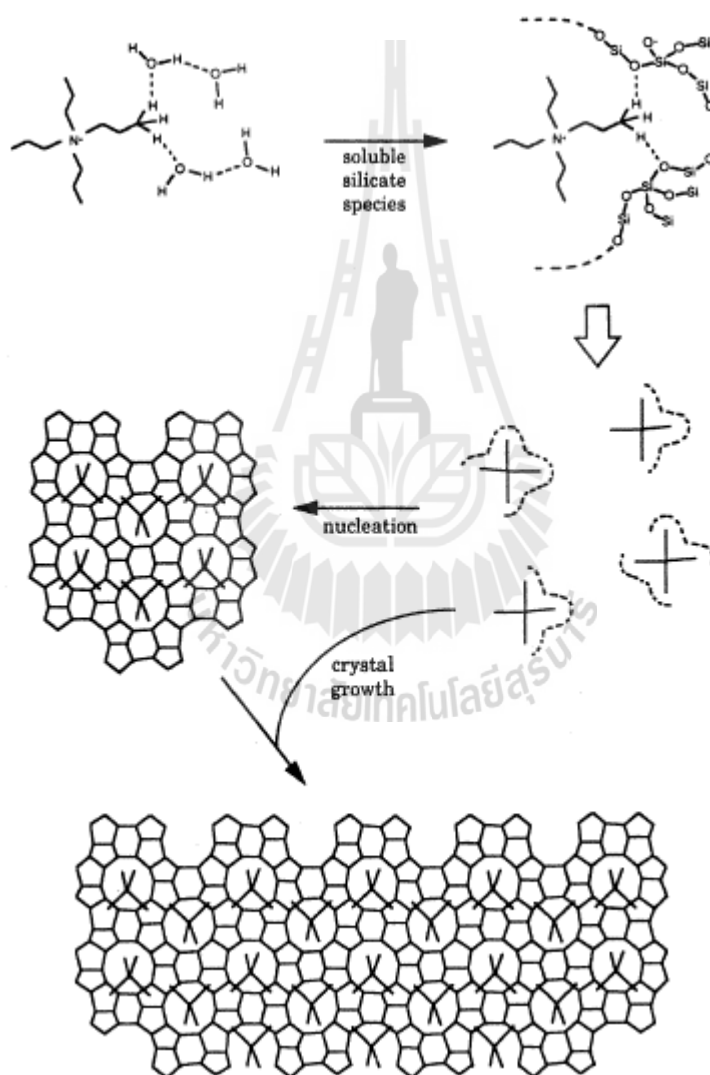


**Figure 1.2** Mechanism of structure direction and crystal growth in the synthesis of TPA-Si-ZSM-5 as investigated by Burkett and Davis (1994).

## 1.2 Zeolite membrane

A zeolite membrane is a thin film of zeolite crystals deposited on a porous and mechanically stable support. MFI is a widely studied structure due to its ease of preparation and suitable pore size for separation of mixtures of commercial importance. A membrane should provide high permeability and selectivity at the same time to be used in industrial applications. Moreover, a large surface area which can be manufactured with a high reproducibility is required together with cost-effective fabrication. Up to now, trials have been done for the membrane quality to be improved by modification of chemical gel composition and variation of crystallization conditions (Noack, Kolsch, Schafer, and Toussaint, 2002). Zeolite membranes are typically prepared on discs or tubular supports with permeable areas at about 5-15 cm<sup>2</sup>. The fluxes through membranes of that thickness on the other hand is too low to be commercialized. Therefore, thin layers of zeolite membranes with good quality are required to combine high permeability with high selectivity.

### 1.2.1 Membrane synthesis

Zeolite membranes are conventionally synthesized by in situ hydrothermal synthesis in batch systems. Hydrothermal synthesis involves crystallization of a zeolite layer onto a porous support from a gel that is usually composed of water, amorphous silica, a source for tetrahedral framework atoms other than Si, a structure directing organic template, and sometimes a mineralizing agent, such as NaOH. This gel is placed in contact with the support in an autoclave, and the time, temperature, and gel composition for crystallization depend on the zeolite. Supports are generally alumina or stainless steel tubes or discs, although other ceramics such as mullite disc can be used.

In hydrothermal synthesis, a zeolite layer is grown onto a porous support which is immersed into an autoclave filled with the synthesis gel or solution. Syntheses are usually carried out at high temperatures around 150-200°C. A polycrystalline zeolite layer forms on the support and this acts as the separating layer. The non-uniform synthesis conditions may result in a non-uniform membrane thickness due to settling of crystals from the bulk and also unwanted phases might form (Caro, Noack, Kolsch, and Schafer, 2000)

Seed crystals are sometimes added to the support prior to the crystallization step to provide sites for zeolite growth and improve control of crystal growth. Using seed crystals is referred to as two-step crystallization. This technique has been used to prepare oriented zeolite membranes, which have increased fluxes by aligning pores in a desired direction (Lai et al., 2002), and to prepare the thin membranes that were mentioned previously. Cationic polymers on the support surface (Hedlund et al., 2002), dip coating (Xiao et al., 2011), and covalent linking (Ha, Lee, Lee, and Yoon, 2000) have increased seed crystal adherence and improved membrane quality.

If template molecules are used during crystallization, they occupy the zeolite pores and small non-zeolite pores in the intercrystalline boundaries. One method to check membranes for large defects is to measure N<sub>2</sub> permeation while the template is in place; if no large defects are present, the membranes are impermeable to N<sub>2</sub>. Successive layers are often crystallized to eliminate defects significantly larger than the zeolite pores. The template is then removed from the membrane pores by calcinating the membrane at temperatures at about 450°C to combust the organic molecules. The temperature required for this process depends on the zeolite and the template used in

synthesis. Even though zeolites are stable at high temperature, care must be taken when calcinating the membranes because the thermal expansion coefficients of zeolites are usually different from that of the support. Ideally, membranes have a low defect concentration to obtain high selectivities, are as thin as possible to obtain high fluxes, and are reliably reproducible. Because they are polycrystalline, however, eliminating every defect or non-zeolite pore is not possible. Proper synthesis techniques reduce the number of non-zeolite pores.

### **1.2.2 Membranes characterization**

Zeolite membranes used in pervaporation measurements have been characterized using some of the methods described below. Zeolite crystal size and shape, and membrane thickness on top of the support are measured with scanning electron microscopy (SEM). Membranes ranging from 0.5  $\mu\text{m}$  to approximately 500  $\mu\text{m}$  thickness have been reported. In addition, SEM gives a qualitative idea of layer uniformity and continuity. Zeolite framework structure and crystallinity are typically determined using X-ray diffraction (XRD).

Zeolite composition is measured with inductively coupled plasma optical emission spectroscopy (ICP-OES) or energy dispersive X-ray spectroscopy (EDX). The surfaces of flat membranes are sometimes analyzed without damaging the membranes, but tubular and monolithic membranes must be broken to carry out these measurements. Zeolite powders that form during membrane synthesis can be analyzed with XRD and ICP, and though these crystals have been shown to be similar to those in the membranes, this is not a direct measure of the membrane. Gas permeation is also a common method of membrane characterization. Ideal selectivity is defined as the ratio of single-gas permeances, and is often used as an indication of membrane quality.

Permeation depends on both adsorption and diffusion, but molecules close to or larger than the zeolite pore size have difficulty entering zeolite channels.

Zeolite membranes used for the separation of gas mixtures, separation of mixtures of hydrocarbons and light gases have been widely studied. Zeolite membranes are also used for separation of liquid mixtures by pervaporation which is a membrane based separation technology. Organic/organic separations, organic/water separations and isomer separations are all accomplished by using zeolite membranes in pervaporation applications.

## **1.3 Pervaporation**

### **1.3.1 Introduction**

Pervaporation is a membrane based separation process to separate liquid mixtures. Figure 1.3 shows a schematic representation of a simple pervaporation unit. The feed side is kept at atmospheric pressure while the permeate side is kept under vacuum to provide the driving force for permeation. The vacuum is established by using a vacuum pump so that the permeate pressure is kept lower than the saturation pressure of the compounds in the mixture at the separation temperature. The permeate stream, rich in the preferentially permeating component, is condensed in the condenser. The retentate stream which is rich in non-preferentially permeating component is either recycled back or used in another process (Bowen, Noble, and Falconer, 2004).

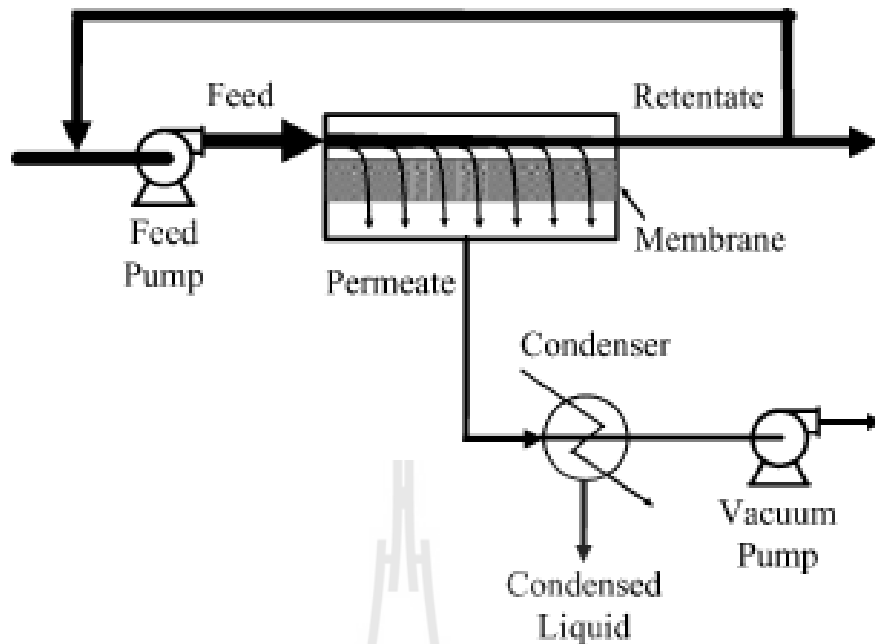


**Figure 1.3** Schematic representation of a typical experimental set up for pervaporation.

Pervaporation involves the following steps: selective sorption into the membrane on the feed side; selective diffusion through the membrane and desorption into a vapor phase on the permeate side.

Pervaporation allows separation of mixtures that are difficult to separate by more conventional techniques like distillation, extraction and sorption. Pervaporation is used to remove a small amount of a liquid sample from a mother liquid sample. Pervaporation is an attractive separation technology when the liquid mixture exhibits an azeotropic composition where distillation cannot be used. Pervaporation is also advantageous for separation of close-boiling mixtures. However, it may not be advantageous to use pervaporation for the complete separation.

Pervaporation is applied for: dehydration applications (removal of water from organic solvents); removal of volatile organic compounds from water; alcohols

from fermentation broths, volatile organic contaminants from waste water, removal of flavor and aromatic compounds, removal of phenolics compounds, polar/non-polar separations; alcohols/aromatics (methanol/toluene), alcohols/aliphatics (ethanol/hexane), alcohols/ethers (methanol/methyl *t*-butyl ether), aliphatics/aromatics (cyclohexane/benzene, hexane/toluene); and isomers (xylene isomers).

The separation performance of zeolite membranes can be described in terms of permeation flux ( $J$ ) and separation factor ( $\alpha$ ) shown below:

$$J = m/At, \alpha_{A/B} = (y_A/y_B) / (x_A/x_B)$$

Where  $m$  is the mass of permeate collected over a period of time ( $t$ ),  $A$  is the effective membrane area for permeation, and  $x_A$ ,  $x_B$ ,  $y_A$  and  $y_B$  denote the mass fractions of components A (ethanol) and B (water) at the feed and permeate sides, respectively.

A good quality membrane is expected to have a high selectivity in combination with high flux. Usually, the selectivity is increased by increasing membrane thickness since a thicker membrane can be more effective to cover defects in zeolite films but the additional resistance to transport reduces the permeability. Defect free thin films are required for industrial applications.

Separation by MFI membranes is based on preferential adsorption of certain molecules rather than molecular sieving. In the case of organic/water separations, both organic and water molecules have sizes smaller than pore size of MFI. Although diffusion would seem to favor water permeation since water molecules have smaller sizes, hydrophobic effects dominate by preferentially adsorbing the organic compounds (Jia and Murad, 2006). Therefore, the permeate side of the MFI membrane is enriched by organic molecules.

### 1.3.2 Factors affecting pervaporation performance of MFI membranes

(a) Feed temperature on pervaporation flux and selectivity is widely studied in literature. An increase in flux is observed with increasing temperature (Bowen, Kalipcilar, and Falconer, 2003). Transport through zeolite pores takes place by two mechanisms: adsorption and diffusion. For pervaporation applications, an increase in temperature increases diffusion and therefore the flux. Since coverages still remain high at high temperatures, diffusion effect dominates. Diffusion increases more than adsorption decreases and fluxes increase with increasing temperature.

With increasing temperature, the selectivities may tend to increase (Tuan, Li, Falconer, and Noble, 2002) or decrease (Lin, Kita, and Okamoto, 2001). A decrease in selectivity for an organics/water mixture with temperature is due to an increase in diffusion of water molecules together with a decrease in organic coverage. The increase in selectivity with temperature is due to the increase in organic diffusion rate compensating the decrease in adsorption coverage.

(b) Feed concentration: For pervaporation of organics/water mixtures, an increase in organic concentration increases both the organic flux and total flux (Sano, Ejiri, Yamada, Kawakami, and Yanagiishita, 1997 and Nomura, Bin, and Kakao, 2002) since organics preferentially permeate through MFI pores.

The separation factor on the other hand usually decreases with increasing organic concentration. The separation factor is a ratio of two ratios; the increase in the ratio in the denominator compensates the increase in numerator, yielding a decrease in separation factor. The increased feed concentration compensates the increase in permeate concentration resulting in lower separation factors.

(c) Permeate pressure: An increase in permeate pressure would decrease the permeate flux. The pervaporation pressures at the permeate side are usually around 0.3-0.4 kPa. The feed pressure has no effect on pervaporation fluxes since pressure has no significant effect on adsorption and permeation of liquid mixtures.

(d) The support material of the membrane influences the separation factors in pervaporation. It is observed that membranes prepared on stainless steel supports exhibit much higher separation factors than the ones prepared on alumina supports (Sano, Kasuno, Takeda, Arazaki, and Kawakami, 1997). For membranes prepared on alumina supports, although no aluminum source is used in the synthesis solution due to aluminum leaching from support; aluminum incorporates into the zeolite framework. When aluminum incorporates into the framework in place of silica, a charge balancing cation is required since aluminum is trivalent. The negatively charged framework and positively charged cations result in electrostatic poles attracting polar molecules. The aluminum incorporation to the framework increases the hydrophilicity of the zeolite, decreasing the separation factor for organic/water mixtures.

The separation factors and fluxes for MFI membranes are not enough to be commercialized for pervaporation applications. Thus, the significance of this research is going on to improve the separation properties of these membranes for liquid mixtures. Thin membranes with high separation factors and fluxes are desired for pervaporation applications.

### **1.3.3 Non-zeolite pores**

Polycrystalline zeolite membranes, however, contain transport pathways in intercrystalline regions, or non-zeolite pores (Figure 1.4). The synthesis procedure,

the type of zeolite, and the calcination conditions affect the number and size of non-zeolite pores. Defects on support surfaces could also be caused by some of the non-zeolite pores present in zeolite membranes. Molecules in non-zeolite pores have different adsorption and diffusion properties from those in zeolite pores. The differences, however, are difficult to quantify because of irregularities in the shape and size of non-zeolite pores. Usually, only non-zeolite pores that are larger than the zeolite pores are considered, but non-zeolite pores have a size distribution, and pores smaller than the zeolite pores may also affect flux and selectivity.

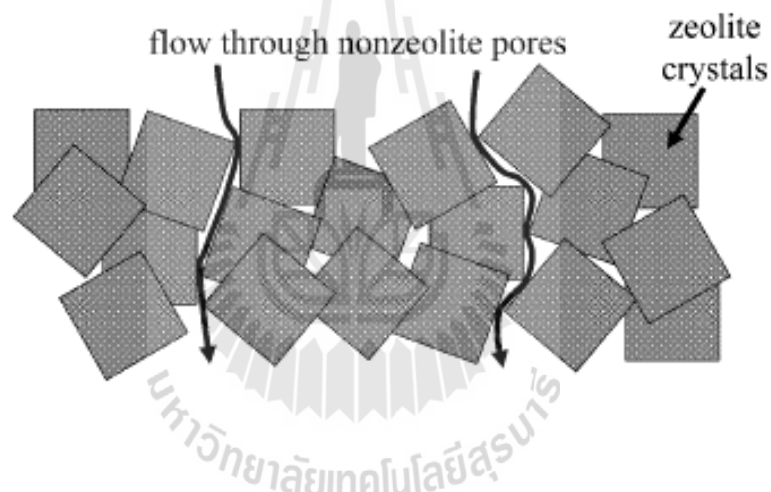


**Figure 1.4** Representation of non-zeolite pores in the intercrystalline boundaries of a zeolite membrane layer.

Non-zeolite pores that are larger than zeolite pores are usually detrimental to the membrane selectivity. Some molecules have difficulty passing each other in zeolite pores, and a larger, slower molecule, such as ethanol, can inhibit diffusion of a smaller, faster molecule, such as H<sub>2</sub>O (Figure 1.5a).

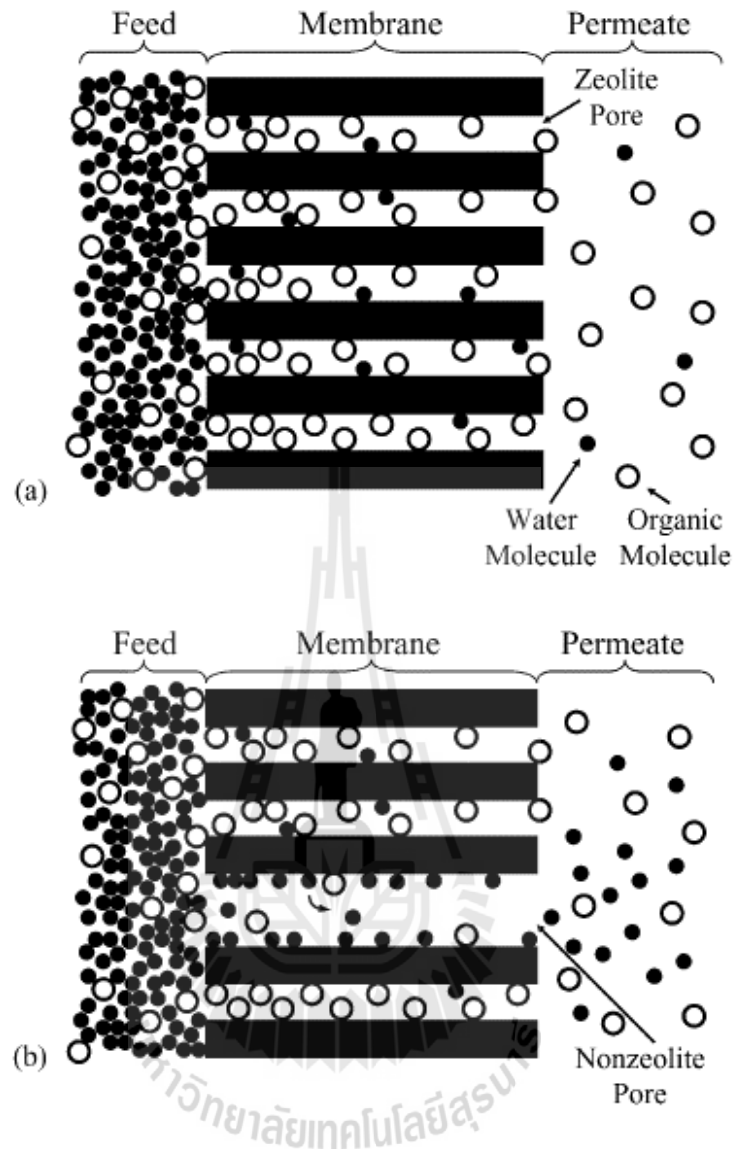


**Figure 1.5** Representation of transport of an organic/water mixture through: (a) hydrophobic zeolite membrane, (b) hydrophobic zeolite membrane containing non-zeolite pores.

A larger, non-zeolite pore, however, allows the faster molecule to pass the slower molecule (Figure 1.5b). In addition, silanol groups in non-zeolite pores are hydrophilic. Both of these non-zeolite pore properties should reduce the organic/H<sub>2</sub>O selectivity of a hydrophobic zeolite membrane.

Presence of non-zeolite pores in the zeolite films has a significant effect on pervaporation flux and separation factor. The Si-OH groups in non-zeolite pores introduce hydrophilic properties to the zeolite (Sano, Kasuno, Takeda, Arazaki, and Kawakami, 1997). Takaba, Koyama, and Nakao (2000) reported a molecular simulation study of ethanol removal from water by a single silicalite crystal. Although no water permeated through the zeolite pores, there were adsorbed water molecules on silanol groups. Presence of silanol groups in non-zeolite pores decreases the separation factor in MFI membranes.

#### 1.4 References

- Ahunbay, M. G., Karvan, O., and Erdem-Senatarlar, A. (2008). MTBE adsorption and diffusion in silicalite-1. **Microporous and Mesoporous Materials**. 115: 93-97.
- Argauer, R. J., and Landolt, G. R. (1972). **US Patent 3702886**. Mobil Co.
- Ban, T., Mitaku, H., Suzuki, C., Matsuba, J., Ohya, Y., and Takahashi, Y. (2005). Crystallization and crystal morphology of silicalite-1 prepared from silica gel using different amines as a base. **Journal of Crystal Growth**. 274: 594-602.
- Bowen, T. C., Kalipcilar, H., Falconer, J. L., and Noble, R. D. (2003). Pervaporation of organic/water mixtures through B-ZSM-5 zeolite membranes on monolith supports. **Journal of Membrane Science**. 215: 235-247.
- Bowen, T. C., Noble, R. D., and Falconer, J. L. (2004). Fundamentals and applications of pervaporation through zeolite membranes. **Journal of Membrane Science**. 245: 1-33.

- Burkett, S. L., and Davis, M. I. (1994). Mechanism of structure direction in the synthesis of pure-silica zeolites. 1. Synthesis of TPA/Si-ZSM-5. **Chemistry of Materials**. 7: 920-928.
- Caro, J., Noack, M., Kolsch, P., and Schafer, R. (2000). Zeolite membrane-state of their development and perspective. **Microporous and Mesoporous Materials**. 38: 3-24.
- Chang, C. D., and Bell, A. T. (1991). Studies on the mechanism of ZSM-5 formation. **Catalysis Letters**. 8: 305-316.
- Chen, H., Li, Y., and Yang, W. (2007). Preparation of silicalite-1 membrane by solution-filling method and its alcohol extraction properties. **Journal of Membrane Science**. 296: 122-130.
- Choudhary, V. R., and Akolekar, D. B. (1988). Crystallization of silicalite-factors affecting its structure, crystal size and morphology. **Materials Chemistry and Physics**. 20: 299-308.
- Cizmek, A., Subotica, B., Kralj, D., Babic-Ivancic, V., and Tonejc, A. (1997). The influence of gel properties on the kinetics of crystallization and particulate properties of MFI-type zeolites. I. The influence of time and temperature of gel ageing on the particulate properties of silicalite-1 microcrystals. **Microporous Materials**. 12: 267-280.
- Coker, E. N., and Jansen, J. C. (1998). Approaches for the synthesis of ultra-large and ultra-small. **Zeolite Crystals Molecular Sieves**. 1: 121-155.
- Davood, V., Ali, A. M., Kamal, M. S., and Mahdi, K. M. (2005). Synthesis of hydrophobic silicalite adsorbent from domestic resources: The effect of

- alkalinity on the crystal size and morphology. **Iranian Journal of Chemistry and Chemical Engineering**. 24: 9-14.
- Delgado, J. A., Maria, A., Sotelo, J. L., Vicente, I., Garcia, A., and Rolda, A. (2012). Separation of ethanol–water liquid mixtures by adsorption on silicalite. **Chemical Engineering Journal**. 180: 137-144.
- Dey, K. P., Ghosh, S., and Naskarn, M. K. (2013). Organic template-free synthesis of ZSM-5 zeolite particles using rice husk ash as silica source. **Ceramics International**. 39: 2153-2157.
- Ha, K., Lee, Y. J., Lee, H. J., and Yoon, K. B. (2000). Facial assembly of zeolite monolayers on glass, silica, aluminar, and other zeolites using 3-halopropylsilyl reagents as covalent linkers. **Advanced Materials**. 12: 1114-1117.
- Hedlund, J., Sterte, J., Anthonis, M., Bons, A. J., Carstensen, B., Corcoran, N., Cox, D., Deckman, H., Gijst, W. D., de Moor, P. P., Lai, F., McHenry, J., Mortier, W., Reinoso, J., and Peeters, J. (2002). High-flux MFI membranes, **Microporous and Mesoporous Material**. 52: 179-189.
- Jia, W., and Murad, S. (2006). Molecular dynamics simulation of pervaporation in zeolite membranes. **Molecular Physics**. 104: 3033-3043.
- Kalpathy, U., Proctor, A., and Shultz, J. (2000). A simple method for production of pure silica from rice hull ash. **Bioresource Technology**. 73: 257-262.
- Kalpathy, U., Proctor, A., and Shultz, J. (2002). An improved method for production of silica from rice hull ash. **Bioresource Technology**. 85: 285-289.
- Kirschhock, C. E. A., Ravishankar, R., Verspeurt, F., Grobet, P. J., Jacobs, P. A., and Martens, J. A. (1999). Identification of precursor species in the formation of

- MFI zeolite in the TPAOH-TEOS-H<sub>2</sub>O system. **The Journal of Physical Chemistry B**. 103: 4965-4971.
- Kokotailo, G. T., Lawton, S. L., Olson, D. H., and Meier, W. M. (1978). Structure of synthetic zeolite ZSM-5. **Nature**. 27: 437-438.
- Kordatos, K., Gavela, S., Ntziouni, A., Pistiolas, K. N., Kyritsi, A., and Kasselouri-Rigopoulou, V. (2008). Synthesis of highly siliceous ZSM-5 zeolite using silica from rice husk ash. **Microporous and Mesoporous Materials**. 115: 189-196.
- Korelskiy, D., Leppajarvi, T., Zhou, H., Grahn, M., Tanskanen, J., and Hedlund, J. (2013). High flux MFI membranes for pervaporation. **Journal of Membrane Science**. 427: 381-389.
- Lai, Z. P., Bonilla, G., Diaz, I., Nery, J. G., Sujaoti, K., Amat, M. A., Kokkoli, E., Terasaki, O., Thompson, R. W., Tsapatsis, M., and Vlachos, D. G. (2002). Microstructure optimization of a zeolite membrane for organic vapor separation. **Science**. 300: 456-460.
- Lin, X., Chen, X., Kita, H., and Okamoto, K. I. (2003). Synthesis of silicalite tubular membranes by in situ crystallization. **American Institute of Chemical Engineers**. 49: 237-247.
- Lin, X., Kita, H., and Okamoto, K. I. (2001). Silicalite membrane preparation, characterization and separation performance. **Industrial & Engineering Chemistry Research**. 40: 4069-4078.
- Liu, Q., Noble, R. D., Falconer, J. L., and Funke, H. H. (1996). Organics/water separation by pervaporation with a zeolite membrane. **Journal of Membrane Science**. 117: 163-174.

- Mansoor, K., and Toraj, M. (2007). Synthesis of MFI zeolite membranes for water desalination. **Desalination**. 206: 547-553.
- Martin, F. M. (1991). Chapter 11 diffusion in zeolite molecular sieves. **Studies in Surface Science and Catalysis**. 58: 391-433.
- Matsuda, H., Yanagishita, H., Negishi, H., Kitamoto, D., Ikegami, T., Haraya, K., Nakane, T., Idemoto, Y., Koura, N., and Sano, T. (2002). Improvement of ethanol selectivity of silicalite membrane in pervaporation by silicone rubber coating. **Journal of Membrane Science**. 210: 433-437.
- Mintova, S., and Valtchev, V. (2002). Effect of the silica source on the formation of nanosized silicalite-1: An in situ dynamic light scattering study. **Microporous and Mesoporous Materials**. 55: 171-179.
- Mosungnoen, W., and Wada, S. (2007). Effect of impurities on the amorphous to cristobalite transformation of rice husk silica. In **The 2nd Work Shop on Rice Husk and Rice Husk Silica**. National Metal and Materials Technology Center (MTEC) and Research Unit of Advanced Ceramics, Bangkok: Chulalongkorn University.
- Noack, M., Kolsch, P., Schafer, R., and Toussaint, P. (2002). Molecular sieve membranes for industrial application: Problems, progress, solutions. **Chemical Engineering & Technology**. 25: 221-230.
- Nomura, M., Bin, T., and Nakao, S. (2002). Selective ethanol extraction from fermentation broth using a silicalite membrane. **Separation and Purification Technology**. 27: 59-66.

- Oumi, Y., Miyajima, A., Miyamoto, J., and Sano, T. (2002). Binary mixture adsorption of water and ethanol on silicalite. **Studies in Surface Science and Catalysis**. 142: 1595-1602.
- Panpa, W., and Jinawath, S. (2009). Synthesis of ZSM-5 zeolite and silicalite from rice husk ash. **Applied Catalysis B: Environmental**. 90: 389-394.
- Rawtani, A. V., and Rao, M. S. (1989). Synthesis of ZSM-5 zeolite using silica from rice husk ash. **Industrial & Engineering Chemistry Research**. 28: 1411-1414.
- Sano, T., Ejiri, S., Yamada, K., Kawakami, Y., and Yanagiishita, H. (1997). Separation of acetic acid-water mixtures by pervaporation through silicalite membrane. **Journal of Membrane Science**. 123: 225-233.
- Sano, T., Kasuno, T., Takeda, K., Arazaki, S., and Kawakami, Y. (1997). Sorption of water vapor on HZSM-5 type zeolites. **Studies in Surface Science and Catalysis**. 105: 1771-1778.
- Shao, C., Li, X., Qiu, S., Xiao, F., and Terasaki, O. (2000). Size-controlled synthesis of silicalite-1 single crystals in the presence of benzene-1,2-diol. **Microporous and Mesoporous Materials**. 39: 117-123.
- Shirazi, L., Jamshidi, E., and Ghasemi, M. R. (2008). The effect of Si/Al ratio of ZSM-5 zeolite on its morphology, acidity and crystal size. **Crystal Research and Technology**. 43: 1300-1306.
- Takaba, H., Koyama, A., and Nakao, S. (2000). Dual ensemble monte carlo simulation of pervaporation of an ethanol/water binary mixture in silicalite membrane based on a Lennard-Jones interaction model. **The Journal of Physical Chemistry B**. 104: 6353-6359.

- Tuan, V. A., Li, S., Falconer, J. L., and Noble, R. D. (2002). Separating organics from water by pervaporation with isomorphously-substituted MFI zeolite membranes. **Journal of Membrane Science**. 196: 111-123.
- Wan, C. W., Louisa, T. Y., Prudence, P. S., Carlos, T. A., and King, L. Y. (2001). Effects of synthesis parameters on the zeolite membrane morphology. **Journal of Membrane Science**. 193: 141-161.
- Xiao, W., Yang, J., Lu, J., and Wang, J. (2009). A novel method to synthesize high performance silicalite-1 membrane. **Separation and Purification Technology**. 67: 58-63.
- Xiao, W., Chen, Z., Zhou, L., Yang, J., Lu, J., and Wang, J. (2011). A simple seeding method for MFI zeolite membrane synthesis on macroporous support by microwave heating. **Microporous and Mesoporous Materials**. 142: 154-160.
- Yalcin, N., and Sevinc, V. (2001). Studies on silica obtained from rice husk. **Ceramics International**. 27: 219-224.
- Yang, R., Meng, F., Wang, X., and Wang, Y. (2011). Influence of Na<sup>+</sup> on the synthesis of silicalite-1 catalysts for use in the vapor phase Beckmann rearrangement of cyclohexanone oxime. **Frontiers of Chemical Science and Engineering**. 5(4): 401-408.
- Zhang, X., Zhu, M., Zhou, R., Chen, X., and Kita, H. (2011). Synthesis of silicalite-1 membranes with high ethanol permeation in ultradilute solution containing fluoride. **Separation and Purification Technology**. 81: 480-484.

## CHAPTER II

### LITERATURE REVIEWS

#### 2.1 Silicalite synthesis

Synthesis of Silicalite or ZSM-5 from low cost silica sources becomes important for industrial production. Rice husk (RH) is an abundantly available agricultural waste material containing maximum amount of siliceous ash. The major constituents of RH are cellulose, lignin and ash varying with the variety, climate and geographic location of growth. Burning of rice husk in air produces rice husk ash containing 85-98% silica (Kordatos et al., 2008) and some amount of organics, alkali oxides and impurities, but with an appropriate washing with dilute acid leaching and burning at 700°C of the husk, the ash can contain >98% (w/w) silica (Yalcin and Sevinc, 2001). According to Mosungnoen and Wada (2007) the amount of amorphous silica in Thai rice husk is about 20% (w/w). RH can be used as an alternative cheap source of amorphous silica. There is a significant interest in its use in the preparation of zeolites due to widespread industrial use of zeolites in separation processes as sorbents (Martin, 1991). Efforts have been made to use RHA as a silica source for the synthesis of ZSM-5 by hydrothermal method.

Rawtani and Rao (1989) synthesized ZSM-5 zeolite from the Na-TPA cation system for the first time using silica from RHA. The molar ratio of  $\text{SiO}_2/\text{Al}_2\text{O}_3$  in the husk was 24.88. Pure ZSM-5 in the obtained final products contained the mole percent of  $\text{SiO}_2$  varied from 70% to 80% and  $(\text{TPA}, \text{Na})_2\text{O}$  from 20% to 35%.

Mohamed, Zidan, and Thabet (2008) synthesized ZSM-5 by hydrothermal method with different Si/Al ratios, 40 and 80 from rice husk ash as silica source. Silica synthesized from raw rice husks through submission to consecutive chemical treatment using NaOH and HCl solution. Transition metal oxides (V, Co) were incorporated with ZSM-5 by impregnation and implication for photocatalytic degradation catalysts.

Kordatos et al. (2008) studied a simple synthesis route that demonstrated towards the efficient production of ZSM-5. RHA was utilized as an alternative silica source for the synthesis of ZSM-5. The reaction of RHA with the organic template TPABr at low temperature and under atmospheric pressure led to the successful transformation of the crystalline ash to ZSM-5. The product was a microporous material having high specific surface area of  $397 \text{ m}^2\text{g}^{-1}$ .

In the study of Panpa and Jinawath (2009), RHA as silica source was prepared from local rice husk. RHA was precleaned and properly heat treated to produce high purity amorphous  $\text{SiO}_2$  for use in the synthesis of ZSM-5 zeolite and silicalite by hydrothermal treatment ( $150^\circ\text{C}$ ) of the precursor gels (pH 11) under autogenous pressure in a short reaction time (4-24 h). A wide range of  $\text{SiO}_2/\text{Al}_2\text{O}_3$  molar ratios (30-2075) and a small template content were employed to fully exploit the potential of rice husk ash.

Naskar, Kundu, and Chatterjee (2012) report a facial and single-steps hydrothermal method for the synthesis of ZSM-5 zeolite powders through the in situ extraction of silica as silicate from RHA. The RHA have  $\text{SiO}_2$  content of 95.45 wt% by its calcination at  $700^\circ\text{C}$  for 6 h in air atmosphere. The molar composition was  $\text{Na}_2\text{O}:100\text{SiO}_2:\text{Al}_2\text{O}_3:20\text{TPAOH}:4000\text{H}_2\text{O}$  and a simple hydrothermal condition at  $130^\circ\text{C}$  to  $170^\circ\text{C}$ . They proposed that in highly alkaline medium, in the present of NaOH

and TPAOH, silica of RHA was converted to silicate ( $M_2O \cdot xSiO_2$ ). The silicate and aluminate ( $AlO_2^-$ ) species in solution self-assembled around  $TPA^+$  cation and polycondensed, leading to the inorganic channel which resembled the molecular shape of  $TPA^+$  toward the formation of ZSM-5.

Recently, Dey, Ghosh, and Naskarn (2013) synthesized ZSM-5 zeolite powder using RHA as a silica source and other low cost water-based precursors, in the absence of any organic template following a single step hydrothermal process at relatively low temperature ( $150^\circ C$ ) under static condition. The BET surface area of powder products was in the range of  $54-78 \text{ m}^2 \text{ g}^{-1}$  and morphology was coffin-shape.

## 2.2 Size-controlled synthesis of silicalite

Because of zeolite specific properties and use for various application such as catalytic processes and adsorption, syntheses of zeolites with various morphologies and sizes have attracted considerable attentions. The range of particle sizes is wide, from colloidal zeolites, a few ten of nm in size, to large crystals in the mm range. Decrease of the crystal size enhances catalytic activity of zeolites in various reactions such as esterification of cyclohexanol with acetic acid (Viswanadham, Kamble, Singh, Kumar, and Dhar, 2009), methanol to propylene reaction (Firoozi, Baghalha, and Asadi, 2009), etc. On the other hand, in the reactions, such as dehydroalkylation of toluene with ethane, in which the shape selectivity needs to be enhanced, zeolite catalysts with relatively large crystal size were preferred (Bresse, Donauer, Sealy, and Traa, 1008).

The optimum compromise between activity and selectivity may depend on both the catalytic process and the type of zeolite used as catalysts. Hence, it is evident that the synthesis also practical importance. However, as crystals of the size in the order of

2  $\mu\text{m}$  and smaller crystals are usually used industrially in order to minimize mass transfer resistance, crystals as large as ten or micrometers limit its application due to diffusion limitation for the bulky molecules to transfer to from the active sites located within the micro pores.

In batch crystallization, crystal size is a function of the ratio between rate of nucleation and rate of growth. Both rates increase with supersaturation, but the exponential law of the nucleation rate rises more sharply than the low-order power law of the growth rate. As a consequence, smaller crystals and rapid syntheses are observed at high supersaturation. The degree of supersaturation of the solution is determined by two main factors are nutrient concentration and temperature. As the nutrient concentration increases, so does the degree of supersaturation, until the formation of an amorphous phase occurs. With the temperature of the system increases, the degree of supersaturation decreases (Coker and Jansen, 1998).

Several parameters (alkalinity, ionic strength, dilution, and temperature) influence silicate solubility and modify the concentration levels in the synthesis system. The presence of an amorphous gel also affects diffusion processes in the mother solution, and stirring effectively modifies crystallization kinetics (Hill, Kinson, and Seddon, 1988; Beyer, Karge, Kiricsi, and Nagy, 1995).

Hill, Kinson, and Seddon (1988) studies the influence of sodium chloride, nucleation temperature and alkalinity on crystal size and product morphology of silicalite. Silicalite prepared from gel composition  $1.04\text{Na}_2\text{O} : 2.95\text{Pr}_4\text{NBr} : 24.6\text{SiO}_2 : 1000\text{H}_2\text{O} : 0-48\text{NaCl}$ . The results show that crystals of silicalite can be readily made in a size ranging from about 1  $\mu\text{m}$  to over 20  $\mu\text{m}$ . A change in silica source from amorphous fumed silica to a commercial gel.

Additionally, They found that silicalite can be made in a range of morphology by variations in salt content as well as variation in alkalinity. Addition of sodium chloride and increasing alkalinity produce crystals with less intergrowth. Increasing the salt content of the gel or increasing the alkalinity is seen to produce crystal with fewer daughters. Nucleating the gel at 90°C before crystallization significantly reduces crystal size.

Shao, Li, Qiu, Xiao, and Terasaki (2000) adding benzene-1,2-diol as complex agent for silicon into the system:  $\text{SiO}_2:\text{TPABr}:\text{NaOH}:\text{R}:\text{H}_2\text{O}$ , R is benzene-1,2-diol. The single crystals of zeolites silicalite with different sized ranging from  $9 \times 3 \times 2 \mu\text{m}$  to  $165 \times 30 \times 30 \mu\text{m}$  were obtained. Experimental showed that crystals synthesized in the presence of benzene-1,2-diol have a much larger size and better morphology than those synthesized in the absence of benzene-1,2-diol.

Song, Justice, Jones, Grassian, and Larsen (2004) synthesized silicalite-1 powders with crystal sizes ranging from 20 to 1000 nm by systematically varying synthesis gel composition, pressure, temperature, and time duration. Silicalite-1 samples were synthesized from clear gel solutions of  $\text{TPAOH}:\text{NaOH}:\text{TEOS}:\text{H}_2\text{O}:\text{EtOH}$ . The effect of crystal size on the physical properties of crystals is observed, including a large increase of both total and external surface area when crystal size decreases. The relationship between particle size and external surface area was modeled by assuming a cubic crystal geometry. The nanosized silicalite samples with crystal sizes less than 100 nm have a higher adsorption capacity for toluene, showing promising potential for its application in volatile organic compound removal.

Davood, Ali, Kamal, and Mahdi (2005) synthesized Silicalite-1 by hydrothermal method at a pH of about 10 from reaction mixture consist of water, amorphous silica and aquaternary ammonium compound. Pure silicalite type zeolite was obtain from the reaction mixture with molar ratio  $(1-5)\text{Na}_2\text{O}:(50-60)\text{SiO}_2:(1-2\text{TPABr}):(600-770)\text{H}_2\text{O}$ . They also investigated the influence of alkalinity percent in the starting gel mixture on the crystal shape and size. It seems that decreasing of alkalinity ( $\text{Na}_2\text{O}$  wt%) grows the particle size. The results shown that the morphology of crystals depend on alkali metal cations concentration could have three different shapes as cyclic, ovate and prolonged ovate alpha quartz and coffin-silicalite shapes.

Hu, Liu, Zhang, Ren, and Tang (2009) used microwave-assisted hydrothermal synthesis of nanozeolites with controllable size. They successfully prepared silicalite-1, ZSM-5, LTL, BEA and LTA zeolite nanocrystals and studied the effects of the starting gel composition such as water content, alkalinity and ratio of  $\text{SiO}_2/\text{Al}_2\text{O}_3$  ratio on the size of the zeolite nanocrystals. Additionally, effects of hydrothermal synthesis condition as temperature and time have been studied. For nanocrystallized of ZSM-5 in low alkalinity systems, both increasing the alkalinity and decreasing the water content accelerate their nucleation process and thereby result in the decrease of their crystal size. Moreover, the change of  $\text{SiO}_2/\text{Al}_2\text{O}_3$  ratio in the starting gel greatly affects the size of nanozeolite ZSM-5.

Qi, Zhao, Xu, and Li (2011) synthesized small and homogeneous silicalite-1 zeolite by hydrothermal method and study the influences of crystallization time, crystallization temperature, different organic solvents and different TPAOH template concentrations. They found that these parameter have played important roles in controlling size of silicalite-1 zeolite. Short crystallization time as well as low

crystallization temperature, adding organic solvent with large dielectric constant and decreasing TPAOH template concentration can obtain small size particle of silicalite.

Xue, Wang, and He (2012) synthesized ultra-high-silica ZSM-5 zeolites with tunable crystal sizes by using silicalite-1 suspension as seed crystals and a small amount of additional tetraalkylammonium bromide as structure-directing agent, highly crystallized ZSM-5 with  $\text{SiO}_2/\text{Al}_2\text{O}_3$  ratios higher than 100. The crystal sizes could be easily tuned from tens of nanometers to about several micrometers by adjusting the amount of seeding suspension. Seeding suspension synthesized from different silica sources and the additional structure-directing agent may also effect the crystal sizes. When tetraethylammonium bromide was used as additional structure-directing agent, crystals with silica-rich cores were observed. While additional nucleation could be found when tetrapropylammonium bromide was used as auxiliary template.

Sari, Younesi, and Kazemian (2014) synthesized nanosized ZSM-5 zeolite by a hydrothermal method with silica extracted from rice husk, available as an inexpensive local biowaste, and without the use of an extra alumina source. Amorphous silica with purity 88 wt% was extracted from rice husk ash by a suitable alkali solution. The  $\text{SiO}_2/\text{Al}_2\text{O}_3$  molar ratio in extracted silica was 176. The molar composition of initial solution is  $0.504\text{Na}_2\text{O}:176\text{Al}_2\text{O}_3:\text{SiO}_2:0.215\text{TPAOH}:16.168\text{H}_2\text{O}$ , crystallization time and temperature that use for synthesis were 96 h and  $150^\circ\text{C}$ . Crystallinity percentages of nanosized ZSM-5 was 89.56 with specific surface area of  $353.5\text{ m}^2\text{g}^{-1}$  and average crystal size was 25.1 nm.

### 2.3 Silicalite membrane and pervaporation

The most common studied separation by MFI membranes is ethanol/water separation. Ethanol removal from fermentation broths is essential for production of biofuel. After fermentation is complete, ethanol purification is required. Purification separates ethanol from other components of fermentation; of these components, water has the largest composition. This step is necessary because fuel purposes require very pure ethanol to properly blend with gasoline (Nomura, Bin, and Kakao, 2002).

Liu, Noble, Falconer, and Funke (1996) synthesized silicalite membranes on alumina supports by hydrothermal treatment. They obtained low separation factors and fluxes for ethanol/water separation. The separation factor for methanol/water was improved from 7 to 15 when membrane was synthesized on a stainless steel support. There are also studies to improve the hydrophobicity of the MFI membranes to increase the separation factor.

Li, Yong, Weizhong, and Changgeng (1998) prepared ZSM-5 type zeolite membranes using a new process on the outer surface of the synthesis sol on ceramic tube. The new process involves the procedures of sol preadsorption and repeated crystallization. The results indicate that using the addition procedure of sol preadsorption favors the formation of zeolite membranes in crystal intergrowth. The influence of the alkalinity of the synthesis sol on the formation of the membrane show that lower alkalinity can form the zeolite membrane in highly interlocking large crystals. When combining both the sol preadsorption and repeating crystallization for four times, a continuous densified ceramic-zeolite membrane with thickness of about 25  $\mu\text{m}$ .

Lai and Gavalas (2000) reported the preparation of supported ZSM-5 membrane using a TPA-free synthesis gel. The membrane were prepared by hydrothermal reaction on asymmetric  $\text{Al}_2\text{O}_3$  tubular supports with the gel composition  $\text{SiO}_2:0.0125\text{Al}_2\text{O}_3:0.2675\text{Na}_2\text{O}:46\text{H}_2\text{O}$ . In the absence of organic cations,  $\text{Na}^+$  function of structure directing species in zeolitization and alkalinity has multifaceted effects on TPA<sup>+</sup>-free synthesis. The results shown that crystal intergrowth improving with increasing alkalinity, but when the  $\text{NaOH}:\text{SiO}_2$  ratio reached 0.6 amorphous material was formed on the support tube. In the studied of variation of the aluminum content, increasing the aluminum content was found to promote the intergrowth of adjacent crystals.

Raileanu et al. (2002) prepared alumina supported silicalite membranes by sol-gel hydrothermal method. They studied the influence of the raw materials used as  $\text{SiO}_2$  source, the temperature of the thermal treatment and the presence of the ceramic support on the crystallization of zeolite. The results shown that the  $\text{SiO}_2$  silica source had a significant effect on the final zeolite. The used of colloidal silica sol as  $\text{SiO}_2$  source in the synthesis led to ZSM-11 crystals, while the sodium silicate solution produced the ZSM-5 type. It is widely recognized fact that the moles of the  $\text{SiO}_2$  from different sources are not equivalent due to their different polymerization degree. The presence of the alumina support influences the crystallization process of ZSM-5, as it improves nucleation and the ordering of the crystals.

Lin, Chen, Kita, and Okamoto (2003) reported the best membrane for ethanol/water separation with a flux of  $0.9 \text{ kg/m}^2\cdot\text{h}$  and a separation factor of 106. The membranes were prepared by in situ crystallization and they concluded that in situ crystallization yielded better membranes when compared with seeding followed by

crystallization. In the study membranes were also prepared on alumina supports and lower separation factors were observed. It was concluded that the silicalite membranes with higher Si/Al ratio showed better separation factors and fluxes.

**Table 2.1** Separation factors and fluxes for the MFI membranes.

Reference	Membrane/ (Thickness)	Support	Feed	Separation factor	Flux (kg/m <sup>2</sup> .h)	Temperature (°C)
Liu et al. (1996)	Silicalite (NA)	Alumina	(9.7 wt%) EtOH/H <sub>2</sub> O	12	0.1	30
Lin et al. (2003)	Silicalite (20-30 μm)	Mullite	(5 wt%) EtOH/H <sub>2</sub> O	106	0.9	60
Matsuda et al. (2002)	Silicalite (NA)	Stainless Steel	(4 wt%) EtOH/H <sub>2</sub> O	125	0.14	30
Chen et al. (2007)	Silicalite (20 μm)	Porous silica tube	(3 wt%) EtOH/H <sub>2</sub> O	69	0.87	60
Zhang et al. (2011)	Silicalite (20 μm)	Mullite	(5 wt%) EtOH/H <sub>2</sub> O	60	2.85	60
Korelskiy et al. (2013)	Silicalite (0.5 μm)	Alumina	(10 wt%) EtOH/H <sub>2</sub> O	5	9	60

Zhang, Liu, and Yeung (2006) prepared five silicalite-1 zeolite seeds of around 100 nm, 600 nm, 1.5 μm, 3 μm and 7.5 μm. The preparation of porous alumina supports seeded using slip-casting technique and silicalite membrane regrown by hydrothermal synthesis. They investigated the effects of seed sizes on the formation of seed layers and zeolite membrane. It has been found that seed sizes have important effects on the formation of seed layers that determines the quality of regrown zeolite membrane. The seed layer and the regrown membranes become from smallest seed (100 nm) are most uniform and densest. With the increase of seed size (from 600 nm to 3 μm), the seed

layers and the membranes become coarser and the intergrowth of the membranes becomes poorer. When using zeolite seeds of 7.5  $\mu\text{m}$ , a continuous membrane cannot be obtained because of the formation of an incontinuous seed layer.

Chen, Li, and Yang (2007) synthesized silicalite membranes with new method called “solution filling (SF)” on porous silica tube. The support tubes were filled with mixed solution of water and glycerol before hydrothermal synthesis. It was found that porous silica tube was suitable for the synthesis of high performance silicalite membrane. Total flux and separation factor for ethanol/H<sub>2</sub>O were 0.87 and 69 kg/m<sup>2</sup>.h, respectively.

Soydas, Culfaz, and Kalipcilar (2009) synthesized MFI-Type zeolite membranes by hydrothermal method. A thin layer on macroporous alumina discs coated with 1  $\mu\text{m}$  MFI-type seed crystals as seed. They studied the effect of soda (Na<sub>2</sub>O) on the morphology of the membranes. Soda concentration and the hydroxyl ion concentration was changed between 0.25 to 6.5 mol/mol gel. When used low soda concentrations the crystals forming the layer exhibited mostly (h0h)/c-axis orientation, but at high soda concentrations a membrane layer formed from randomly oriented crystals.

Xiao et al. (2011) prepared thin and defect-free zeolite membranes by effective seeding method and used secondary growth method on macroporous tubular supports. The permeation properties of the as-prepared membranes depend strongly on the seeding method of zeolite crystals during which the whole support surface should be covered uniformly and sufficiently. They explained that the seeding have three step: (a) pre-modified the support surface by hot dip-coating in large seed (1.2  $\mu\text{m}$ ) suspension; (b) rub off the excess large seeds which stick on the support surface;

(c) further modified the support by hot dip-coating in another seed (0.4  $\mu\text{m}$ ) suspension. After the composite seeding process, silicalite-1 membrane was synthesized by microwave heating at 423 K for 2 h using the synthesis solution of  $1\text{SiO}_2:0.3\text{TPAOH}:80\text{H}_2\text{O}:4\text{C}_2\text{H}_5\text{OH}$ . The results showed the as-prepared zeolite membrane was dense and continuous with a thickness of about 4  $\mu\text{m}$ .

Zhang, Zhu, Zhou, Chen, and Kita (2011) synthesized the defect free silicalite membrane on tubular mullite supports in ultradilute solution containing fluoride by hydrothermal synthesis. The flux and separation factor were 2.85 and 60  $\text{kg}/\text{m}^2\cdot\text{h}$ , respectively, for 5 wt% of ethanol/ $\text{H}_2\text{O}$  mixture.

Korelskiy et al. (2013) prepared MFI membrane with a thickness of 0.5  $\mu\text{m}$  on  $\alpha$ -alumina support and separation mixture of 10 wt% ethanol/water by pervaporation. High flux was about 9  $\text{kg}/\text{m}^2\cdot\text{h}$  and separation factor of ca. 5 was obtained.

However, it is very difficult to manufacture defect-free commercial-scale silicalite-1 membranes. On the other hand, silicalite-1 membranes are expected to be more expensive than polymer membranes on a unit area basis. Combining the advantages of inorganic membrane and polymeric membrane for obtaining high ratio of membrane performance/cost, hybrid membranes consisting of silicalite-1 particles dispersed in PDMS have been attracted more and more interest for pervaporation separation of ethanol/water.

Up to now, many researchers have investigated a number of pervaporation membranes for recovery alcohol from fermentation broth as modified zeolite membrane, zeolite-PDMS mixed matrix membranes and so on.

Sano, Hasegawa, Ejiri, Kawakami, and Yanagishita (1995) modified silicalite membranes that prepared on porous stainless-steel supports with silane coupling

reagents (octyltrichlorosilane or octadecyltrichlorosilane). The pervaporation performance of each modified membrane was investigated using an aqueous ethanol solution 5% (v/v). The results found that the ethanol concentration of the permeate through the modified silicalite membrane was markedly increased, indicating that the modification with the silane coupling reagent is very effective for the improvement of the separation performance of the zeolite membrane. The pervaporation performance of unmodified silicalite membrane were 5 and 0.843 kg/m<sup>2</sup>.h for separation factor and flux, respectively. When modified silicalite membrane with octadecyltrichlorosilane its show the highest of separation factor was 45 with flux value 0.133 kg/m<sup>2</sup>.h.

Matsuda et al. (2002) synthesized a silicone-coated silicalite membrane. The silicone was added to fill the non-zeolite pores. A high separation factor of 125 was obtained with a 0.14 kg/m<sup>2</sup>.h flux for the coated membrane. On the other hand the separation factor was 51 for the non-coated membrane synthesized under the same conditions. Silicone coating reduced the flux only with a fraction of 1%.

Zhan, Li, Chen, and Huang (2009) prepared thin-film zeolite-filled silicone/PVDF composite membranes by incorporating zeolite particles into PDMS (poly(dimethylsiloxane)) membrane. The effect of zeolite loading and Si/Al ratio of zeolite particles on pervaporation performance of ethanol/water mixtures was investigated. With the increase of zeolite loading from 10% to 30%, the total flux increased significantly from 0.265 kg/m<sup>2</sup>.h to 0.821 kg/m<sup>2</sup>.h with 5 wt% ethanol feed concentration at 50°C and the separation factor increased from 11.3 to 13.7. The results effect of operation temperature and ethanol feed concentration show that the temperature increased form 40°C to 80°C, the separation factor varied from 12.1 to 13.7

which maintained the maximum value at 50°C, and the total flux increased exponentially from 0.436 kg/m<sup>2</sup>.h to 2.993 kg/m<sup>2</sup>.h with 30% zeolite loading.

Liu, Xiangli, Wei, Liu, and Jin (2011) improved performance of PDMS/Ceramic composite pervaporation membranes. A surface graft/coating approach was developed from homogeneously dispersing ZSM-5 zeolite in PDMS for preparing ZSM-5 filled PDMS mixed matrix/ceramic composite membranes. It was found that surface modification of zeolite particles could highly improve their interaction with PDMS matrix. In the FT-IR analysis and contact angle measurements, the prepared ZSM-5 filled PDMS membranes exhibited less hydroxyl groups and became hydrophobic with increasing zeolite loading. The pervaporation experiment in 5 wt% ethanol/water mixture shown that the homogeneous incorporated ZSM-5 particles improved the selectivity of PDMS membrane and separation factor of surface-modified ZSM-5 filled PDMS membrane increased gradually with zeolite loading. The separation factor reach a maximum of 14 at the zeolite loading 40% with flux 0.408 kg/m<sup>2</sup>.h.

## 2.4 References

- Beyer, H. K., Karge, H. G., Kiricsi, I., and Nagy, J. B. (1995). Studies in surface science and catalysis. **Catalysis by Microporous Materials**. 94: 517-524.
- Bressel, A., Donauer, T., Sealy, S., and Traa, Y. (2008). Influence of aluminum content, crystallinity and crystallite size of zeolite Pd/H-ZSM-5 on the catalytic performance in the dehydroalkylation of toluene with ethane. **Microporous and Mesoporous Materials**. 109: 278-286.

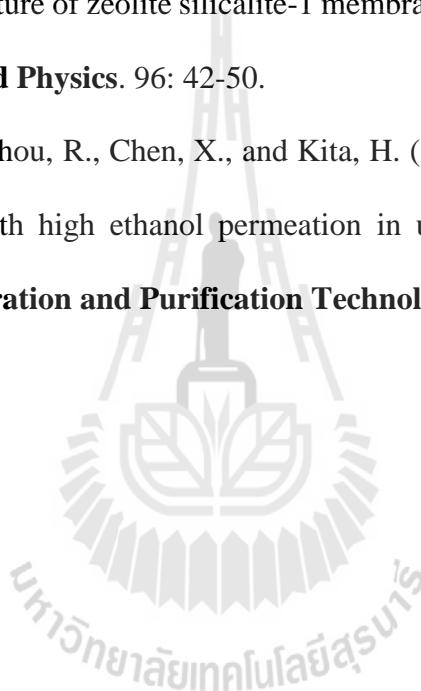
- Chen, H., Li, Y., and Yang, W. (2007). Preparation of silicalite-1 membrane by solution-filling method and its alcohol extraction properties. **Journal of Membrane Science**. 296: 122-130.
- Coker, E. N., and Jansen, J. C. (1998). **Molecular sieves**. Berlin: Springer. pp. 121-155.
- Davood, V., Ali, A. M., Kamal, M. S., and Mahdi, A. M. (2005). Synthesis of hydrophobic silicalite adsorbent from domestic resources: The effect of alkalinity on the crystal size and morphology. **Iranian Journal of Chemistry and Chemical Engineering**. 24(4): 9-14.
- Dey, K. P., Ghosh, S., and Naskarn, M. K. (2013). Organic template-free synthesis of ZSM-5 zeolite particles using rice husk ash as silica source. **Ceramics International**. 39: 2153-2157.
- Firoozi, M., Baghalha, M., and Asadi, M. (2009). The effect of micro and nano particle sizes of H-ZSM-5 on the selectivity of MTP reaction. **Catalysis Communications**. 10: 1582-1585.
- Hill, G. S., Kinson, K., and Seddon, D. (1988). The crystal size and morphology of silicalite as influenced by gel nucleation temperature, alkalinity and sodium chloride concentration. **Australian Journal of Chemistry**. 41: 783-789.
- Hu, Y., Liu, C., Zhang, Y., Ren, N., and Tang, Y. (2009). Microwave-assisted hydrothermal synthesis of nanozeolites with controllable size. **Microporous and Mesoporous Materials**. 119: 306-314.
- Kordatos, K., Gavela, S., Ntziouni, A., Pistiolas, K. N., Kyritsi, A., and Kasselouri-Rigopoulou, V. (2008). Synthesis of highly siliceous ZSM-5 zeolite using silica from rice husk ash. **Microporous and Mesoporous Materials**. 115: 189-196.

- Korelskiy, D., Leppajarvi, T., Zhou, H., Grahn, M., Tanskanen, J., and Hedlund, J. (2013). High flux MFI membranes for pervaporation. **Journal of Membrane Science**. 427: 381-389.
- Lai, R., and Gavalas, G. R. (2000). ZSM-5 membrane synthesis with organic-free mixtures. **Microporous and Mesoporous Materials**. 38: 239-245.
- Li, Y., Yong, S., Weizhong, J., and Changgeng, P. (1998). A novel route of synthesis of ZSM-5 zeolite membranes. **Materials Letters**. 37: 221-226.
- Lin, X., Chen, X., Kita, H., and Okamoto, K. I. (2003). Synthesis of silicalite tubular membranes by in situ crystallization. **American Institute of Chemical Engineers**. 49: 237-247.
- Liu, G., Xiangli, F., Wei, W., Liu, S., and Jin, W. (2011). Improved performance of PDMS/ceramic composite pervaporation membranes by ZSM-5 homogeneously dispersed in PDMS via a surface graft/coating approach. **Chemical Engineering Journal**. 174: 495-503.
- Liu, Q., Noble, R. D., Falconer, J. L., and Funke, H. H. (1996). Organics/water separation by pervaporation with a zeolite membrane. **Journal of Membrane Science**. 117: 163-174.
- Martin, F. M. (1991). Chapter 11 diffusion in zeolite molecular sieves. **Studies in Surface Science and Catalysis**. 58: 391-433.
- Matsuda, H., Yanagishita, H., Negishi, H., Kitamoto, D., Ikegami, T., Haraya, K., Nakane, T., Idemoto, Y., Koura, N., and Sano, T. (2002). Improvement of ethanol selectivity of silicalite membrane in pervaporation by silicone rubber coating. **Journal of Membrane Science**. 210: 433-437.

- Mohamed, M. M., Zidan, F. I., and Thabet, M. (2008). Synthesis of ZSM-5 zeolite from rice husk ash: Characterization and implications for photocatalytic degradation catalysts. **Microporous and Mesoporous Materials**. 108: 193-203.
- Mosungnoen, W., and Wada, S. (2007). Effect of impurities on the amorphous to cristobalite transformation of rice husk silica. In **The 2nd Work Shop on Rice Husk and Rice Husk Silica**. National Metal and Materials Technology Center (MTEC) and Research Unit of Advanced Ceramics, Bangkok: Chulalongkorn University.
- Naskar, M. K., Kundu, D., and Chatterjee, M. (2012). A facial hydrothermal conversion of rice husk ash to ZSM-5 zeolite powders. **Journal of the American Ceramic Society**. 95(3): 925-930.
- Nomura, M., Bin, T., and Nakao, S. (2002). Selective ethanol extraction from fermentation broth using a silicalite membrane. **Separation and Purification Technology**. 27: 59-66.
- Panpa, W., and Jinawath, S. (2009). Synthesis of ZSM-5 zeolite and silicalite from rice husk ash. **Applied Catalysis B: Environmental**. 90: 389-394.
- Qi, J., Zhao, T., Xu, X., and Li, F. (2011). Hydrothermal synthesis of size-controlled silicalite-1 crystals. **Journal of Porous Materials**. 18: 509-515.
- Raileanu, M., Popa, M., Moreno, J. M. C., Stanciu, L., Bordeianu, L., and Zaharescu, M. (2002). Preparation and characterization of alumina supported silicalite membranes by sol-gel hydrothermal method. **Journal of Membrane Science**. 210: 197-207.
- Rawtani, A. V., and Rao, M. S. (1989). Synthesis of ZSM-5 zeolite using silica from rice husk ash. **Industrial & Engineering Chemistry Research**. 28: 1411-1414.

- Sano, T., Hasegawa, M., Ejiri, S., Kawakami, Y., and Yanagishita, H. (1995). Improvement of the pervaporation performance of silicalite membranes by modification with a silane coupling reagent. **Microporous Materials**. 5: 179-184.
- Sari, Z. G. L. V., Younesi, H., and Kazemian, H. (2014). Synthesis of nanosized ZSM-5 zeolite using extracted silica from rice husk without adding any alumina source. **Appl Nanosci**. 5(6): 737-745.
- Shao, C., Li, X., Qiu, S., Xiao, F., and Terasaki, O. (2000). Size-controlled synthesis of silicalite-1 single crystals in the presence of benzene-1,2-diol. **Microporous and Mesoporous Material**. 39: 117-123.
- Song, W., Justice, R. E., Jones, C. A., Grassian, V. H., and Larsen, S. C. (2004). Size-dependent properties of nanocrystalline silicalite synthesized with systematically varied crystal sizes. **Langmuir**. 20: 4696-4702.
- Soydas, B., Culfaz, A., and Kalipcilar, H. (2009). Effect of soda concentration on the morphology of MFI-Type zeolite membranes. **Chemical Engineering Communications**. 196: 182-193.
- Viswanadham, N., Kamble, R., Singh, M., Kumar, M., and Dhar, G. M. (2009). Catalytic properties of nano-sized ZSM-5 aggregates. **Catalysis Today**. 141: 182-186.
- Xiao, W., Chen, Z., Zhou, L., Yang, J., Lu, J., and Wang, J. (2011). A simple seeding method for MFI zeolite membranes synthesis on macroporous support by microwave heating. **Microporous and Mesoporous Materials**. 124: 154-160.
- Xue, T., Wang, Y. M., and He, M. (2012). Synthesis of ultra-high-silica ZSM-5 zeolites with tunable crystal sizes. **Solid State Sciences**. 14: 409-418.

- Yalcin, N., and Sevinc, V. (2001). Studies on silica obtained from rice husk. **Ceramics International**. 27: 219-224.
- Zhan, X., Li, J., Chen, J., and Huang, J. (2009). Peravaporation of ethanol/water mixtures with high flux by zeolite-filled PDMS/PVDF composite membranes. **Chinese Journal of Polymer Science**. 27(6): 771-780.
- Zhang, X., Liu, H., and Yeung, K. L. (2006). Influence of seed size on the formation and microstructure of zeolite silicalite-1 membranes be seed growth. **Materials Chemistry and Physics**. 96: 42-50.
- Zhang, X., Zhu, M., Zhou, R., Chen, X., and Kita, H. (2011). Synthesis of silicalite-1 membranes with high ethanol permeation in ultradilute solution containing fluoride. **Separation and Purification Technology**. 81: 480-484.



# CHAPTER III

## HYDROTHERMAL SYNTHESIS OF SILICALITE FROM RICE HUSK ASH

### 3.1 Abstract

The objective of this research work was to evaluate the hydrothermal synthesis of silicalite with high crystallinity and small particle size. The current study focused on investigating the effects of silica sources such as rice husk ash (RHA) and silica gel (SG), crystallization time, and ratios of NaOH/SiO<sub>2</sub>, H<sub>2</sub>O/NaOH, and SiO<sub>2</sub>/TPABr. The crystallinity, particle size, and morphology were characterized by FT-IR, XRD, particle size analyzer, and SEM. The conclusion of the main findings indicated that the XRD patterns of these samples clearly showed a pure phase of MFI structure corresponding to FT-IR spectra with vibration mode at 550 and 1223 cm<sup>-1</sup>. The highest crystallinity was obtained at reaction time of only 6 h with the mole ratios of NaOH/SiO<sub>2</sub>, H<sub>2</sub>O/NaOH and SiO<sub>2</sub>/TPABr as 0.24, 155, and 30, respectively. When SG was used as a silica source, it was found that the particle size was smaller than that from RHA. The morphologies of all silicalite samples were coffin and cubic-like shape.

### 3.2 Introduction

Silicalite or high silica ZSM-5 possesses MFI structure. It contains two intersecting channel systems composing of 10-membered ring straight and sinusoidal channels with

a unique pore structure dimension of 0.54-0.56 nm. According to a variety of its useful properties such as strong hydrophobicity, excellent shape selectivity, good catalytic activity and high thermal stability, hence, it has been widely used in industrial applications for adsorption (Ahunbay, Karvan, and Erdem-Senatarlar, 2008), catalysis (Yang, Meng, Wang, and Wang, 2011), and gas and liquid separation (Xiao, Yang, Lu, and Wang, 2009; Nomura, Bin, and Kakao, 2002).

Typically, silicalites are synthesized by the hydrothermal method from the gel compositions of silica, alkaline and organic cation as a template. Several types of silica source were applied in the synthesis of silicalite such as fumed silica in a molar composition of  $\text{SiO}_2:0.2\text{TPABr}:0.5\text{NaOH}:30\text{H}_2\text{O}$  at  $180^\circ\text{C}$  for 7 days (Shao, Li, Qiu, Xiao, and Terasaki, 2000), water glass in a reaction mixture of  $(1-5)\text{Na}_2\text{O}:(50-60)\text{SiO}_2:(1-2)\text{TPABr}:(600-770)\text{H}_2\text{O}$  at  $200^\circ\text{C}$  for 72 h (Davood, Ali, Kamal, and Mahdi, 2005) and TEOS in a molar composition of  $\text{SiO}_2:0.12\text{TPAOH}:0.008\text{NaOH}:60\text{H}_2\text{O}$  at  $95^\circ\text{C}$  for 7 days (Rider, Klementova, Bravec, and Kocirik, 2005). However, TEOS, fumed silica and colloidal silica are much more expensive compared to rice husk ash which is a potential silica source containing about 20% (w/w) of amorphous silica (Kamath and Proctor, 1998) and is considered as a by-product in form of an industrial waste abundance in agricultural countries. Moreover, another benefit of silica from rice husk is it is highly reactive silica which can be simply extracted to high purity silica (about 98%) by digesting with dilute acid and burning at  $700^\circ\text{C}$  for 4 h (Yalcin and Sevinc, 2001).

As a result, the major aim of the present work focused on synthesizing high crystalline silicalite using rice husk ash under considering the effect of silica sources, reaction times and gel compositions by hydrothermal method.

### 3.3 Materials and methods

#### 3.3.1 Materials

Silica from the rice husk from a local rice mill in the target area i.e. in Nakhon Ratchasima Province, Thailand was used as the starting material in the initial mixture for the silicalite synthesis together with pellets of sodium hydroxide (Merck), tetrapropylammonium bromide, TPABr (Sigma-Aldrich), and distilled water. Simultaneously hydrochloric acid 37% (Carlo-Erba) was used to prepare 1 M HCl.

#### 3.3.2 Methods

The preparation of the rice husk ash (RHA) extracted from rice husk and silica gel (SG) was carried out in the following steps.

Firstly, the rice husk was thoroughly washed with deionized water and dried at 110°C overnight. Next, the dried rice husk was digested with dilute acid, by boiling with 1 M HCl for 3 h and then repeatedly washed with water until neutral and dried at 110°C overnight. After that the acid digested rice husk was burned at 700°C for 4 h until it became clearly noticeable white ash. Finally, the white ash was ground till it became fine powder and later was sieved through a mesh no.100.

Silica gel was prepared by dissolving RHA with 1 M NaOH through boiling by covering its container to form sodium silicate solution. Then, the solution was filtered to remove carbon and silica residue. After the solution was cool, it was titrated with 1 M HCl until pH 4 was obtained and then it was left overnight to allow aging in order to form gel. Later, the gel was crushed and repeatedly washed with distilled water until the water was free from chloride ions and it was left overnight to dry at 120°C. Finally, the product was ground and sieved with the similar process as RHA.

### 3.3.3 Synthesis procedure

The procedure of silicalite synthesis was carried out from the system  $\text{SiO}_2\text{-NaOH-TPABr-H}_2\text{O}$  system with the mole ratios of  $\text{NaOH/SiO}_2$ ,  $\text{H}_2\text{O/NaOH}$  and  $\text{SiO}_2\text{/TPABr}$  within the ranges of 0.24-0.48, 155-618 and 30-60, respectively. After the required amount of NaOH, TPABr, silica and water was mixed together, the resulting mixture was stirred continuously for 5 minutes. Then, the hydrothermal treatment was carried out in a stainless steel bomb lined with PTFE at  $187^\circ\text{C}$  under autogenous pressure and various reaction times. Next, after reaching the desirable reaction time, the reaction was quenched with distilled water. Then, it was allowed to cool. Later, it was carefully filtered, and thoroughly and repeatedly washed with distilled water. Lastly, it was dried overnight at  $120^\circ\text{C}$ . The synthesized silicalite samples under different conditions were denoted as SL1 to SL21 (see Table 3.2).

### 3.3.4 Ethanol adsorption

The ethanol adsorption experiments were carried out with 2.5-10 wt% of ethanol. The solutions were added to the dried sorbents using 100 mg of the solid per mL of solution. After 1 h at room temperature, the liquid was analyzed on a gas chromatograph.

### 3.3.5 Characterization

Fourier transform infrared (FT-IR) spectroscopy was carried out using Perkin Elmer, SpectrumGX. The spectra were recorded within the range of  $2000\text{-}400\text{ cm}^{-1}$  with 32 scans at a resolution of  $4.0\text{ cm}^{-1}$ , using KBr pellet technique. Powder X-ray diffraction (XRD) was collected on Siemens D5005 diffractometer using  $\text{Cu K}_\alpha$  radiation. The percentage of the relative crystallinity was calculated from the ratio of the area of the highest intense reflection peak at 101, 200, 501, 151 and 133 as

a reference and as the area of those peaks from the other samples. The chemical compositions of RHA and SG were determined by X-ray fluorescence spectrometer (Oxford DE200). The BET specific surface area and particle size were carried out measured with a Micromeritics ASAP 2000 and Malvern instruments, respectively. The morphologies of the samples were detected by SEM after gold coating with the operation of a JEOL instrument at 20 KV.

### 3.4 Results and discussion

The chemical compositions and BET surface areas of silica sources are shown in Table 3.1.

**Table 3.1** The chemical compositions and BET surface areas of silica sources.

Silica source	RHA	SG
<b>Chemical composition, %wt.</b>		
SiO <sub>2</sub>	98.78	99.29
Al <sub>2</sub> O <sub>3</sub>	0.52	0.52
MgO	0.12	ND
CaO	0.36	ND
Others	0.22	ND
BET surface area, m <sup>2</sup> /g	247	790

The purity of white RHA product is 98.78% with a little impurity of natural metal oxides. While the metal oxide and unburned carbon were removed during the procedure to prepare, SG could be clearly observed. Interestingly, the BET surface area was greatly increased from 247 to 790 m<sup>2</sup>/g.

**Table 3.2** Mole ratios of gel compositions for silicalite synthesis.

Synthesized silicalite (SL)	Silica source	SiO <sub>2</sub>	NaOH/SiO <sub>2</sub>	H <sub>2</sub> O/NaOH	SiO <sub>2</sub> /TPABr	Reaction time (h)	Relative crystallinity (%)
SL1	RHA	1	0.24	309	60	24	43
SL2	RHA	1	0.24	309	30	24	90
SL3	RHA	1	0.24	309	15	24	84
SL4	RHA	1	0.24	309	7	24	88
SL5	RHA	1	0.24	309	4	24	83
SL6	RHA	1	0.24	309	30	6	73
SL7	RHA	1	0.24	309	30	12	96
SL8	RHA	1	0.24	309	30	18	91
SL9	RHA	1	0.12	618	30	12	67
SL10	RHA	1	0.48	155	30	12	69
SL11	RHA	1	0.24	155	30	12	95
SL12	RHA	1	0.24	618	30	12	67
SL13	RHA	1	0.24	155	30	6	98
SL14	RHA	1	0.24	155	30	4	84
SL15	RHA	1	0.24	155	30	3	amorphous
SL16	SG	1	0.24	155	30	3	42
SL17	SG	1	0.24	155	30	4	93
SL18	SG	1	0.24	155	30	6	100
SL19	SG	1	0.12	309	30	6	63
SL20	SG	1	0.48	77	30	6	80
SL21	SG	1	0.24	309	30	6	92

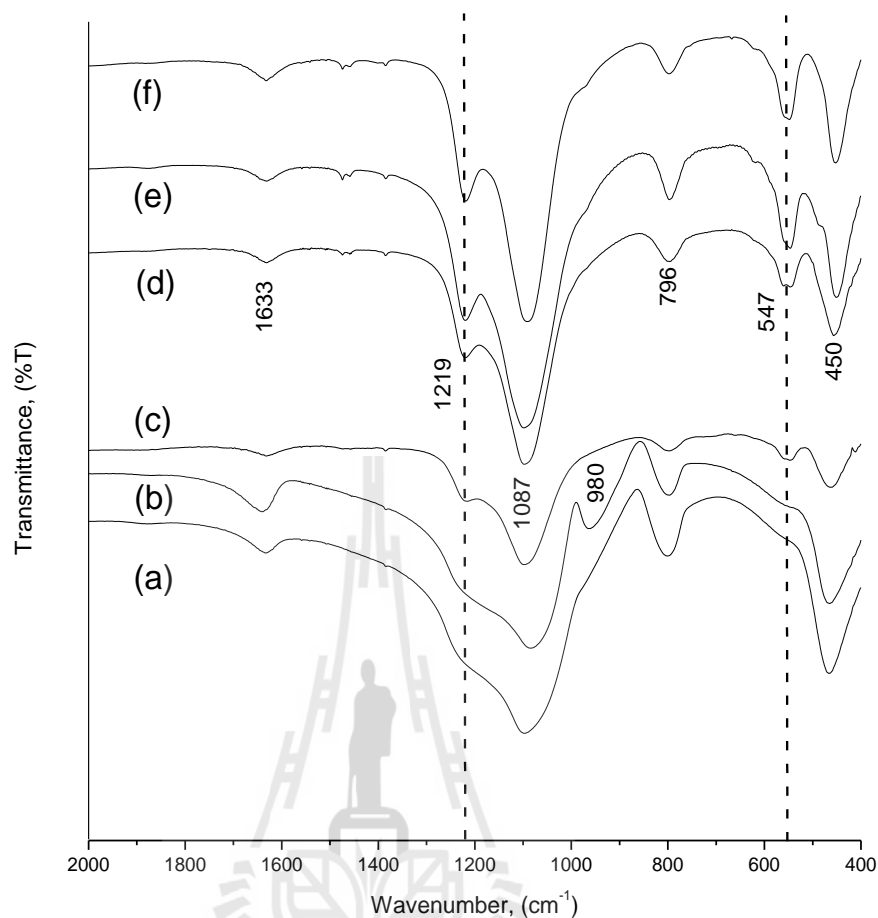


**Figure 3.1** FT-IR spectra of silica source: RHA(a), SG(b) and silicalite samples: SL1(c), SL12(d), SL13(e) and SL18(f) with different gel compositions (see Table 3.2).

### 3.4.1 Fourier transform infrared spectroscopy

The FT-IR spectra of the samples are shown in Figure 3.1. All the synthesized silicalite samples (see Figure 3.1(c), (d), (e) and (f)) reflect the vibration bands at 450, 796 and 1087  $\text{cm}^{-1}$  corresponding to the typical Si-O-Si bending, Si-O-Si symmetric stretching (outer  $\text{SiO}_4$  tetrahedron) and Si-O-Si asymmetric stretching (inner  $\text{SiO}_4$  tetrahedron) within silica framework, respectively (Panpa and Jinawath, 2009).

The clearly observed vibration modes at 547 and 1219  $\text{cm}^{-1}$  are attributed to double ring tetrahedral vibration and asymmetric stretching of Si tetrahedral in the zeolite framework, correspondingly, resulting in MFI-structured zeolite (Armaroli et al., 2006; Shirazi and Ghasemi, 2008) and they were not observed in amorphous silica. The bending vibration of adsorbed water appears at 1633  $\text{cm}^{-1}$ . When compared the spectrum of RHA and SG ((see Figure 3.1(a) and (b)), the additional band of Si-OH at 980  $\text{cm}^{-1}$  is noticeable for SG.

### 3.4.2 X-ray fluorescence

The elemental analysis of silicalite determined by X-ray fluorescence was shown in Table 3.3. The synthesized of silicalites have high silica content and low impurity of other metals. Especially, silicalite that prepared from SG give the purity higher than silicalite prepared from RHA.

**Table 3.3** The chemical compositions of silicalite SL13 and SL18.

Sample	SL13	SL18
<b>Chemical composition, %wt.</b>		
SiO <sub>2</sub>	99.50	99.64
Al <sub>2</sub> O <sub>3</sub>	0.13	0.01
CaO	0.10	0.03
NaO	0.26	0.30
Others	0.01	0.02

### 3.4.3 X-ray diffraction

Figure 3.2 shows the XRD patterns of all silicalite samples demonstrating a pure phase of MFI structure. RHA and SG show amorphous phase with a broad hump at the  $2\theta$  of around 20-22° (see Figure 3.2(a) and (b)). The typical characteristic pattern

of silicalite zeolite indicates its indexable peaks as (101), (200), (501), (151) and (133) reflections (Qi, Zhao, Xu, Li, and Sun, 2011; Naskar, Kundu, and Chatterjee, 2012). The crystallinity of silicalite is strongly influenced by the starting gel compositions as shown in Table 3.2. When RHA was used as a silica source with higher ratio of  $\text{SiO}_2/\text{TPABr}$  (SL1-SL2), a crystallinity percentage sharply decreased from 90% to 43% due to a lower amount of template. Obviously, the  $\text{SiO}_2/\text{TPABr}$  mole ratio of 30 is optimal for silicalite synthesis. Similarly, with a higher mole ratio of  $\text{H}_2\text{O}/\text{NaOH}$ , the crystallinity percentage greatly dropped from 95% to 67%.

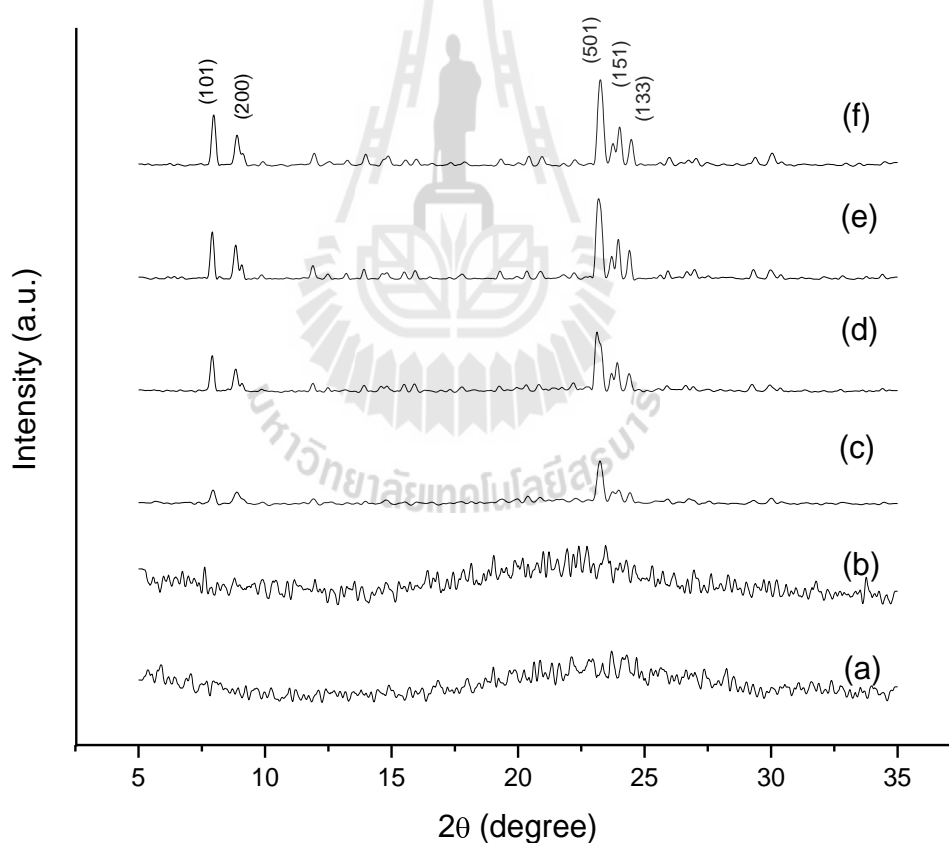


**Figure 3.2** X-ray diffraction patterns of silica source: RHA(a), SG(b) and silicalite sample: SL1(c), SL12(d), SL13(e), and SL18(f) with different gel compositions (see Table 3.2).

With a higher mole ratio of NaOH/SiO<sub>2</sub>, the amount of TPABr decreases due to a reaction with NaOH solution producing tripropylamine and propane (Cundy and Cox, 2003). As a result, the percentage of crystallinity decreases. The optimal condition of the silicalite synthesis with RHA as silica source was observed with the mole ratio of NaOH/SiO<sub>2</sub>, H<sub>2</sub>O/NaOH and SiO<sub>2</sub>/TPABr equal to 0.24, 155, and 30, respectively, under only 6 h of reaction time. When RHA was manipulated to improve some properties to become SG (see Table 3.1), this SG was then further applied as silica source for silicalite synthesis under the same optimal condition as RHA. The highest crystallinity is the result. Moreover, a very small amount of template, TPABr, was used in the synthesis of silicalite in this work, compared to those reported elsewhere (Shao, Li, Qiu, Xiao, and Terasaki, 2000; Rider, Klementova, Bravec, and Kocirik, 2005).

#### **3.4.4 Scanning electron microscope**

The scanning electron micrographs of silicalite are shown in Figure 3.3. The SEM images reveal that all silicalite products emerge in forms of two morphologies, coffin and cubic-like shape. In addition, it indicates the presence of amorphous nanoparticle on the crystal face of all silicalite samples when RHA is used as silica source. On the opposite, if SG is used as silica source (SL18), a clean surface clearly occurs. Figure 3.4 demonstrates the particle size distribution of two silicalite samples synthesized from RHA and SG under the condition of SL13 and SL18, accordingly. An average particle size of silicalite synthesized from RHA (~10 μm in length) is larger than that from SG (~5 μm). This can be evidently explained that silica moiety of SG whose surface area is larger could be depolymerized by NaOH more rapidly than that of RHA resulting in inducing faster nucleation. Additionally, with SG as silica source, a narrower size distribution was observed.

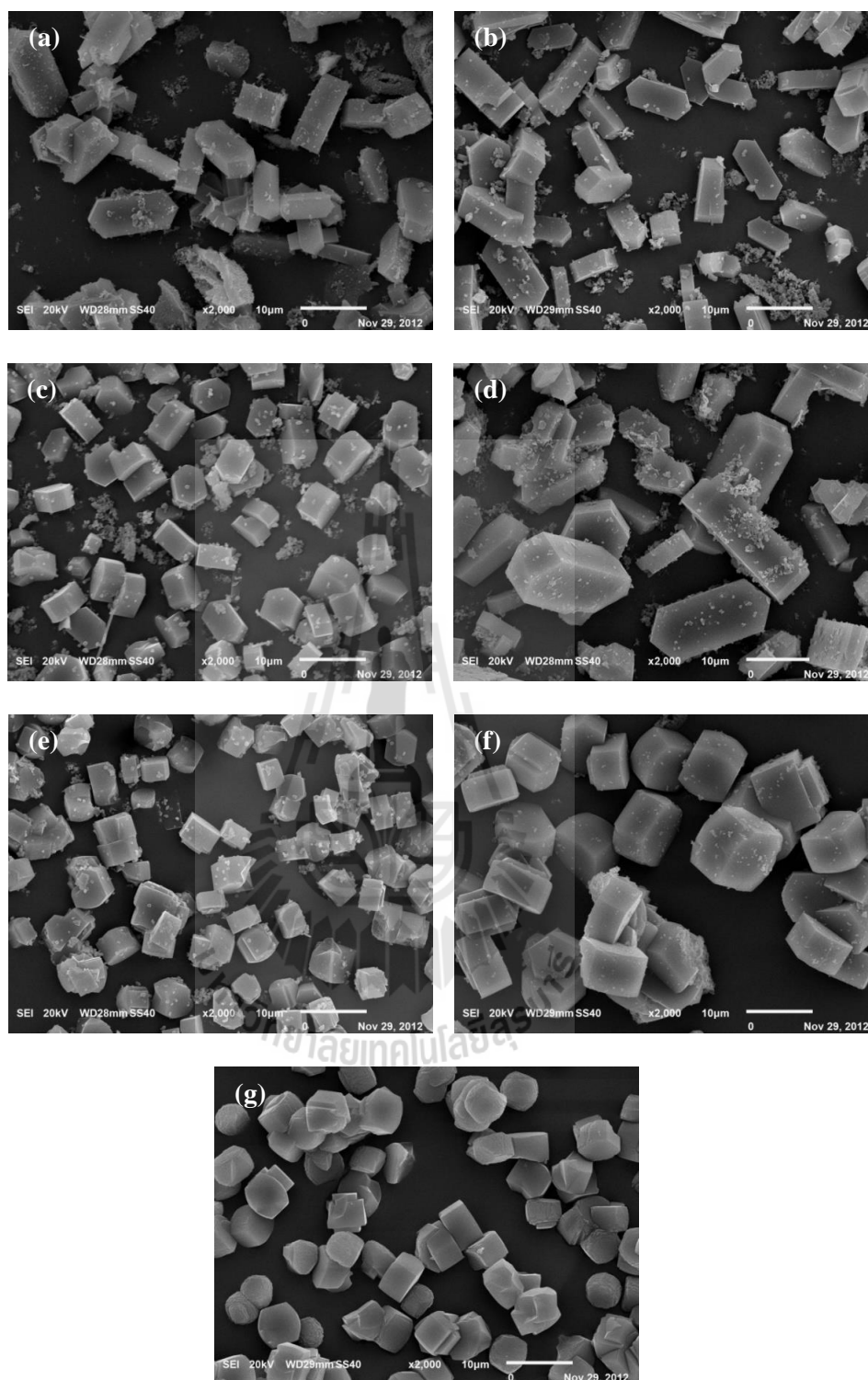


**Figure 3.3** Scanning electron micrographs of SL1(a), SL2(b), SL10(c), SL11(d), SL12(e), SL13(f), and SL18(g), referred in Table 3.2.

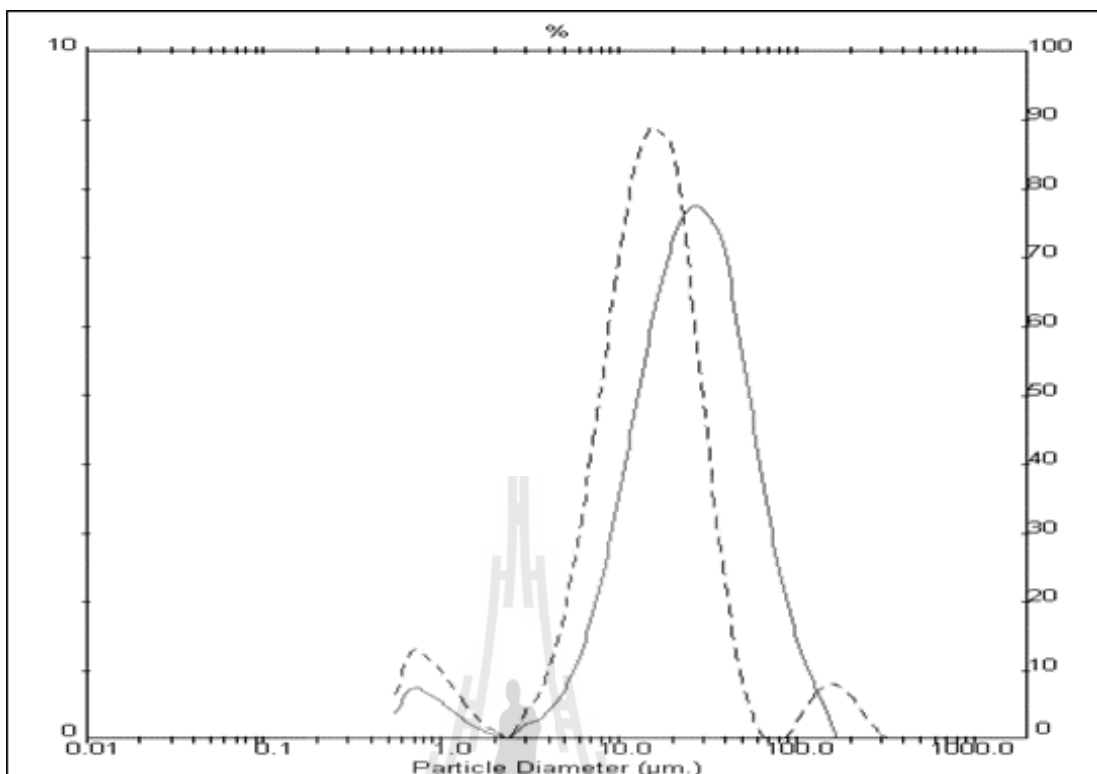


**Figure 3.4** Particle size distribution of silicalite synthesized from RHA (SL13) in solid line and SG (SL18) in dash line.

### 3.4.5 Ethanol adsorption properties

Silicalite sample of SL18 showed higher ethanol adsorption than SL13 that prepared from RHA due to its smaller size, narrower size distribution and higher crystallinity. The adsorption was increased with an increase in ethanol concentration in the solution. Ethanol adsorption of SL18 with 2.5 wt% ethanol solution was 61 mg ethanol/g. It was nearby the reports of Cekova, Kocev, Kolcakovska, and Stojanova (2006) that used silicalite as adsorbents for 2 wt% ethanol adsorption. The value of adsorption was 82 mg ethanol/g.

**Table 3.4** Ethanol adsorption of silicalite (2.5 wt% to 10 wt% ethanol solutions, 100 mg/mL).

Sorbent	Ethanol concentration / wt%	mg ethanol/g sorbent
SL13	2.5	55
	5	73
	10	112
SL18	2.5	61
	5	95
	10	125

### 3.5 Conclusions

It is obvious that silica source and synthesis gel composition strongly influences crystallinity, particle size and morphology of silicalite. An improvement of some properties of rice husk ash such as an increment of a specific surface area and a reduction of impurity can be successfully done by gel formation with a suggested procedure as an outcome of this study. The highest crystallinity, a narrow size distribution and a smaller particle size of synthesized silicalite are efficiently achieved from silica gel as a silica source by hydrothermal method.

### 3.6 References

- Ahunbay, M. G., Karvan, O., and Erdem-Senatalar, A. (2008). MTBE adsorption and diffusion in silicalite-1. **Microporous and Mesoporous Materials**. 115: 93-97.

- Armaroli, T., Simon, L. J., Digne, M., Montanari, T., Bevilacqua, M., Valtchev, V., Patarin, J., and Busca, G. (2006). Effects of crystal size and Si/Al ratio on the surface properties of H-ZSM-5 zeolites. **Applied Catalysis A**. 306: 78-84.
- Cekova, B., Kocev, D., Kolcakovska, E., and Stojanova, D. (2006). Zeolites as alcohol adsorbents from aqueous solutions. **APTEFF**. 37: 83-87.
- Cundy, C. S., and Cox, P. A. (2003). The hydrothermal synthesis of zeolites: History and development from the earliest days to the present time. **Chemical Reviews**. 103: 663-701.
- Davood, V., Ali, A. M., Kamal, M. S., and Mahdi, K. M. (2005). Synthesis of hydrophobic silicalite adsorbent from domestic resources: The effect of alkalinity on the crystal size and morphology. **Iranian Journal of Chemistry and Chemical Engineering**. 24: 9-14.
- Kamath, S. R., and Proctor, A. (1998). Silica gel from rice hull ash: Preparation and characterization. **Cereal Chemistry**. 75: 484-487.
- Naskar, M. K., Kundu, D., and Chatterjee, M. (2012). A facile hydrothermal conversion of rice husk ash to ZSM-5 zeolite powders. **Journal of the American Ceramic Society**. 95: 925-930.
- Nomura, M., Bin, T., and Nakao, S. (2002). Selective ethanol extraction from fermentation broth using a silicalite membrane. **Separation and Purification Technology**. 27: 59-66.
- Panpa, W., and Jinawath, S. (2009). Synthesis of ZSM-5 zeolite and silicalite from rice husk ash. **Applied Catalysis B: Environmental**. 90: 389-394.
- Qi, J., Zhao, T., Xu, X., Li, F., and Sun, G. (2011). Hydrothermal synthesis of size-controlled silicalite-1 crystals. **Journal of Porous Materials**. 18: 509-515.

- Rider, M., Klementova, M., Bravec, L., and Kocirik, M. (2005). Morphology and structure of silicalite-1 crystals. Evidence of twinning by x-ray and electron diffraction. **Studies in Surface Science and Catalysis**. 158: 741-748.
- Shao, C., Li, X., Qiu, S., Xiao, F., and Terasaki, O. (2000). Size-controlled synthesis of silicalite-1 single crystals in the presence of benzene-1,2-diol. **Microporous and Mesoporous Materials**. 39: 117-123.
- Shirazi, L., Jamshidi, E., and Ghasemi, M. R. (2008). The effect of Si/Al ratio of ZSM-5 zeolite on its morphology, acidity and crystal size. **Crystal Research and Technology**. 43: 1300-1306.
- Xiao, W, Yang, J., Lu, J., and Wang, J. (2009). A novel method to synthesize high performance silicalite-1 membrane. **Separation and Purification Technology**. 67: 58-63.
- Yalcin, N., and Sevinc, V. (2001). Studies on silica obtained from rice husk. **Ceramics International**. 27: 219-224.
- Yang, R., Meng, F., Wang, X., and Wang, Y. (2011). Influence of Na<sup>+</sup> on the synthesis of silicalite-1 catalysts for use in the vapor phase Beckmann rearrangement of cyclohexanone oxime. **Frontiers of Chemical Science and Engineering**. 5(4): 401-408.

# **CHAPTER IV**

## **FACIAL HYDROTHERMAL SYNTHESIS OF SIZE- CONTROLLED SILICALITE CRYSTALS FROM RICE HUSK ASH**

In the chapter III, silicalite was successfully synthesized by conventional hydrothermal method from rice husk ash (RHA) and silica gel (SG) as silica source. Silicalite prepared from SG gave highest crystallinity, narrow size distribution and smaller particle size than that from RHA. However, the method used for preparation of SG took a long time and the obtained synthesized silicalite crystals were also agglomerated. In this chapter, the facial hydrothermal synthesis of silicalite that gave a single morphology with easily tunable crystal size was proposed.

### **4.1 Abstract**

This study is the first one which yields the controllable size of highly crystallized silicalite from the rice husk ash, one of the most accessible agricultural byproducts. Moreover, this silicalite was successfully obtained through the simplest hydrothermal method with these materials as silica source i.e. rice husk ash (RHA), sodium silicate and potassium silicate, prepared by dissolving RHA with NaOH and KOH. Its crystal size could be easily tuned from 3  $\mu\text{m}$  to 23  $\mu\text{m}$  by adjusting the molar ratio of NaOH:SiO<sub>2</sub> or KOH:SiO<sub>2</sub> in the system of SiO<sub>2</sub>-TPABr-NaOH/KOH-H<sub>2</sub>O

through the synthesis process with the temperature at 187°C for 6 h. This synthesized samples were then characterized by infrared spectroscopy, X-ray powder diffraction and scanning electron microscopy. Thus, the significant outcomes of the research come in forms of controllable size of crystallized silicalite, cost effectiveness and accessibility of its silica sources, RHA.

## 4.2 Introduction

Silicalite or high silica ZSM-5 with the framework type of MFI composes of 10 member ring straight and parallel channels intersected with 10 membered ring sinusoidal channels whose unique pore structure dimension is 0.54-0.56 nm. It has been widely used in industrial applications such as catalysis (Mohamed, Zidan, and Thabet, 2008; Panpa and Jinawath, 2009), adsorption (Lua, Xua, Wang, Huang, and Cai, 2009; Ali, Hassan, Shaaban, and Soliman, 2011), gas separation (Arruebo, Coronas, Menendez, and Santamaria, 2001; Xiao, Yang, Lu, and Wang, 2009) and membrane separation (Qureshi, Meagher, Huang, and Hutkins, 2001; Zhoua, Sua, Chen, Yi, and Wan, 2010) because of its strong hydrophobicity, excellent shape selectivity and thermal stability.

Typically, silicalite can be synthesized by conventional hydrothermal method at 120-200°C under autogeneous pressure from gel composition of silica source, alkaline, water and organic cation as a template. For the past few years, some notable related studies focusing the synthesis of silicalite as silica source with different conditions are as follows. Firstly, Shao, Li, Siu, Xiao, and Terasaki (2000) synthesized silicalite by hydrothermal method from fume silica with a molar composition of  $\text{SiO}_2:0.2\text{TPABr}:0.5\text{NaOH}:30\text{H}_2\text{O}$  for 7 days at 180°C. Secondly, Li, Mihailova,

Creaser, and Sterte (2000) prepared silicalite from tetraethyl orthosilicate (TEOS) with a molar composition of 9 TPAOH:25SiO<sub>2</sub>:0.13Na<sub>2</sub>O:595H<sub>2</sub>O:100EtOH for 32 h at 100°C. Thirdly, Davood, Ali, Kamal, and Mahdi (2005) synthesized silcalite by using water glass as silica source from reaction mixture (1-5)Na<sub>2</sub>O:(50-60)SiO<sub>2</sub>:(1-2)TPABr:(600-770)H<sub>2</sub>O for 72 h at 200°C. The rate of crystallization at crystallization temperature below 160°C was found to be very slow (Ming, Baoquan, and Xiu, 2008).

However, cost effectiveness is one of the main factors in running a business. It is clear that the materials used as silica source for silicalite synthesis in the former studies are all expensive. For instance, the common types of silica source generally used for silicalite synthesis were TEOS, fumed silica and colloidal silica. All of these are far more expensive than natural silica source such as diatomite (Sanhueza, Kelm, Cid, and Lopez-Escobar, 2004), lignite fly ash (Chareonpanich, Namto, Kongkachuichay, and Limtrakul, 2004), kaolin (Wang, Shen, Shen, Peng, and Gao, 2007) and mudstone (Tuana et al., 2010). Among these, rice husk ash is one of the most interesting choices of candidates. This is because it has high silica content and it is industrial waste which is abundant in agricultural countries. That is rice husk contains amorphous silica about 20% w/w (Kamath and Proctor, 1998). This special silica from the rice husk is reactive silica that can be simply extracted by the digestion with dilute acid or base. After it is burned at 700°C the ash product has silica content about 98% which is very suitable for silicalite synthesis.

Apart from the advantages of the rice ash in terms of its cost effectiveness, accessibility and especially a characteristic type of its zeolite, its crystal size plays an important role on catalytic and adsorption process. The more the catalytic activity

increases, the smaller the crystal size becomes. On the contrary, the more the selectivity increases, the bigger the crystal size becomes. In fact, the optimum compromise between activity and selectivity depends on both of the catalytic process and the selected zeolite type. However, there are a few reports on the synthesis of high silica zeolite with tunable crystal sizes (Hu, Liu, Zhang, Ren, and Tang, 2009; Xue, Wang, and He, 2012). Furthermore, what is more interesting and important to industrial applications is the control crystal sizes with facial and less expensive way. All of these give rise to this present study whose major purpose is to control crystal size of silicalite with a simple but a highly efficient method using rice husk as silica source for synthesizing high crystalline silicalite with the consideration of the cost effectiveness through the lowest amount of template used and the shortest reaction time.

### **4.3 Materials and methods**

#### **4.3.1 Materials**

The specific materials used in the synthesis of silicalite in this present study are rice husk ash (RHA), pellets of sodium hydroxide (Merck), potassium hydroxide (Merck), hydrochloric acid (Merck), tetrapropylammonium bromide, TPABr (Fluka).

#### **4.3.2 Methods**

RHA as silica source was extracted from rice husk in order to prepare sodium silicate solution and potassium silicate solution denoted as SS and KS, respectively. To start with, RHA was prepared by burning the acid leached rice husk at 700°C for 4 hs until a white ash was formed. Then, it was ground until it became fine powder and sieving through a mesh number 100. Next, sodium silicate solution (SS)

was prepared by dissolving 10 g of RHA with 100 mL of 1M NaOH through boiling it by covering its container for 1 h to form sodium silicate solution. After that, the solution was filtered to remove indissoluble polymeric silica and other impurity of carbon residue which a volume of the filtrate was made up to 100 mL. Then, it was left overnight. Also, potassium silicate solution (KS) was prepared in the same manner of sodium silicate but KOH was used instead of NaOH.

### 4.3.3 Synthesis procedure

Silicalite syntheses were carried out using the gel molar compositions of the starting materials, namely  $\text{SiO}_2:0.24\text{NaOH}:0.03\text{TPABr}:37\text{H}_2\text{O}$ ,  $\text{SiO}_2:0.48\text{NaOH}:0.03\text{TPABr}:74\text{H}_2\text{O}$  and  $\text{SiO}_2:0.60\text{NaOH}:0.03\text{TPABr}:92.5\text{H}_2\text{O}$  with the molar ratios of base/ $\text{SiO}_2$  as 0.24, 0.48, and 0.60, respectively. Briefly, in synthesizing the sample of RHA1 (see Table 4.2), i.e. the specific amounts of NaOH (0.16 g), TPABr (0.15 g) template and  $\text{H}_2\text{O}$  (11.2 g) were added to RHA (1.00 g). Then, the mixture was stirred for 5 minutes to obtain a dispersion. Particularly, the hydrothermal treatment in this study was performed in a stainless steel bomb lined autoclave with PTFE under autogenous pressure at  $187^\circ\text{C}$  for 6 h. Next, hydrothermal reaction as powder was collected by filtration, followed by washing with deionized water several times until the pH of the filtrated became neutral. Finally, the powder was dried overnight at  $120^\circ\text{C}$ .

For the synthesis of silicalite from SS and KS, at first, the sample of SS1 (see Table 4.2), such as the specific amount of NaOH, TPABr, and  $\text{H}_2\text{O}$  as in the sample of RHA1 was added to 10 mL of SS/KS. Then the mixture was added with 6M HCl to adjust the molar ratio of  $\text{H}_2\text{O}/\text{base}$  to be constant at 155. Similarly, the hydrothermal treatment was performed under the same condition as referred above.

#### 4.3.4 Characterization

The chemical compositions of RHA was determined by X-ray fluorescence spectrometer (Oxford DE200). The morphologies and crystal sizes of the samples were determined by scanning electron microscopy (SEM) using a JEOL instrument operating at 10 keV. X-ray powder diffraction (XRD) measurements were performed with a Siemens D5000 diffractometer (Cu  $K_{\alpha}$ ,  $\lambda = 1.5406 \text{ \AA}$ ). While, Fourier transform infrared (FT-IR) spectroscopy was carried out by Perkin Elmer, SpectrumGX, the spectra were recorded in the range of  $2000\text{-}400 \text{ cm}^{-1}$  with 32 scans at a resolution of  $4.0 \text{ cm}^{-1}$  and using KBr pellet technique.  $^{29}\text{Si}$  and  $^{27}\text{Al}$  solid-state MAS NMR spectra were recorded on a Bruker spectrometer, Ascend 500.

### 4.4 Results and discussion

#### 4.4.1 Silica source properties

Table 4.1 shows the chemical composition of RHA. The sample has high purity of  $\text{SiO}_2$  as 98.78% with a little amount of metal oxide.

**Table 4.1** The chemical composition of the local RHA determined by XRF.

Chemical composition	% wt.
$\text{SiO}_2$	98.78
$\text{Al}_2\text{O}_3$	0.52
MgO	0.12
CaO	0.36
Others	0.22

The gel compositions for silicalite synthesis with difference of bases (NaOH and KOH) are listed in Table 4.2. Although, the molar ratios of base/SiO<sub>2</sub> were varied from 0.24 to 0.60, the molar ratio of H<sub>2</sub>O/NaOH, SiO<sub>2</sub>/TPABr were kept constant at 155 and 30, respectively. In addition, Table 4.2 shows the crystal size with different size ranking from 3 x 3 x 2 μm to 26 x 17 x 18 μm. The sample products were characterized by FT-IR, XRD and SEM. The results are presented in this section.

**Table 4.2** Molar ratios of gel composition and crystal size of silicalite synthesized at 187°C for 6 h.

Sample	SiO <sub>2</sub>	NaOH/	KOH/	H <sub>2</sub> O/	SiO <sub>2</sub> /	Crystals size L x W x T (μm)	Crystals agglomerated
		SiO <sub>2</sub>	SiO <sub>2</sub>	NaOH	TPABr		
RHA1	1	0.24	-	155	30	9 x 6 x 4	Yes
RHA2	1	-	0.24	155	30	26 x 17 x 18	Yes
SS1	1	0.24	-	155	30	16 x 20 x 13	No
SS2	1	0.48	-	155	30	11 x 13 x 9	No
SS3	1	0.60	-	155	30	21 x 23 x 17	No
KS1	1	-	0.24	155	30	6 x 11 x 3	No
KS2	1	-	0.48	155	30	3 x 3 x 2	No
KS3	1	-	0.60	155	30	4 x 6 x 3	No

#### 4.4.2 Fourier transform infrared spectroscopy

The FT-IR spectra of the synthesized samples are shown in Figure 4.1. All the samples show the vibrational band at 450, 796, and 1087 cm<sup>-1</sup> corresponding to a typical Si-O-Si bending, Si-O-Si symmetric stretching (outer SiO<sub>4</sub> tetrahedron) and Si-O-Si asymmetric stretching (inner SiO<sub>4</sub> tetrahedron) within silica framework, respectively. Also, the bending mode of adsorbed water appeared at 1633 cm<sup>-1</sup> (Qi, Zhao, Xu, Li, and Sun, 2011). The vibrational modes at 547 and 1219 cm<sup>-1</sup> are the

characteristic of MFI-structured zeolite. These are consistent with the previous report (Jian, Tianbo, Xin, and Fengyan, 2011; Milan, Debtosh, and Minati, 2012). Furthermore, they are assigned to double ring tetrahedral vibration and asymmetric stretching of Si tetrahedral in the zeolite framework, respectively.

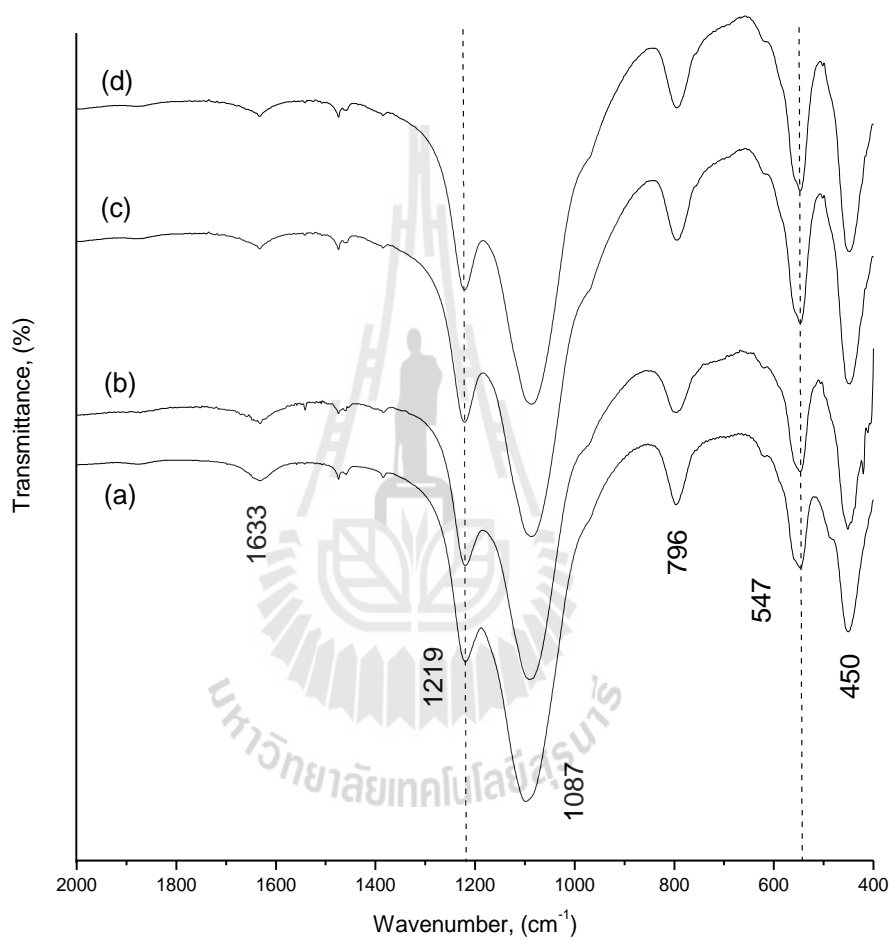


**Figure 4.1** FT-IR spectra of as-synthesized silicalite prepared from RHA1(a), RHA2(b), SS2(c), and KS2(d).

#### 4.4.3 X-ray power diffraction

XRD patterns of the synthesized samples are shown in Figure 4.2. All the samples show the typical characteristic patterns of silicalite with their peaks indexable

as (011), (020), (501), (303), and (133) reflections (Ji, Yao, and Zhang, 2011). The result shows a pure phase of silicalite with high crystallinity.

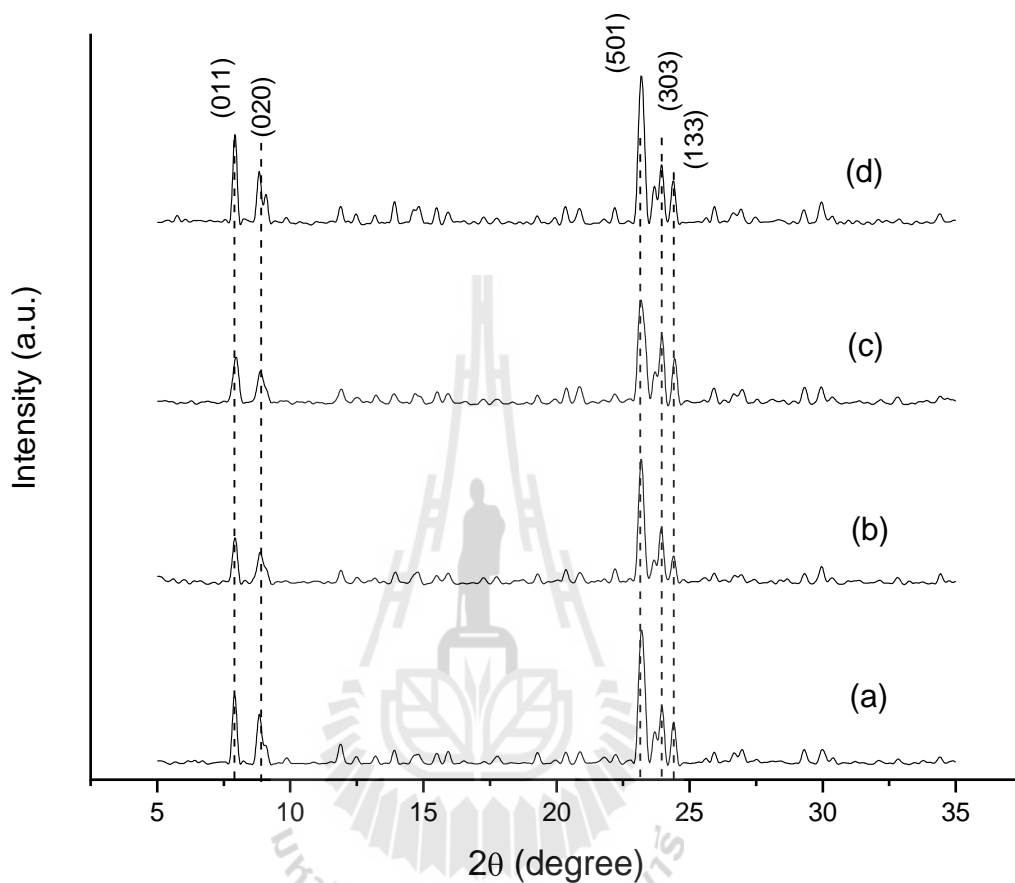


**Figure 4.2** X-ray diffraction patterns of RHA1(a), RHA2(b), SS2(c), and KS2(d).

#### 4.4.4 $^{29}\text{Si}$ and $^{27}\text{Al}$ NMR

$^{29}\text{Si}$  NMR spectra of SS3 appear in Figure 4.3. Si spectra are dominated by broad, overlapping lines. The spectra exhibit two broad features associated with Q3 [-95 to -104 ppm] and Q4 [-104 to -115 ppm] Si connectivities. Peaks in the Q3 region are due to silanol groups Si(3Si, 1OH) or aluminum content Si(3Si, 1Al) species, while those in the Q4 are attributed to Si connected to 4 T-atoms through O atoms Si(4Si) (Xue et al., 2012). Silanol groups of silicalite were ascribed to the framework defects.

Non-closed Si-O-Si linkages produce two  $\text{SiO}^-$  anions. One of these anions compensates with  $\text{TPA}^+$  and cation as  $\text{Na}^+$  and  $\text{K}^+$ . After calcination at  $550^\circ\text{C}$  the template ion was replaced by Si-OH group (Hunger, Freude, and Pfeifer, 1990).

Oumi, Miyajima, Miyamoto, and Sano (2002) studied the adsorption behaviors of water and ethanol on silicalite with difference of structural defects. The structure of silicalite with less defect is capable to adsorb less amount of water. On the other hand, ethanol was adsorbed preferentially on silicalite structure with less defect. In addition, Sano, Kasuno, Takeda, Arazaki, and Kawakami (1994) studied the adsorption of water and alcohol on powder silicalite and ZSM-5, they found that the amount of water adsorbed was strongly influenced by the amount of silanol groups of zeolite crystals.

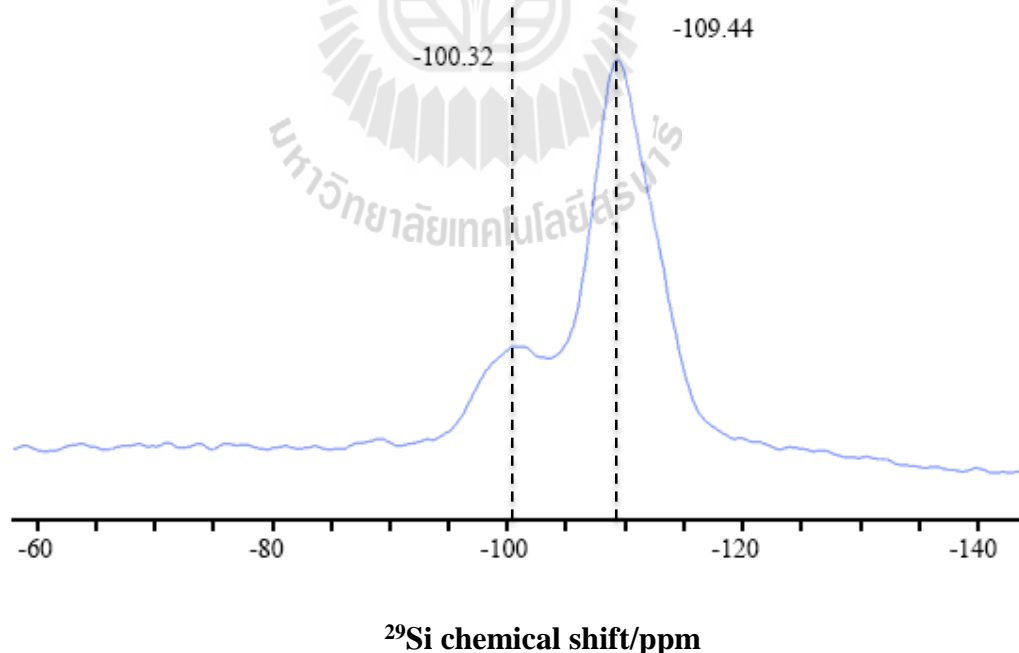


**Figure 4.3**  $^{29}\text{Si}$  MAS NMR signal of SS3 sample.

The  $^{27}\text{Al}$  NMR spectra of SS3 sample shows in Figure 4.4. The major feature at about 55-58 ppm is assigned to aluminum in tetrahedral framework sites (Xue et al., 2012).

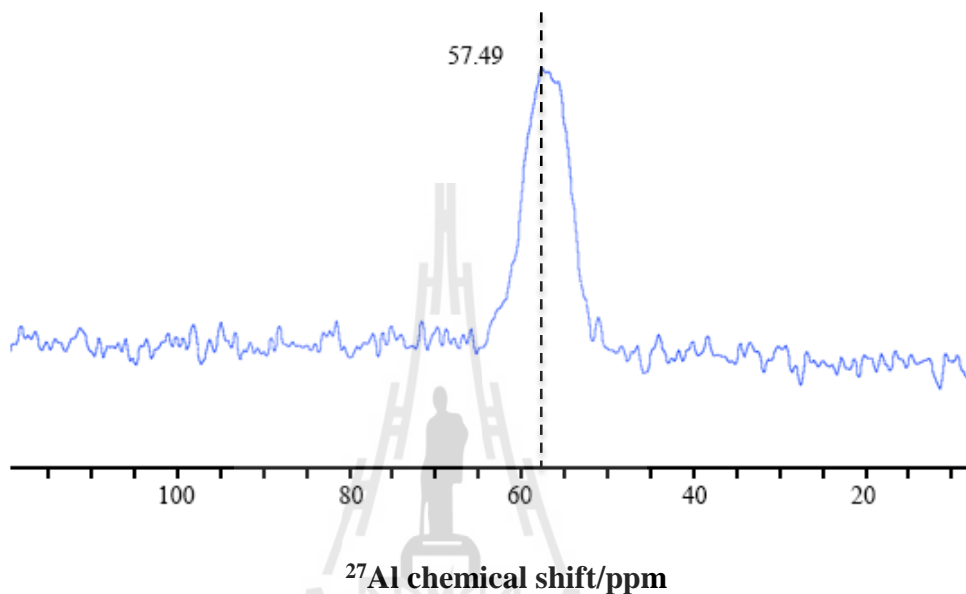


**Figure 4.4**  $^{27}\text{Al}$  NMR spectra of SS3 sample.

#### 4.4.5 Scanning electron microscopy

The morphologies of silicalite crystals prepared from solid of RHA and clear solution of SS and KS are shown in Figure 4.5. All the synthesized samples obtained from RHA are coffin and cubic-like shapes. The result demonstrates that the crystals are agglomerated with a wide range of size distribution ((a) and (b)). Clearly, its smaller crystal size could be observed when NaOH was used as an alkali compared to KOH. This could be explained in terms of depolymerization of silica that NaOH is a stronger base than KOH. Hence it could depolymerize silica source more rapidly and faster induce nucleation than KOH. As a result, the larger crystals size of silicalite was achieved when KOH was used.

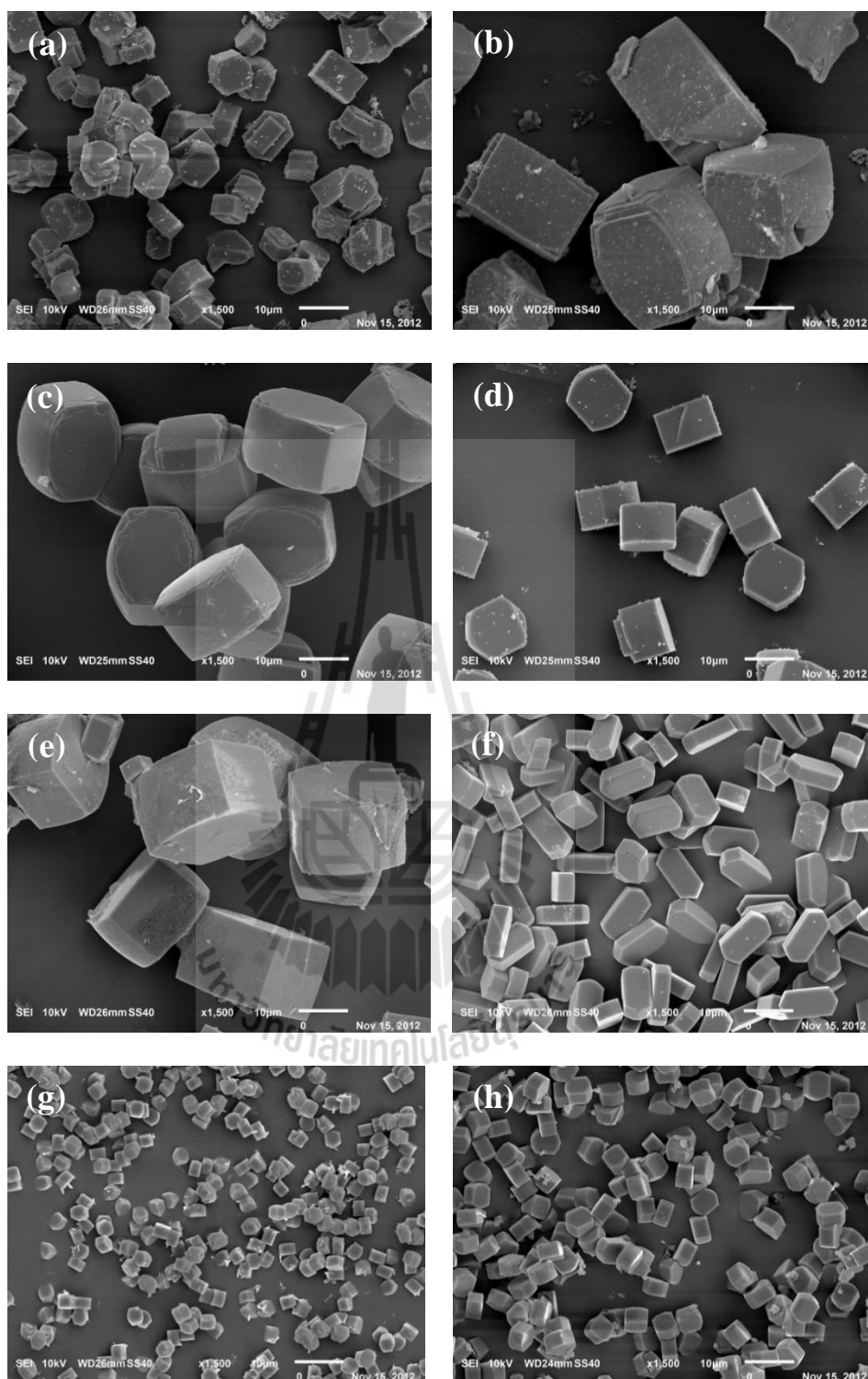


**Figure 4.5** Scanning electron micrographs of as-synthesized silicalite samples RHA1(a), RHA2(b), SS1(c), SS2(d), SS3(e), KS1(f), KS2(g) and KS3(h).

In synthesizing silicalite from clear solutions of SS and KS, the result reflects that all of the products ((c) to (h)) show mainly a coffin-like shape morphology and a little of cubic-like shape. With the same ratio of base/SiO<sub>2</sub>, it is obvious that a larger crystal size was obtained from SS. The largest crystals size (23 μm along the Width (W)) was achieved with molar ratio of 0.60 NaOH/SiO<sub>2</sub> while the smallest crystals size was observed from SS and KS with molar ratio of 0.48 base/SiO<sub>2</sub> (see Table 4.2) with the crystals size 13 and 3 μm along the W for SS and KS, respectively.

Davood, Ali, Kamal, and Mahdi (2005) investigated the influence of alkalinity (Na<sub>2</sub>O) in the starting gel mixture on the crystal shape and size. Water glass was exchanged with H<sup>+</sup> to produce silica sol used as silica source. Pure silicalite was obtained from gel composition of (1-5)Na<sub>2</sub>O:(50-60)SiO<sub>2</sub>:(1-2)TPABr:(600-770)H<sub>2</sub>O. It was found that a decreasing of Na<sub>2</sub>O grows the particle size. Crystal size of products varied from 8.3 to 32 μm. Shao, Li, Qiu, Xiao, and Terasaki (2000) synthesized single crystals of silicalite and size-controlled silicalite by adding benzene-1,2-diol into the gel composition of SiO<sub>2</sub>:TPABr:NaOH:H<sub>2</sub>O. The crystal size and morphology of silicalite were largely influenced by the content of benzene-1,2-diol. The formation of silicon-benzene-1,2-diol make silicon species to form silicalite slowly during crystallization, thus the crystal size was increased with an increase in benzene-1,2-diol content. Crystals sizes of the products were ranging from 9 x 3 x 2 μm to 165 x 30 x 30 μm.

Generally, the crystal size is a function of the ratio between the rate of nucleation and that of crystal growth. This is affected by various factors such as temperature, aging, seeding, and OH<sup>-</sup>/SiO<sub>2</sub> ratio (Hill, Kinson, and Seddon, 1988; Burkett and Davis, 1995; Coker and Jansen, 1998). In the terms of a crystal size, it

depends on inorganic cations as  $\text{Na}^+$  and  $\text{K}^+$  which play an important role as a part of template effect (Petrik, Connor, and Schwarz, 1995; Singh and Dutta, 2003).

## 4.5 Conclusions

- (1) The high crystalline silicalite can successfully be synthesized by a conventional hydrothermal method from RHA, sodium silicate solution (SS) and potassium silicate solution (KS) with the minimal amount of TPABr template according to the procedure suggested.
- (2) The size of crystal is successfully prepared by both adjusting a molar ratio of base/ $\text{SiO}_2$  and using alkali cations of  $\text{Na}^+$  and  $\text{K}^+$ .
- (3) The single morphology and the narrow particle size distribution are effectively achieved by using silica source as SS and KS.

## 4.6 References

- Ali, I. O., Hassan, A. M., Shaaban, S. M., and Soliman, K. S. (2011). Synthesis and characterization of ZSM-5 zeolite from rice husk ash and their adsorption of  $\text{Pb}^{2+}$  onto unmodified and surfactant-modified zeolite. **Separation and Purification Technology**. 83: 38-44.
- Arruebo, M., Coronas, J., Menendez, M., and Santamaria, J. (2001). Separation of hydrocarbons from natural gas using silicalite membranes. **Separation and Purification Technology**. 25: 275-286.
- Burkett, S. L., and Davis, M. E. (1995). Mechanisms of structure direction in the synthesis of pure-silica zeolites. 1. Synthesis of TPA/Si-ZSM-5. **Chemistry of Materials**. 7: 920-928.

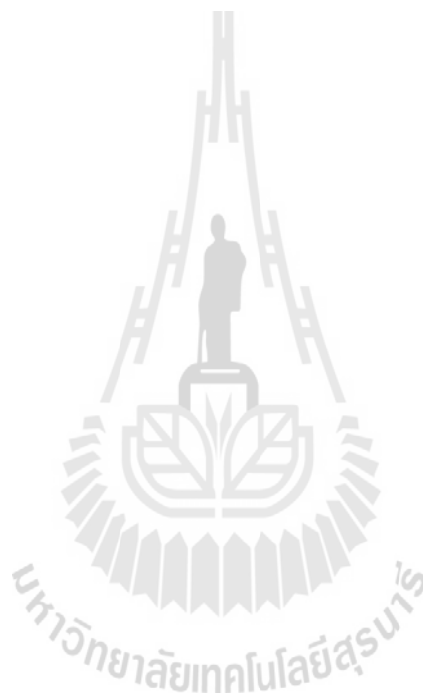
- Chareonpanich, M., Namto, T., Kongkachuichay, P., and Limtrakul, J. (2004). Synthesis of ZSM-5 zeolite from lignite fly ash and rice husk ash. **Fuel Processing Technology**. 85: 1623-1634.
- Coker, E. N., and Jansen, J. C. (1998). **Molecular sieves**. Berlin: Springer. pp. 121-155.
- Davood, V., Ali, A. M., Kamal, M. S., and Mahdi, A. M. (2005). Synthesis of hydrophobic silicalite adsorbent from domestic resources: The effect of alkalinity on the crystal size and morphology. **Iranian Journal of Chemistry and Chemical Engineering**. 24: 9-14.
- Hill, S. G., Kinson, K., and Seddon, D. (1988). The crystal size and morphology of silicalite as influenced by gel nucleation temperature, alkalinity and sodium-chloride concentration. **Australian Journal of Chemistry**. 41: 783-789.
- Hu, Y., Liu, C., Zhang, Y., Ren, N., and Tang, Y. (2009). Microwave-assisted hydrothermal synthesis of nanozeolites with controllable size. **Microporous Mesoporous Mater**. 119: 306-314.
- Hunger, M., Freude, D., and Pfeifer, H. (1990). MAS NMR studies of silanol groups in zeolites ZSM-5 synthesized with an ionic template. **Chemical Physics Letters**. 167: 21-26.
- Ji, W., Yao, J., and Zhang, L. (2011). Fast synthesis and morphology control of silicalite-1 in the presence of polyvinyl alcohol. **Journal of Porous Materials**. 18: 451-454.
- Jian, Q., Tianbo, Z., Xin, X., and Fengyan, L. (2011). Hydrothermal synthesis of size-controlled silicalite-1 crystals. **Journal of Porous Materials**. 18: 509-515.

- Kamath, S. R., and Proctor, A. (1998). Silica gel from rice hull ash: Preparation and characterization. **Cereal Chemistry**. 75: 484-487.
- Li, Q., Mihailova, B., Creaser, D., and Sterte, J. (2000). The nucleation period for crystallization of colloidal TPA-silicalite-1 with varying silica source. **Microporous and Mesoporous Materials**. 40: 53-62.
- Lua, J., Xua, F., Wang, D., Huang, J., and Cai, W. (2009). The application of silicalite-1/fly ash cenosphere (S/FAC) zeolite composite for the adsorption of methyl tert-butyl ether (MTBE). **Journal of Hazardous Materials**. 165: 120-125.
- Milan, K. N., Debtosh, K., and Minati, C. (2012). A Facile hydrothermal conversion of rice husk ash to ZSM-5 zeolite powders. **Journal of the American Ceramic Society**. 95: 925-930.
- Ming, Z., Baoquan, Z., and Xiu, F. L. (2008). Oriented growth and assembly of zeolite crystals on substrates. **Chinese Science Bulletin**. 53: 801-816.
- Mohamed, M. M., Zidan, F. I., and Thabet, M. (2008). Synthesis of ZSM-5 zeolite from rice husk ash: Characterization and implications for photocatalytic degradation catalysts. **Microporous and Mesoporous Materials**. 108: 193-203.
- Oumi, Y., Miyajima, A., Miyamoto, J., and Sano, T. (2002) **Studies in Surface Science and Catalysis**. 142: 1595-1602.
- Panpa, W., and Jinawath, S. (2009). Synthesis of ZSM-5 zeolite and silicalite from rice husk ash. **Applied Catalysis B: Environmental**. 90: 389-394.
- Petrik, L. F., O' Connor, C. T., and Schwarz, S. (1995). **Catalysis by microporous material**. Amsterdam: Elsevier. pp. 517-524.
- Qi, J., Zhao, T., Xu, X., Li, F., and Sun, G. (2011). Hydrothermal synthesis of size-controlled silicalite-1 crystals. **Journal of Porous Materials**. 18: 509-515.

- Qureshi, N., Meagher, M. M., Huang, J., and Hutkins, R. W. (2001). Acetone butanol ethanol (ABE) recovery by pervaporation using silicalite–silicone composite membrane from fed-batch reactor of *Clostridium acetobutylicum*. **Journal of Membrane Science**. 187: 93-102.
- Sanhueza, V., Kelm, U., Cid, R., and Lopez-Escobar, L. (2004). Synthesis of ZSM-5 from diatomite: A case of zeolite synthesis from a natural material. **Journal of Chemical Technology and Biotechnology**. 79: 686-690.
- Sano, T., Kasuno, T., Takeda, K., Arazaki, S., and Kawakami, Y. (1997). Sorption of water vapor on HZSM-5 type zeolites. **Studies in Surface Science and Catalysis**. 105: 1771-1778.
- Shao, C., Li, X., Qiu, S., Xiao, F., and Terasaki, O. (2000). Size-controlled synthesis of silicalite-1 single crystals in the presence of benzene-1,2-diol. **Microporous and Mesoporous Materials**. 39: 117-123.
- Singh, R., and Dutta, P. K. (2003). **MFI: A case study of zeolite synthesis**. New York-Basel: Marcel Dekker Inc. pp. 21-63.
- Tuana, H. T., Bae, I., Jang, Y., Chae, S., Chae, Y., and Suhr, D. (2010). Hydrothermal synthesis of ZSM-5 zeolite using siliceous mudstone. **Journal of Ceramic Processing Research**. 11: 204-208.
- Wang, P., Shen, B., Shen, D., Peng, T., and Gao, J. (2007). Synthesis of ZSM-5 zeolite from expanded perlite/kaolin and its catalytic performance for FCC naphtha aromatization. **Catalysis Communications**. 8: 1452-1456.
- Xiao, W., Yang, J., Lu, J., and Wang, J. (2009). A novel method to synthesize high performance silicalite-1 membrane. **Separation and Purification Technology**. 67: 58-63.

Xue, T., Wang, Y. M., and He, M. (2012). Synthesis of ultra-high-silica ZSM-5 zeolites with tunable crystal sizes. **Solid State Sciences**. 14: 409-418.

Zhoua, H., Sua, Y., Chen, X., Yi, S., and Wan, Y. (2010). Modification of silicalite-1 by vinyltrimethoxysilane (VTMS) and preparation of silicalite-1 filled polydimethylsiloxane (PDMS) hybrid pervaporation membranes. **Separation and Purification Technology**. 75: 286-294.



# **CHAPTER V**

## **SEPARATION OF ETHANOL FROM ETHANOL/WATER MIXTURES USING PERVAPORATION MEMBRANE**

In this research we have studied continuously to attempt to prepare silicalite membranes on mullite porous support by hydrothermal method through the condition of silicalite synthesis that was studied in the Chapter IV. In addition, the 2-stage of crystallization temperature applied to the hydrothermal synthesis of silicalite membrane and using PhTES for modifying the membranes in order to improve its pervaporation performance were exhibited in the Chapter V.

### **5.1 Abstract**

Polycrystalline silicalite membranes were synthesized on the outer surface of porous mullite disc by conventional hydrothermal method in batch system. In the synthesis, the silicalite membrane was synthesized from clear solutions with a molar composition of  $0.80\text{KOH}:\text{SiO}_2:0.03\text{TPABr}:123\text{H}_2\text{O}$ . Crystallization was carried out at 2 stage temperature for  $90^\circ\text{C}$  for 17 h and  $170^\circ\text{C}$  for 24 h. The modified of silicalite with phenyltriethoxysilane (PhTES) was carried out by reflux silicalite membrane with PhTES in toluene at  $80^\circ\text{C}$  for 6 h. The membranes were characterized by fourier transform infrared for evaluate PhTES, X-ray diffraction for phase identification and scanning electron microscopy for morphology determination. The membranes was used for separation of ethanol from ethanol/water mixture by pervaporation. The high

ethanol permselectivity with a separation factor 8.43 and the flux 0.42 kg/m<sup>2</sup>h was achieved for a 5 wt% aqueous ethanol solution at 60°C.

## 5.2 Introduction

Ethanol is an important renewable energy that can be produced from byproducts of agricultural products such as cassava, corn, potato, sorghum and sugar cane etc. via chemical and bio-fermentation processes. A large number of separation techniques are available for separation of liquid mixtures, such as distillation, adsorption, liquid-liquid extraction and fractional crystallization. Many studies have been reported on separation of organic compounds from organic/water mixtures by pervaporation (Araki, Imasaka, Tanaka, and Miyake, 2011; Li, Tuan, Falconer, and Noble, 2003). Pervaporation is expected to enable separation of azeotropic mixtures, thermally degradable mixtures, and organic aqueous solutions of low concentration. Moreover, pervaporation should reduce the device volume and energy consumption, with the possibility of continuous operation.

The permeation through the zeolite membrane on PV was usually explained by the adsorption-diffusion model which is based on the solution diffusion model. Each component of the permeating molecules was adsorbed to the inlet of the zeolite micropores and diffused through the zeolite pores due to the concentration gradient. The membrane separation performance is related to the quality of zeolite layer with high crystallinity should be thin and defect-free. Normally, to prepare zeolite membranes is to control the formation of zeolite growth on porous supports. It is known that the formation of zeolite layers is involved in the complex chemical reactions, which are affected by many interacting factors such as the chemical composition, silica source, hydrothermal synthesis conditions, seeds and so on (Wong, Au, Lau, Ariso, and

Yeung, 2001). Typically a technique which are often used to synthesize the zeolite membrane on a flat or tubular porous support under hydrothermal reaction condition is in situ crystallization, crystal growth on an untreated support from a solution or a gel of aluminosilicate.

Using of hydrophobic membranes is effective when the organic concentration in the mixtures is low. Generally, high flux, selectivity and chemical and mechanical stability are required of the membranes for using in a pervaporation process, and it is necessary to control the pore sizes to obtain high flux and selectivity (Bowen, Noble, and Falconer, 2004)

Silicalite membrane seems to have great potential for the ethanol recovery by PV (Vane, 2005). Silicalite exhibits hydrophobic property with MFI structure and it is one of  $\text{Al}_2\text{O}_3$  free zeolite which avoid dealumination. It is very difficult to prepare silicalite membranes that show the same membrane performance, although the membranes are prepared by the same method. Such difference in the performance may be attributed to the slight difference in the membrane thickness or the number of small pores formed during the thermal treatment which is carried out to remove a template in the channel of the silicalite crystals. Therefore, in order to improve the separation performance of the silicalite membrane, the enhancement of the hydrophobicity of the membrane and control of small pores that originate from silicalite crystals must be conducted.

In this study, MFI-type zeolite membranes were synthesized over porous mullite supports from clear synthesis solutions with a molar composition of  $(0.24-1.0)\text{NaOH/KOH}:\text{SiO}_2:0.03\text{TPABr}:123\text{H}_2\text{O}$ . The synthesis solution was then transferred to a stainless steel autoclave and the porous support was immersed in the solution. The crystallization procedure was carried out at  $90^\circ\text{C}$  for 17 h and

crystallization at 170°C with various times (0-24 h). To improve the PV performance of silicalite membrane, PhTES was used as silane coupling reagent that enhance the hydrophobicity of silicalite membrane. The membranes were investigated by FT-IR, XRD and SEM.

## **5.3 Materials and methods**

### **5.3.1 Materials**

Kaolin clay, Rice husk ash, pellets of potassium hydroxide (Merck), hydrochloric acid (Merck), tetrapropylammoniumbromide, TPABr, (Fluka), and distilled water were used in the synthesis of silicalite membrane. Phenyltriethoxysilane (Fluka) used for modification of silicalite membrane.

### **5.3.2 Methods**

#### **Porous supports preparation**

Porous supports were prepared from kaolin clay which was thermally converted to mullite via high temperature calcination. Disc-shape (50 mm in diameter and 2 mm in thickness) was conveniently made by 13 gram of kaolin clay which was put into a mold and hydraulically pressed to form disc-shape, then calcined at 1400°C with a heating rate of 4°C/min for 2 h (Mansoor and Toraj, 2007).

#### **Silicalite membrane synthesis**

The thin film of silicalite on porous support was prepared as follows. Briefly, a clear solution of synthesis mixture with a molar composition of 0.24-1.0NaOH/KOH:SiO<sub>2</sub>:0.03TPABr:123H<sub>2</sub>O. The synthesis solution was then transferred to a stainless steel autoclave and the porous support was immersed in the solution. The crystallization procedure was carried out at 90°C for 17 h and 170°C for various times (0-24 h). Finally, the membrane samples were taken out, washed carefully

with DI water, dried and calcined at 550°C to remove the template for 5 h with heating rate of 1°C/min (Wan, Louisa, Prudence, Carlos, and King, 2001; Nomura, Bin, and Nakao, 2002).

### **Silicalite membrane surface modification**

Modification of the silicalite membrane with a silane coupling reagent was conducted as follows. The silicalite membrane was soaked into toluene (45 g) containing the silane coupling reagent (Phenyltriethoxysilane, 1.5 g) and kept temperature at 80°C for 6 h. After the treatment, the membrane thus obtained was washed with hexane and acetone to remove the free silane coupling reagent from the membrane (Sano, Hasegawa, Ejiri, Kawakami, and Yanagishita, 1995; Araki, Imasaka, Tanaka, and Miyake, 2011).

### **Pervaporation performance**

The pervaporation measurements were performed under an aqueous ethanol solution of 5% (w/w) to 20% (w/w), and temperature varied from 30°C to 60°C. The pervaporation were done with a homemade pervaporation apparatus. Liquid nitrogen was used as a cooling agent for the cool trap. The compositions of the feed and the permeate were determined by gas chromatography. The performance was evaluated by the separation factor and flux.

#### **5.3.3 Characterization**

The silicalite membranes, and the supports during the membrane synthesis were analyzed by X-ray diffraction (XRD) (Philips PW1840 diffractometer) between 5 and 50° Bragg angles using Ni filtered Cu-K $\alpha$  radiation. Fourier transform infrared (FT-IR) spectroscopy was carried out by Perkin Elmer, SpectrumGX. The spectra were recorded within the the range of 3000-400 cm<sup>-1</sup> with 32 scans at a resolution of 4.0 cm<sup>-1</sup> and using KBr pellet and mull technique. Membrane morphology

was determined by a JEOL JSM-6400 scanning electron microscope on gold-coated samples at an accelerating voltage of 10 kV. The composition of permeate streams were analyzed by gas chromatography (Hewlette Packard, GC-HP6890) equipped with a flame ionization detector (FID) and the capillary column used was HP-INNOWAX polyethylene glycol with 0.32 ID and 0.15  $\mu\text{m}$  film thickness.

## 5.4 Results and discussion

### 5.4.1 Mullite disc porous support

Figure 5.1(b) the mullite disc exhibits a more porous micro-structure. The particles combined each other due to the sintering, resulting in the formation of larger sintered particles.

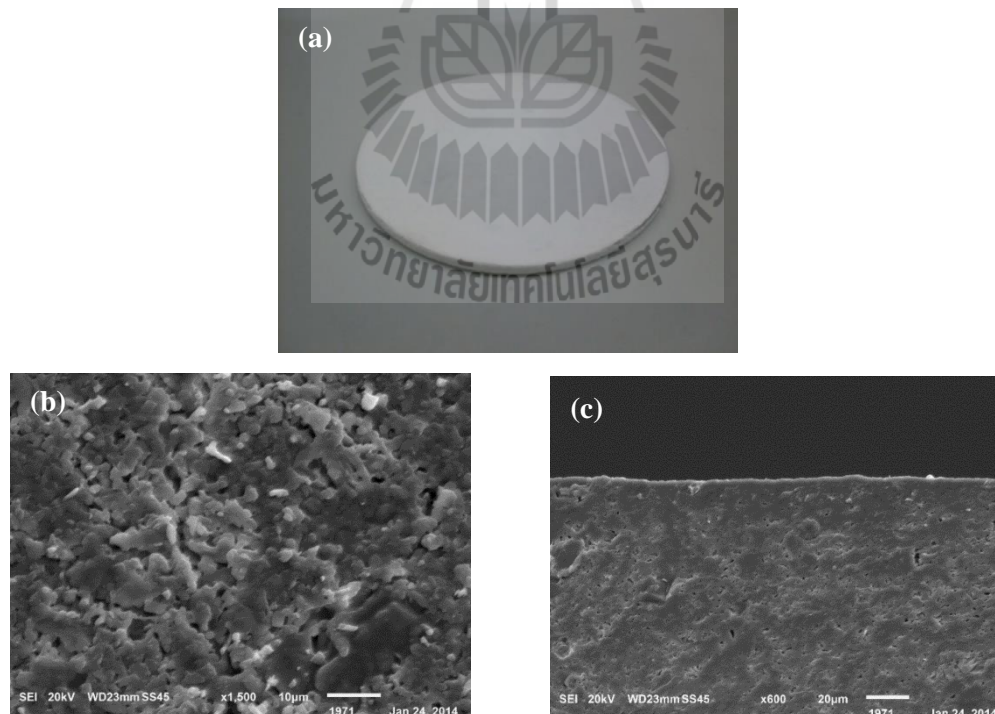


**Figure 5.1** SEM of the mullite (a) mullite disc with diameter 5 cm, (b) surface, and (c) cross-section of mullite disc.

To study the effect of synthesis gel composition, silicalite membranes were prepared by hydrothermal method with various base/SiO<sub>2</sub> ratio (Table 5.1). The results were found that the only sample SLM8 was successfully synthesized thin film of silicalite crystal on the porous support.

**Table 5.1** Mole ratios of chemical compositions of preparation condition of silicalite membranes synthesis at 2 stage temperature for 24 h.

Membrane	SiO <sub>2</sub>	NaOH/ SiO <sub>2</sub>	KOH/ SiO <sub>2</sub>	H <sub>2</sub> O/ NaOH	SiO <sub>2</sub> / TPABr	Crystal growth Results
SLM1	1	0.24		155	30	defect
SLM2	1	0.48		155	30	defect
SLM3	1	0.60		155	30	defect
SLM4	1	0.80		155	30	defect
SLM5	1		0.24	155	30	defect
SLM6	1		0.48	155	30	defect
SLM7	1		0.60	155	30	defect
SLM8	1		0.80	155	30	thin film silicalite
SLM9	1		1.00	155	30	defect

#### 5.4.2 Time dependent layer morphology

Morphological features of the membrane layers (SLM8) was shown in Figure 5.2 as a function of synthesis time ( $t_c$ ). The micrographs present a top view of each membrane and the order of the formation events can be briefly summarised as follows:

$t_c$  2 h : an amorphous gel layer, consisting of colloidal aluminosilicate species, is deposited on the support surface.

$t_c$  4 h : small clusters of nuclei start to coalesce and crystallize to form a matrix of crystallite clusters in close proximity to each other.

$t_c$  12 h : the additional growth planes on each crystal start to fuse together to form larger, defined crystal faces. The round edges show that fusion and growth proceeds rapidly.

$t_c$  24 h : crystal faces are now well-defined into the cubic morphology. Sharp edges indicate that nutrients are depleted and growth has ended.

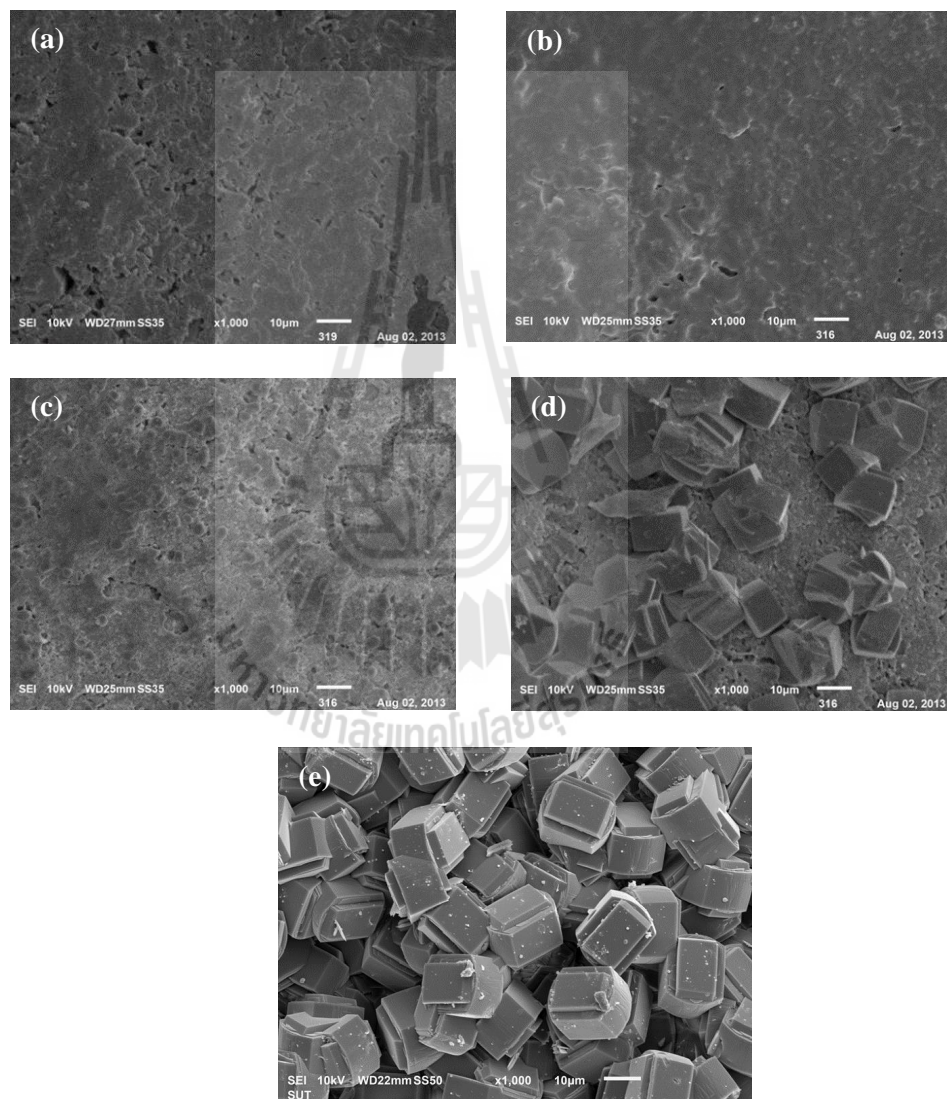


**Figure 5.2** SEM imaging of silicalite membrane formation against time,  $t_c$ . Top views of single layered membranes after  $t_c = 0$  h (a), 2 h (b), 4 h (c), 12 h (d), and 24 h (e).

Figure 5.3 shows the cross section image of silicalite membranes. The thin film of silicalite zeolite were grown on the surface of the mullite support with the thickness about 40  $\mu\text{m}$ . The membrane layer was continuous with no detectable inter-zeolite pores, the crystals on membrane have a length of approximately 20  $\mu\text{m}$ .

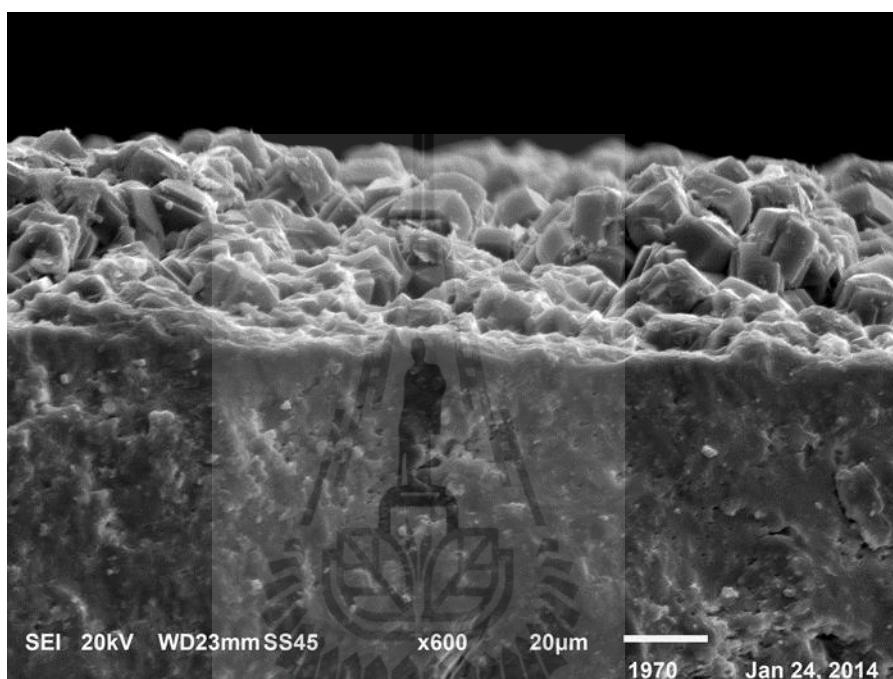


**Figure 5.3** Cross-sections through the layered of zeolites membrane corresponding to synthesis times of 24 h.

#### 5.4.3 Silicalite crystallinity

Figure 5.4 shows X-ray diffraction patterns of silicalite membrane synthesized with reaction time of 24 h supported on porous mullite disc. The reflection peaks corresponding to MFI structure were observed in the X-ray diffraction patterns. The peaks derived from the mullite porous supports were not observed.

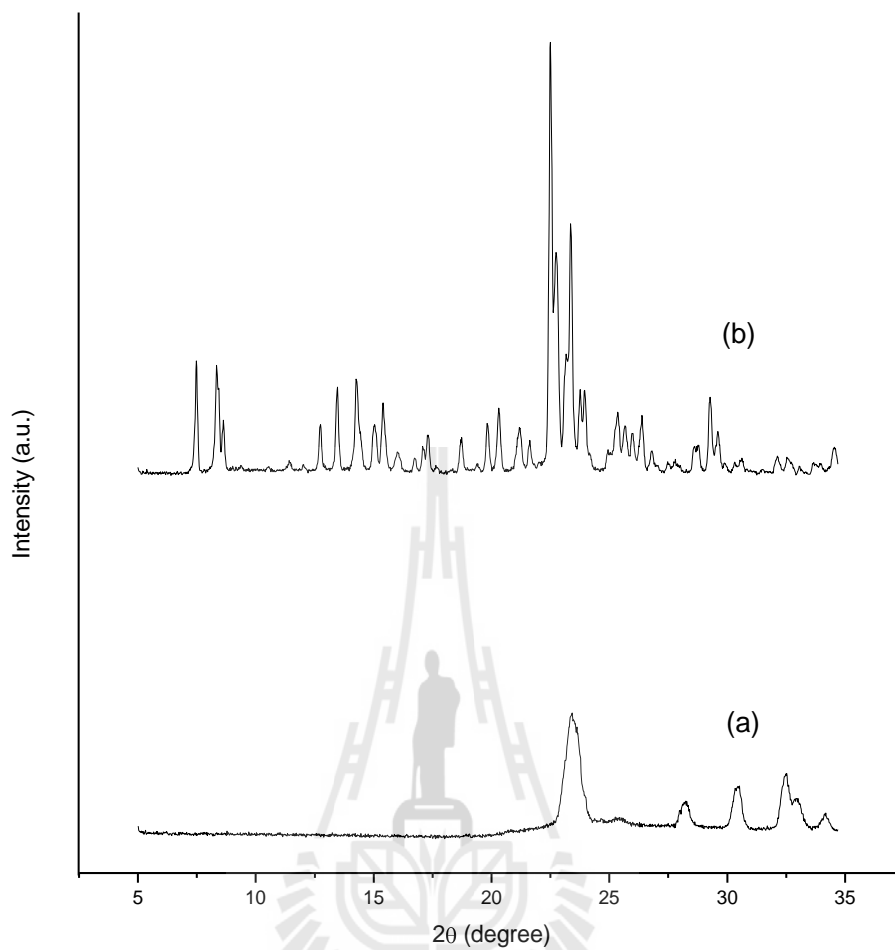


**Figure 5.4** X-ray diffraction patterns of the (a) mullite disc support and (b) silicalite membrane synthesized with reaction time of 24 h.

#### 5.4.4 Modified silicalite membrane

##### SEM images and FT-IR study

SEM images before and after surface modification of silicalite membrane with PhTES are presented in Figure 5.5. PhTES were first coated on the external surfaces of silicalite crystal and it increased hydrophobic properties of the membrane.

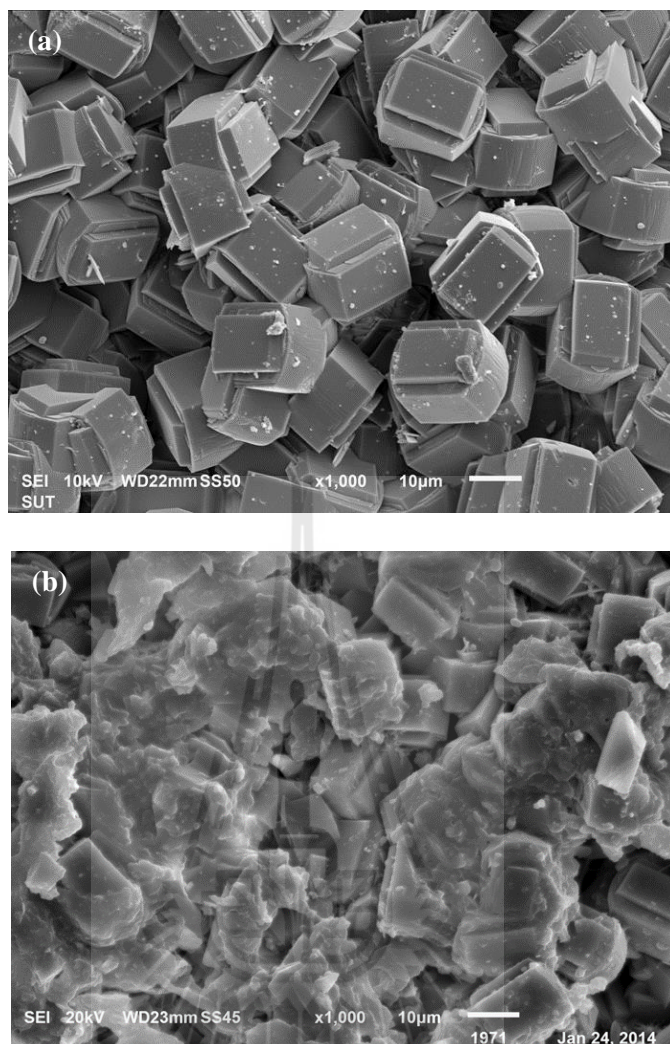


**Figure 5.5** Surface of silicalite membrane (a) and silicalite membrane modified with PhTES (b).

FT-IR absorption spectra after surface modification are shown in Figure 5.6. Organic C-H peaks were observed in the  $2800\text{-}3000\text{ cm}^{-1}$  region with low intensity. The absorption band observed at  $1620\text{-}1585\text{ cm}^{-1}$  corresponds to  $\text{-C=C-}$  in plane stretching vibrations of benzene ring (Araki, Imasaka, Tanaka, and Miyake, 2011; Ou and Seddon, 1997). The broad band in the region around  $1050\text{-}1100\text{ cm}^{-1}$  confirmed the existence of Si-O-Si groups.

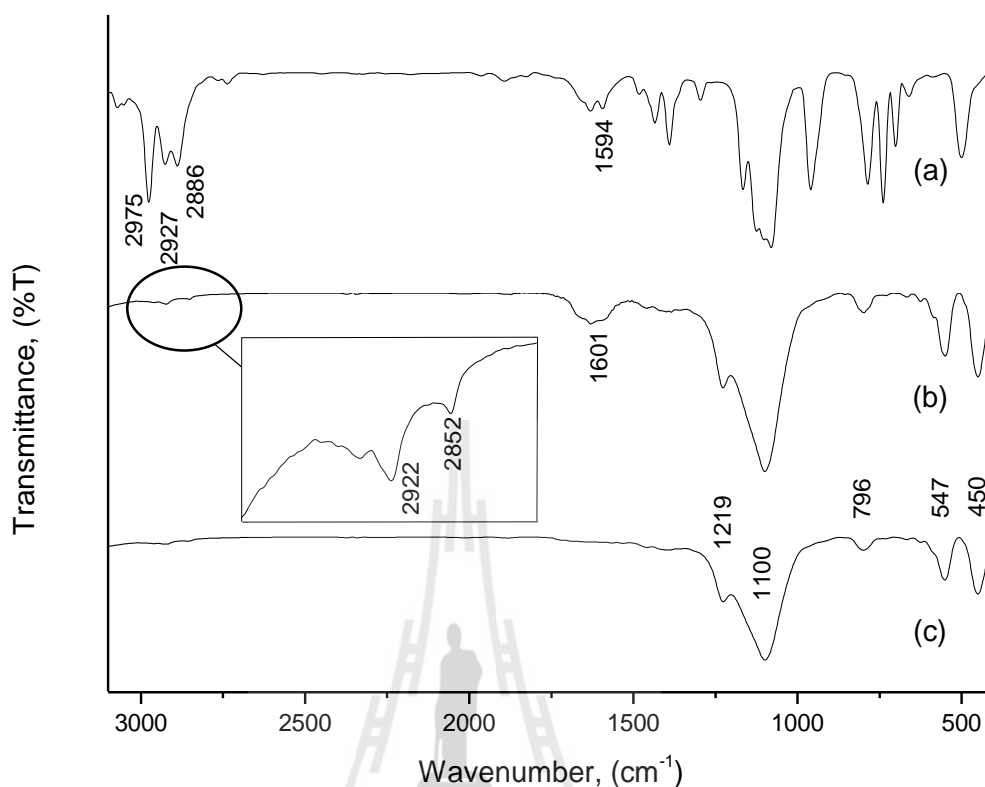


**Figure 5.6** FT-IR spectra of PhTES (a), silicalite membrane after modified with PhTES (b), and silicalite membrane (c).

#### 5.4.5 Pervaporation

##### Effect of temperature

The influence of the feed temperature at 30, 45 and 60°C on the pervaporation performance was studied using modified silicalite membrane supported on a mullite disc. The separation factor and flux increased with an increase in the feed temperature due to the higher vapor pressure of the components of the feed. The highest value of separation factor (S.F.) and flux were 8.4 and 0.42 kg/m<sup>2</sup>.h, respectively.

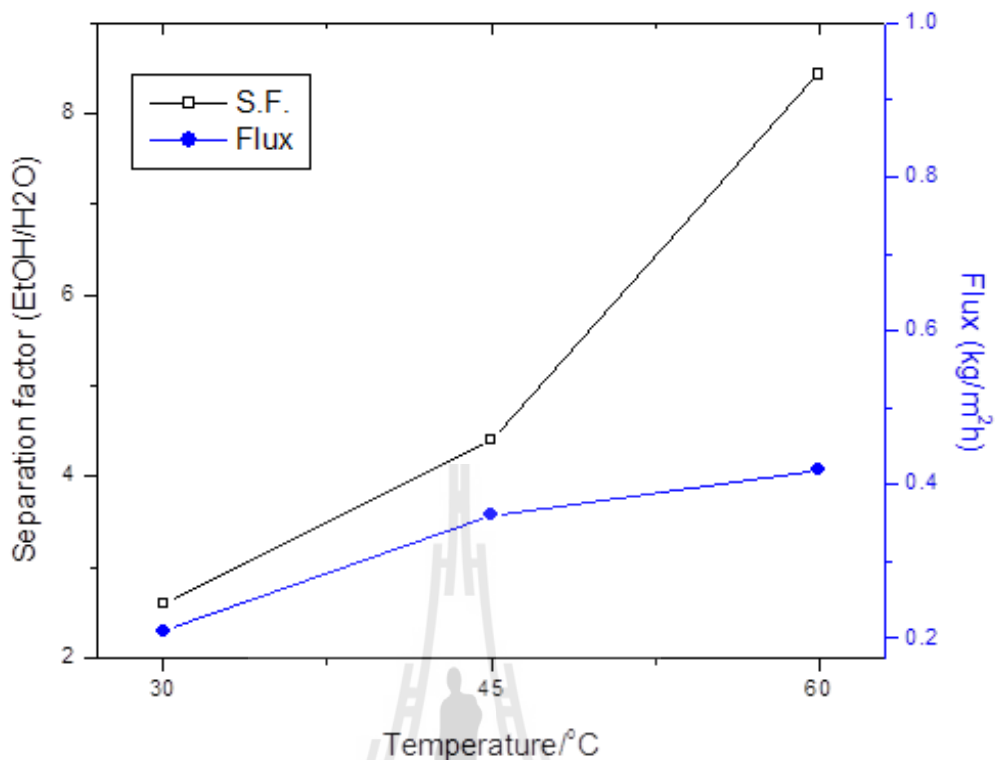


**Figure 5.7** Influence of feed temperature on pervaporation performances through silicalite membrane modified with PhTES. Feed ethanol concentration: 5 wt%.

#### **Effect of feed ethanol concentration.**

Figure 5.7 illustrates the relationship between separation factor and flux as function of feed ethanol concentration. Total flux rapidly increased with increasing feed ethanol concentration. In contrast, separation factor decreases with increasing ethanol concentration. The results suggest that selective adsorption of ethanol on the surface of the silicalite membrane takes place.

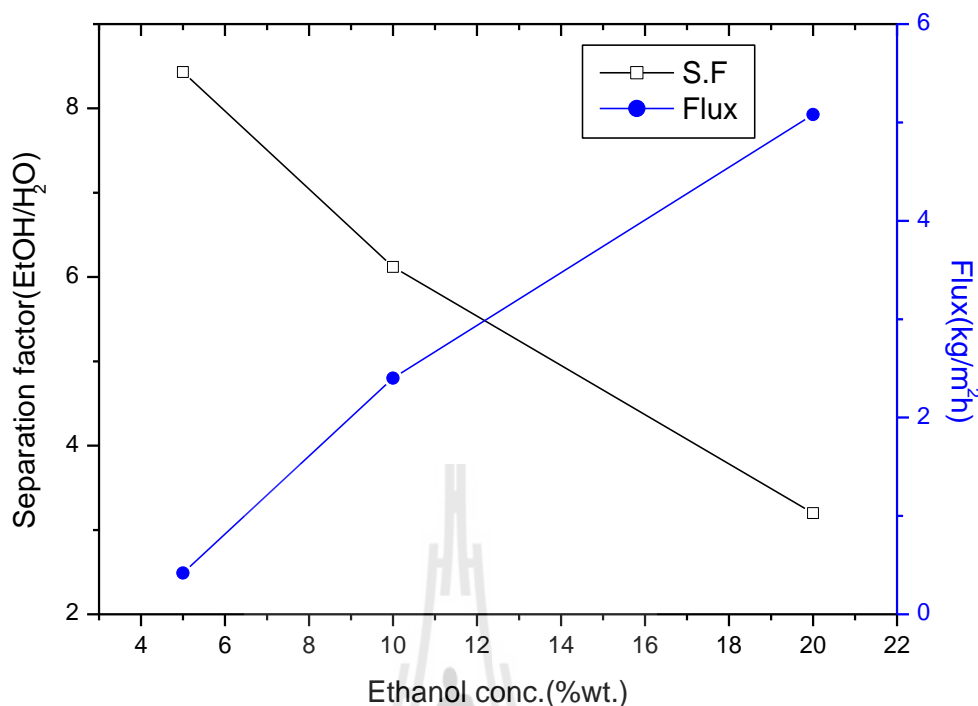


**Figure 5.8** Influence of feed ethanol concentration on pervaporation performance.

Feed temperature: 60°C.

The comparison between silicalite membrane and modified silicalite membrane for pervaporation performances are listed in Table 5.2. The silicalite membranes showed higher separation factor compared to the mixed matrix membrane and modified silicalite membrane for ethanol/water mixture separation. In this work, silicalite membrane cannot separate the ethanol/water mixture by pervaporation. It results from non-zeolite pores occurring during the synthesis in the membrane. Non-zeolite pores are selective for water over organic molecule. The synthesis procedure affects the number and size of non-zeolite pores. Thus, the reduction of non-zeolite pore over the silicalite membrane is necessary. In this work, PhTES was used to reduce non-zeolite pores and to increase hydrophobicity of the zeolite.

**Table 5.2** Pervaporation performance of silicalite membrane and silicalite membrane modified for ethanol/water mixture separation.

Membrane	Feed conc. (EtOH wt%)	T (°C)	Flux (kg/m <sup>2</sup> .h)	$\alpha$	Ref.
Silicalite	5.0	30	0.760	60	Sano et al. (1994)
Silicalite	5.0	30	0.40	69.2	Nomura et al. (2002)
Silicalite	5.0	60	2.26	59	Lin et al. (2001)
Silicalite filled PDMS	5.0	40	0.408	14	Liu et al. (2011)
Silicalite filled PDMS/PVDF	5.0	60	1.290	13.4	Zhan et al. (2009)
Silicalite modified with OTCIS	5.0	50	0.133	45	Sano et al. (1995)
Silicalite membrane	5.0	60	0.76	-	This work
Silicalite modified with PhTES	5.0	60	0.42	8.4	This work

## 5.5 Conclusions

Silicalite membrane with thin film top layer about 40  $\mu\text{m}$  was prepared by cheap material as RHA silica source with TPABr used as organic template and porous mullite support was prepared from kaolin clay. The PV performance of the membrane was improved by modified silicalite membrane with PhTES in order to enhance the hydrophobicity and reduce non-zeolite pores in the membrane. The modified silicalite membrane gave a total flux of 0.42 kg/m<sup>2</sup>.h and a separation factor of 8.3 with 5 wt% ethanol concentration at 60°C. As the temperature was increased from 30°C to 60°C,

the separation factor and flux increased from 2.6 to 8.4 and 0.21 kg/m<sup>2</sup>.h to 0.42 kg/m<sup>2</sup>.h, respectively. When concentration of ethanol feed increased from 5 wt% to 20 wt%, the flux increased from 0.42 kg/m<sup>2</sup>.h to 5.08 kg/m<sup>2</sup>.h, while the separation factor decreased from 8.4 to 3.2. The modified silicalite membrane showed a good pervaporation performance in the low concentration range of ethanol feed.

## 5.6 References

- Araki, S., Imasaka, S., Tanaka, S., and Miyake, Y. (2011). Pervaporation of organic/water mixtures with hydrophobic silica membranes functionalized by phenyl groups. **Journal of Membrane Science**. 380: 41-47.
- Bowen, T. C., Noble, R. D., and Falconer, J. L. (2004). Fundamentals and applications of pervaporation through zeolite membranes. **Journal of Membrane Science**. 245: 1-33.
- Li, S., Tuan, V. A., Falconer, J. L., and Noble, R. D. (2003). Properties and separation performance of Ge-ZSM-5 membranes. **Microporous and Mesoporous Materials**. 58: 137-154.
- Lin, X., Kita, H., and Okamoto, K. I. (2001). Silicalite membrane preparation, characterization and separation performance. **Industrial & Engineering Chemistry Research**. 40: 4069-4078.
- Liu, G., Xiangli, F., Wei, W., Liu, S., and Jin, W. (2011). Improved performance of PDMS/ceramic composite pervaporation membranes by ZSM-5 homogeneously dispersed in PDMS via surface graft/coating approach. **Chemical Engineering Journal**. 174: 495-503.

- Mansoor, K., and Toraj, M. (2007). Synthesis of MFI zeolite membranes for water desalination. **Desalination**. 206: 547-553.
- Nomura, M., Bin, T., and Nakao, S. (2002). Selective ethanol extraction from fermentation broth using a silicalite membrane. **Separation and Purification Technology**. 27: 59-66.
- Ou, R. D., and Seddon, A. B. (1997). Near and mid-infrared spectroscopy of sol-gel derived ormosils: Vinyl and phenyl silicates. **Journal of Non-Crystalline Solids**. 210: 187-203.
- Sano, T., Hasegawa, M., Ejiri, S., Kawakami, Y., and Yanagishita, H. (1995). Improvement of the pervaporation performance of silicalite membranes by modified with silane coupling reagent. **Microporous Materials**. 5: 179-184.
- Sano, T., Yanagishita, H., Kiyozumi, Y., Mizukami, F., and Haraya, K. (1994). Separation of ethanol/water mixture by silicalite membrane on pervaporation. **Journal of Membrane Science**. 95: 221-228.
- Vane, L. M. (2005). A review of pervaporation for product recovery from biomass fermentation processes. **Journal of Chemical Technology and Biotechnology**. 80: 603-629.
- Wong, W. C., Au, L. T. Y., Lau, P. P. S., Ariso, C. T., and Yeung, K. L. (2001). Effects of synthesis parameters on the zeolite membrane morphology. **Journal of Membrane Science**. 193: 141-161.
- Zhan, X., Li, J., Chen, J., and Huang, J. (2009). Pervaporation of ethanol/water mixtures with high flux by zeolite-filled PDMS/PVDF composite membranes. **Chinese Journal of Polymer Science**. 27: 771-780.

## SUMMARY

The crystalline silicalite were synthesized by extraction of silica from rice husk in the presence of NaOH, TPABr, and H<sub>2</sub>O following a facial hydrothermal method. The highest crystallinity was obtained at reaction time only 6 h with the mole ratios of NaOH/SiO<sub>2</sub>, H<sub>2</sub>O/NaOH, and SiO<sub>2</sub>/TPABr as 0.24, 155, and 30, respectively. The vibration bands of the crystals appeared at around 550 and 1223 cm<sup>-1</sup> are characteristics of double 5-ring in ZSM-5. The XRD patterns of all silicalite samples also demonstrates a pure phase of MFI structure with indexable peaks as (101), (200), (501), (151), and (133) reflections. An improvement of some properties of rice husk ash such as an increment of a specific surface area and a reduction of impurity can be successfully done by gel formation with a suggested procedure as an outcome of this study. The highest crystallinity, a narrow size distribution and a smaller particle size of synthesized silicalite are efficiently achieved from silica gel as a silica source by hydrothermal method. Moreover, silicalite prepared from silica gel showed higher ethanol adsorption than silicalite prepared from RHA.

A fast and facial process for the synthesis of silicalite by using RHA as silica source with controllable crystal sizes was obtained. The crystal size of products ranging from 3 μm to 23 μm were achieved by adjusting the molar ratio of NaOH:SiO<sub>2</sub> or KOH:SiO<sub>2</sub> in the system of SiO<sub>2</sub>-TPABr-NaOH/KOH-H<sub>2</sub>O through the hydrothermal synthesis with the temperature at 187°C for 6 h. Single morphology of silicalite was synthesized with sodium and potassium silicate as silica source.

The silicalite membranes were synthesized on the outer surface of the porous mullite disc from clear solutions with a molar composition of  $0.80\text{KOH}:\text{SiO}_2:0.03\text{TPABr}:123\text{H}_2\text{O}$ . Crystallization was carried out at 2 stage temperature for  $90^\circ\text{C}$  for 17 h and  $170^\circ\text{C}$  for 24 h. To improve hydrophobicity of silicalite membrane, modified silicalite membrane was prepared by reflux silicalite membrane with PhTES in toluene at  $80^\circ\text{C}$  for 6 h. The modified silicalite membrane was applied to separation ethanol from ethanol/water mixture by pervaporation. The pervaporation performance gave a total flux of  $0.42\text{ kg/m}^2\cdot\text{h}$  and a separation factor of 8.3 with 5 wt% ethanol concentration at  $60^\circ\text{C}$ .

RHA by-product showed the potential to produced advanced and high-added value materials. The locally RHA waste material can be converted to advanced zeolite materials in an economic and environmental friendly process.



# CURRICULUM VITAE

**CHAIWAT KONGMANKLANG**

**Born:** August 24, 1974, Nakhon Ratchasima, Thailand

**Citizenship:** Thai

**Marital status:** Married

---

## **Degree:**

- |           |                                                                                              |
|-----------|----------------------------------------------------------------------------------------------|
| 2009-2015 | Ph.D. candidate Chemistry<br>Suranaree University of Technology, Nakhon Ratchasima, Thailand |
| 2003      | M.Sc. Analytical Chemistry<br>Khon Kaen University, Khon Kaen, Thailand                      |
| 1996      | B.Sc. Chemistry<br>Ubonratchathani Rajabhat Institute, Ubonratchathani, Thailand             |

## **Working experiences:**

- 1998-Present Scientist, The Center for Scientific and Technological Equipment,  
Suranaree University of Technology, Nakhon Ratchasima

## **Publications:**

1. Kongmanklang, C., and Rangsiwatananon, K. (2015). Facial hydrothermal synthesis of size-controlled silicalite crystals from rice husk ash. **Journal of Chemical Engineering of Japan**. Submitted.
2. Kongmanklang, C., and Rangsiwatananon, K. (2014). Hydrothermal synthesis of high crystalline silicalite from rice husk ash. **Journal of Spectroscopy**. Article ID 696513.